FORMULATION AND IMPLEMENTATION OF TRANSITION DIPOLE MOMENT AND ELECTRIC RESPONSE PROPERTIES USING MULTI-REFERENCE METHODS

THESIS SUBMITTED TO
SAVITRIBAI PHULE PUNE UNIVERSITY
FOR AWARD OF DEGREE OF
DOCTOR OF PHILOSOPHY
IN CHEMISTRY

BY
DEBARATI BHATTACHARYA

Dr. SOURAV PAL
(RESEARCH GUIDE)

Dr. NAYANA VAVAL
(RESEARCH CO-GUIDE)

PHYSICAL CHEMISTRY DIVISION
CSIR - NATIONAL CHEMICAL LABORATORY
PUNE - 411008

JUNE 2015

DECLARATION

I, **Ms. Debarati Bhattacharya** do hereby declare that the work incorporated in the thesis entitled,

'Formulation and implementation of transition dipole moment and electric response properties using multi-reference methods'

submitted by me for the degree of **Doctor of Philosophy in Chemistry** to **Savitribai Phule Pune University** is the record of work carried out by me during the period from February 2012 to June 2015 under the guidance of **Dr. Sourav Pal** and has not formed the basis for the award of any degree, diploma, associateship, fellowship, titles in this or any other University or other institution of Higher learning.

I further declare that the material obtained from other sources has been duly acknowledged in the thesis.

Date :

Place : Pune

Debarati Bhattacharya

Dedicated to

My parents, responsible for me seeing the light of day and to my both set of grandparents.

Acknowledgements

The path towards the completion of my doctoral thesis was very fascinating. I had the pleasure of experiencing life to the fullest. Not only did I grow as a researcher but also had the opportunity to discover myself in the process.

Dr. Sourav Pal played a great role as an advisor and deserves every bit of praise that can be showered on him. My basic knowledge about the quantum world grew around his lectures. His time to time encouragement, his friendly chat sessions, his guidance when astray helped me overcome the obstacles that came my way during the span of this research work. I will be forever grateful to him for accepting me as one his students and helping me as and when required. I hope the journey that I started under his guidance will continue lifelong and that I get to learn from his experience and wisdom.

Without doubt the next person is the most gentle and caring person I have come across till date. She had been there in those trying starting sessions, when I neither heard nor understood the words 'Coupled Cluster'. She painstakingly took me under her tutelage and explained the working of codes. Dr. Nayana Vaval is not only my co-advisor but also the fastest coder, a tea time companion, someone to rush to, in times of trouble and above all a gem of a person. I have actually lost counts of the number of occasions that I went to her for help and she has always rendered aid with a smile.

I am grateful for my hardworking and friendly labmates. I am amazed at the amount of effort that everyone puts into their research and this has been my source of inspiration for a long time. Some of them have been long gone from this lab while some others remain. I thank them all for bearing with me and for their patience. I thank the 'boy gang' in my lab for those wonderful and spirited sea side trips. Achintya, Susanta, Turbasu, Manzoor, Himadri, Aryya, Sudip and Deepak are the present batch of people whom I am grateful to for giving me so many reasons to laugh. I also thank Arijit da, Rahul da, Subrata da, Himadri da and Sumanatra da, Jitendra and Mudit for their scientific discussions and suggestions. I specially thank Jitendra for those rigorous and heated scientific discussion sessions in lab. The 'girl gang' comprised Tuhina, Lalitha, Bhakti, Deepti, Sapna, Sayali, Kamalika, Anagha, Madhulita, Saba and Vidhika. Thanks to all of them for the small chitchat sessions. A

special thanks to Shantanu, Amrita, Nisha, Jaya, Yuvraj and Jugal for being my lunch time buddies. I also thank Manoj, Samik, Rahul, and Baljinder for their support in one way or the other (making me smile also counts!). Special thanks to Dr. Kumar Vanka, Souvik, Chandan, Prithvi and Shubhodeep.

This thesis would not have been complete without mentioning the contribution of those people who have been there through thick and thin. I could not have asked for a better roommate than Nivedita. She has seen me and been at my side no matter what the situation had been. She encouraged me in times of depression, she cautioned me in times of ecstasy, she held my hand when everyone had left, she showed me light when all I perceived was darkness, she fought for me, fought by me, shared with me, stayed up for me... and I could just go on. She is one person who has had perhaps the most significant contribution in this thesis in a non-scientific manner. Among my cherished friends, I thank Sananda, Swagata, Sutapa di, Kamalika, Veena and Sayali. Each one of them is also very special in my doctoral journey and I know this bond will not break that easily !

It seems impossible to thank my family. A child can never thank her parents for their daily sacrifice. They are the replica of whatever is good in this world. I thank Dr. Hiranmay Bhattacharya and Radha Bhattacharya (parents) for their undying love, faith, trust and belief in me. I thank them for their encouragement, dare to dream big attitude, pursuit of dreams, positivity to name a few. I thank my maternal grandparents for their courage. I thank my uncles: Jethu, Kaka, Choto mashai, Mashai, Swapan Mashai, Sintu Kaku and Babu Kaku. My aunties: Boro Pisi, Jemma, Kamma, Bunu masi, Gubli masi, Putai masi, Mummum, Lily Kamma for their support in everything that I pursue. My sisters, Didibhai, Putus, Titir, Boni and Ping who are also my 3 am buddies; my responsible brothers, Bubul and Bon. Even if the name does not feature here, I thank everyone of my family members for their moral support, love and encouragement. Lastly, but definitely not the least, the one person whom I happened to meet by luck and who has now become an integral part of my life; I thank my fiancé, Supratim for being a constant support in this short span of time. I thank him for his patience, caring nature and his scientific aptitude.

Debarati Bhattacharya

Table of contents

Abstract

This thesis mainly focuses on the development of novel and efficient ways to generate transition moments within the class of Fock-space multi-reference coupled cluster (FSMRCC) framework. Certain perturbative approximate methods within FSMRCC are also formulated and presented with reduced scaling, showcasing their effect on difference energies, electric dipole moment, polarizabilities and on transition dipole moments.

Transition dipole moment (TDM) is an important quantity as it provides a basis (along with the rotational-vibrational levels) to calculate Einstein transition probabilities [1] and oscillator strengths. However, the calculation of this is challenging, mainly because of the explicit occurrence of excited wave function. It has been realized that a high level of correlated wave function is necessary for an adequate description of the excited states. Multi-reference coupled cluster (MRCC) [2-14] theory, in the Fock-space version, has been known to be an accurate method of choice in that it includes a combination of dynamic and static correlation arising from the multi-configurational nature of reference space. Using restricted Hartree-Fock determinant of ground closed shell as vacuum, a suitable one hole – one particle *(1,1)* determinant set, constructed within an active set of holes and particles, serves as a suitable reference space for low-lying excited states.

A Fock-space coupled cluster (FSCC) [2-11] theory using such a reference has been well developed for excitation energies and response properties [15-18]. Though, in principle, the theory provides the excited state wave function, its use in the calculation of transition dipole moment has been scarce, mainly because of the description of the conjugate (left) vector of not just the ground state but also the excited state. Once the wave functions have been constructed, it is straightforward to generate the one-electron dipole induced matrix elements. In this thesis, we have formulated and implemented a couple of formalisms to calculate the same, one using a straightforward conjugate of the ground and excited state (called FSCC-T) and the other involving a bi-orthogonal approach [19-22] for the left or conjugate ground and excited states (FSCC-Λ). The first one involves a non-terminating series in the context of coupled cluster method, thus requiring a forced truncation. The second approach linearizes the conjugate states and hence, is naturally terminating. However

this suffers from the fact that additional amplitudes have to be calculated. In the context of FSCC, this implies the evaluation of these amplitudes till the Fock-space sector in question. The two approaches are the expectation value and bi-orthogonal approach and have been used to evaluate TDM of closed shell systems and open shell molecules (only doublet species). Apart from the two methods, a third method is developed to calculate TDM of closed shell molecules: the semi-bi-orthogonal approach. It is a hybrid of the expectation value (FSCC-T) and the bi-orthogonal (FSCC-Λ) approaches and differ from the two in a manner the conjugate states are defined. We have abbreviated this semi-bi-orthogonal approach as the FSCC-ΛT method.

The above methods are constructed within FSCC singles and doubles (SD) methodology. However, the treatment of larger molecular systems become tedious under the same approximation. Certain perturbative approximations have been introduced within FSMRCCSD scheme to check for their effects on the difference energies (e.g. ionization potential (IP), electron affinity (EA) and excitation energies) and electric response properties (like, dipole moment and polarizability). These perturbative approximations help in reduced scaling and lowers the computational cost. Hence, it can be applied to larger systems at a minimal loss of accuracy. Apart from dipole moment and polarizability the effect of such lower scaling methods have also been studied with respect to TDM.

The thesis is organized as follows,

Chapter I : The single reference coupled cluster (SRCC) theory is discussed briefly highlighting the need for a genuine multi-reference method. This is followed by a detailed discussion of Fock space multi-reference theory under the singles and doubles scheme. The discussion includes all the relevant working equations to evaluate difference energies like, IP and EA. Excitation energies are described for the low lying states only, which are depicted in the Fock-space methodology as *(1,1)* sector. A general introduction to constrained variation approach (CVA) and its use in the context of FSCC have also been highlighted. The nature and scope of this thesis form the concluding remarks of this chapter.

Chapter II : The second chapter gives a general introduction to transition dipole moment and its connection with other experimental observables. It is then followed

by a short account of some of the previous work done within CC theory to evaluate TDM. A brief overview of the FSMRCC wave equations are also presented. The methods developed by us within FSCC formulation to evaluate dipole strength comes next. Dipole strength is the square of the transition dipole moment and is related to the experimental observable quantity, oscillator strength. We have formulated two new methods to calculate the dipole strength for ground to low lying excited states of closed as well as open shell molecules. The first formalism uses a straightforward conjugate of the ground and excited state and is abbreviated as FSCC-T. The second one involves a bi-orthogonal approach for the left or conjugate ground and excited states. This is abbreviated as FSCC-Λ. Both the methods are discussed in details for closed as well as open shell systems.

Chapter III : This chapter brings forth the implementation of dipole strength for closed shell molecules from ground to a few low lying excited states. The theory that has been developed and detailed in the previous chapter is implemented through certain molecular systems. Generally, a large number of optically allowed transitions arising from the ground state to electronically excited states are singlet in nature. We have evaluated a few such optically allowed transitions and their oscillator strengths for some small molecules. The methods developed by us are compared against other available theoretical methods and any other available experimental oscillator strength. Apart from the two approaches formulated in the previous chapter, a third hybrid method is introduced in this chapter for the calculation of dipole strength. This is a semi-bi-orthogonal approach where the left and right transition moments are calculated from the bi-orthogonal and expectation value approaches respectively. This new method is tested against the other two FSCC methods as well as other theoretical methods.

Chapter IV : This chapter implements the dipole strength for doublet species. In the Fock-space methodology the doublet species are represented as either (0,1) or (1,0) sectors. The former is equivalent to a IP case, while the latter signifies the EA case. These doublet radical systems are open shell systems and hence even the ground state of such molecules have to described by multi-reference theory. This chapter recapitulates the theory given in chapter II followed by the relevant working equations for the (0,1) sector pertaining to transition moments. The tables are represented with a comparison made against other theoretical methods, wherever applicable.

Chapter V : The previous chapters described and implemented transition moments within FSMRCC theory under the singles and doubles (SD) scheme. In this chapter we describe various approximate methods within the same and their effect on difference energies and first and second order electric response properties. The approximations are based on a perturbative analysis of the ground state similarity transformed Hamiltonian. The various methods are abbreviated as FSCC(n), where *n* $\left(2 \le n \le 4\right)$ depicts that the correlation energy is correct at least up to n^{th} order. At higher values of n, the FSCC(n) will converge towards the full FSCCSD energies. This truncation scheme is size extensive through all orders. It is important to point out, that no truncation scheme has been applied to the higher sectors of FS. The effective Hamiltonian of *(0,1), (1,0)* and *(1,1)* sectors are complete with respect to the truncated effective Hamiltonian of the ground state. This chapter presents the hierarchy of FSCC(n) methods, explicitly stating the terms contributing to the effective Hamiltonian at each level of truncation and the working equations related to it. A general trend is also presented in terms of the root mean squared average values for the difference energies and also for the response properties of each sector.

Chapter VI : This chapter focuses on the general trend of the transition moment following the wake of the various truncation schemes as detailed in the previous chapter. The dipole strengths are calculated in the two lower scaling methods: FS-CC2 and FSCC(2). These are compared against the full FSCCSD calculations for some closed shell ground to low lying excited states of a few molecules.

Chapter VII: This thesis aims on method development as well as implementation of the same to evaluate various properties within Fock-space multi-reference framework. This chapter gives a general conclusion of the work carried out in this thesis and paves the way for ongoing research and future research in this area.

References

[1]. R. C. Hilborn, *Am. J. Phys*. **1982**, 50, 982

[2]. W. Kutzelnigg, *J. Chem. Phys*. **1982**, 77, 3081

[3]. I. Lindgren, *Int. J. Quantum Chem. S***1978**, 12, 33

[4]. I. Lindgren, D. Mukherjee, *Phys. Rep*. **1987**, 151, 93

[5]. D. Mukherjee, *Pramana***1979**, 12, 203

[6]. A. Haque, U. Kaldor, *Chem. Phys. Lett*. **1985**, 117, 347

[7]. S. Pal, M. Rittby, R.J. Bartlett, D. Sinha, D. Mukherjee, *J. Chem. Phys*. **1988**, 88, 4357

[8]. U. Kaldor, *Theo. Chim. Acta*.**1991**, 80, 427

[9]. D. Mukherjee, S. Pal, *Adv. Quantum Chem*. **1989**, 20, 291

[10]. D. Mukherjee, R. K. Moitre, A. Mukhopadhyay, *Mol. Phys*. **1975**, 30, 1861

[11]. S. Pal, *Mol. Phys*. **2010**, 108, 3033

[12]. B. Jeziorski, H. J. Monkhorst, *Phys. Rev. A*, **1981**, 24, 1668

[13]. A. Banerjee, J. Simons, *Int. J. Quantum Chem*. **1981**, 19, 207

[14]. A. Balkova, S. A. Kucharski, L. Meissner, R.J. Bartlett, *J. Chem. Phys*. **1991**, 95, 4311

[15]. S. Pal, *Int. J. Quantum Chem*. **1992**, 41, 443

[16]. K.B. Ghose, S. Pal, *Phys. Rev. A*, **1992**, 45, 1518

[17]. P. U. Manohar, S. Pal, *Chem. Phys. Lett*. **2007**, 438, 321

[18]. J. Gupta, N. Vaval, S. Pal, *J. Chem. Phys*. **2013**, 139, 074108

[19]. P. Jorgensen, T. Helgaker, *J. Chem. Phys*. **1988**, 89, 1560

[20]. N. C. Handy, H.F. Schaefer III, *J. Chem. Phys*. **1984**, 81, 5031

[21]. P. G. Szalay*Int. J. Quantum Chem*. **1995**, 55, 151

[22]. K. R. Shamasunder, S. Asokan, S. Pal, *J. Chem. Phys*. **2004**, 120, 6381

Chapter 1

Introduction

A general overview of the developments in the field of quantum chemistry is presented first that leads up to the subject matter of the thesis. A brief summary of some of the relevant theories and concepts leading to single reference coupled cluster theory is discussed. The need for genuine multi-reference based methods is highlighted, followed by the effective Hamiltonian formalism in MRCC methods. This finally paves way for the Fock-space based CC method. The constrained variation approach within the *(1,1)* sector of FSMRCC is also stated. The first chapter is concluded with the objective and scope of the thesis.

1.1 Introduction

The last few decades have seen spectacular developments in many body theoretical methods (also known as the correlated methods) [1–5] that can accurately describe a range of chemical phenomena. Studies pertaining to electron correlation effects in the ground state of closed-shell systems resulted in a multitude of methods like, the configuration interaction (CI) method, [6-9] the many-body perturbation theory (MBPT), [10-14] and the coupled-cluster (CC) method. [15-19] Size-extensivity and size-consistency criteria have also been an important factor in selecting methods for practical applications. These methods are collectively known as single-reference (SR) methods because of their ability to treat electron correlation effects in systems, with a single dominating configuration.

The success of SR methods in explaining structure and properties of ground state of closed-shell atomic and molecular systems, inspired the extension of these methods for further research in excited states, to treat electron-correlation effects in degenerate and near-degenerate situations (commonly referred to as quasi-degeneracy) e.g. open-shell molecules, curve crossing, etc. The non-dynamical correlation effect, arising from the quasi-degeneracy of such systems, results in the dominance of more than one configuration. This attributed to the development of multi-reference (MR) based methods. Analogous to SR methods, these include MRCI [20,21], MR-MBPT [22-26] and MRCC [27, 36] approaches. In these methods, the dynamical correlation effects are incorporated in a similar fashion like that of their SR counterparts.

The separabilitity, scaling features and accuracy of SRCC methods, boosted the development of MRCC methods. The MRCC class of methods can be divided into two main categories: single root MRCC [32,34-37] i.e. state specific approach and multi-root description i.e. effective Hamiltonian based approaches. The second class of MRCC methods can be further subdivided into two basic classes, namely, Hilbert-space (HS) MRCC [31] and Fock-space (FS) or the valence universal (VU) MRCC [28, 29, 33]. Both these approaches differ in a manner the dynamic correlation is introduced and hence, are applicable for different types of situations. Each of these MRCC methods, have its own window of applicability as well as limitations. HSMRCC is suitable for studying potential energy surfaces whereas, FSMRCC is

suitable for the calculation of ionization potential [38], electron affinity and excitation energies [38-41]. Due to many theoretical and computational difficulties associated with them, the MRCC methods are not as popular as their SR counterparts. In particular, they do not offer an expedient block-box type of solution. They continue to be developed even today and an obvious method of choice is yet to be decided.

Parallel to the MRCC approaches, the equation of motion coupled cluster (EOM-CC) method [42-45] is well known to incorporate a balanced description of the dynamic and non-dynamic correlation within the SRCC framework. Thus, this method presents a black box type of approach for the calculation of energy [45-46], structure [46-49] and properties [50] of open shell molecules and molecular excited states.

In this thesis, we will focus on new developments within the class of FSMRCC for excited state properties and compare our results with other available theoretical methods e.g. EOM-CC. This chapter will highlight some of the earlier developments within SRCC and FSMRCC, including the constrained variation approach (CVA). The FSMRCC theory will be discussed in details for the specific case of excited state which will pave way for the scope of this thesis.

1.2 Overview of previous developments

1.2.1 Hartree-Fock theory

The, Hartree-Fock (HF) theory is central to all attempts made towards solving the Schrodinger equation for many electron system [6, 51-53]. It is based on the fact that stationary states, in particular, the ground states of atoms and molecules with even number of electrons can be represented by a single Slater determinant. Each electron is assumed to be independent of the other, i.e. the electrons are assumed to be moving in a spherically averaged inter electronic repulsion potential. Thus, Hartree - Fock theory is also known as an independent particle model. The HF procedure, directs to a orthonormal set of spin-orbitals, which are the Eigen functions of the Fock operator and the corresponding Eigen values are the orbital energies. The 'N' spin-orbitals with lowest energies are occupied in HF configuration and the corresponding determinant is known as the Hartree-Fock wave function. The remaining unoccupied orbitals in HF configuration are termed as virtual orbitals. The physical significance

of orbital energies is provided by Koopmans' theorem, which states that the energy of an occupied orbital in HF ground state is negative of the energy required for removing an electron from the orbital without relaxing the rest of the orbitals. Koopmans' theorem can accurately predict the ionization potential (IP) because of the fact that the relaxation and correlation effects partially cancel each other. Koopmans' theorem also predicts the first electron affinity. However, these are found to be quite absurd, since, the correlation and relaxation errors add up in this case. For atoms, the HF equations can be exactly solved as an integro-differential equation. However, for molecules, the explicit integration of the two-electron interaction term is difficult, as the orbitals involved are centered at different nuclei. So, following Roothan [54] a finite set of Gaussian functions are introduced to define the spatial parts of atomic orbitals, which are then transformed to molecular orbital basis to achieve ortho-normalization. For closed-shell systems, the spin-orbitals with opposite (spin-up and spin-down) spin functions are paired up and the problem can be simplified by using only spatial orbitals after spin-integration. This leads to a Roothan Hall set of equations and the method is known as restricted HF (RHF). The open-shell systems also have most of the electrons paired up and can be solved by open-shell RHF (ROHF) method. This simplification of electron pairing may not be considered at all and one may explicitly solve the HF equations using spin-orbitals. This method of solving the HF equations is called unrestricted HF (UHF) and leads to the Pople-Nesbet equations. While an RHF or ROHF determinant is a pure Eigen function of total spin operator, UHF determinant, in general, is not. Brillouin's theorem is a result of HF theory and states that configurations obtained by excitation of a single electron from the HF configuration do not directly interact with the HF configuration through the exact Hamiltonian. This feature can be treated as the defining condition of HF approximation.

The important feature of HF theory is the simplification of many-electron problem to an independent particle picture by treating the electron-electron repulsion in a spherically averaged manner. The HF determinant recovers almost 95 to 99 percent of the total energy. The difference between the exact energy and HF energy is termed as the correlation energy as it arises due to partial neglect of the electron-electron interactions. The correlation energy can be recovered by improving the approximations made in HF theory. This leads to various branches of theories

collectively termed as many-body methods or electron correlated methods. Due to the inherent simplicity and its ability to recover most of the ground state energy, HF configuration is generally used as a starting reference for the many-body theories.

1.2.2 An ideal theory

To prove its universal use and acceptance as a practical theory, certain conditions need to be fulfilled. These criteria, as were proposed by Pople et. al. [55] about half a century back and later on quoted and modified by Bartlett [56] can be stated as follows.

1. The method should be independent of certain choices of configurations and symmetry and should it be applicable to a wide range of molecular systems
2. The method should be invariant with respect to a class of transformations. Particularly, unitary transformations should not change the orbital degeneracy.
3. The method should be size-consistent and size-extensive.
4. The method should be computationally efficient as well cost-effective, in order to extend its applicability to various molecular systems.
5. The method should be applicable for open shell systems and excited states.

Among the above stated conditions, size-consistency and size-extensivity are the most important criteria, as the efficiency and accuracy of the method are primarily determined by these factors.

1.2.2.1 Size consistency and extensivity

As defined by Pople and co-workers [55] and Bartlett [56], size-consistency of a method refers to its behaviour when it is applied to a collection of N non-interacting monomers. A method is termed size-consistent if the energy obtained in its application to this collection of monomers, is N times the energy obtained in its separate application to the monomer. In other words, when a size-consistent method is applied to a molecule AB dissociating into two fragments A and B, the energy of the molecule calculated at the dissociating limit (or infinite separation limit) is equal to the sum of the energies of both fragments calculated by separately applying the method to individual fragments. If a method is size consistent, it usually means that

the method can qualitatively predict a correct dissociation curve. Hence, size-consistency is a desirable feature for any approximate method.

Size-extensivity, is a concept related to size-consistency wherein, it refers to the mathematical scaling of energy with the number of electrons [30,57]. A method is size-extensive if the energy a many-electron system calculated by the method, even in the presence of interactions, is approximately proportional to the number of electrons *N* and becomes exact as N tends to infinity. In other words, the energy and the error in energy should increase in proportion with the size of the system. Size-extensivity is especially important for methods treating electron correlation. If a method is not size-extensive, the error in correlation energy shows either sub-linear or super-linear dependence on the number of electrons (or equivalently the size of the system). In the former case, fraction of the exact correlation energy recovered per electron decreases as the size of the system increases, eventually leading to zero correlation energy in the limit of $N \rightarrow \infty$. In the latter case, the same fraction increases with the system size leading to a prediction of infinite correlation energy per electron as $N \rightarrow \infty$. Therefore, all non size-extensive methods show progressively unphysical behaviour as the size of the system increases. Size-extensive methods are considered to be particularly suitable for large systems, as they strive to recover a roughly constant fraction of the exact correlation energy with increasing system size.

Another related concept that is useful in discussion on size-consistency and size-extensivity is the separability. As discussed by Primas [58], separability is related to the behavior of certain quantities of a system composed of two sub-systems interacting with each other in the limit of vanishing interaction strength [58,59]. An additively separable quantity of the system, as the interaction vanishes, should be the sum of the same quantity for individual sub-systems. Similarly, a multiplicatively separable quantity should be the product of the same quantity for individual systems. For example, the total energy of many-electron systems is an additively separable quantity. Similarly, the wave function is multiplicatively separable. Evidently, separability condition is a generalization of size-consistency condition on energy, with respect to an arbitrary division of the system into sub-systems.

1.2.3 Many body methods

There are three very popular methods for the proper treatment of correlation effects: linear variation based configuration interaction, many-body perturbation theory and coupled cluster method. We will discuss the first two methods briefly followed by a detailed analysis of the coupled cluster theory.

1.2.3.1 Configuration Interaction method

CI is conceptually, perhaps the simplest and the most traditional method, where the wave function is expressed as a linear combination of Slater determinants; the coefficients are determined by a linear variation method. Since it is a variational method, CI gives variational upper bound to the energies. Use of a linear variation method to determine expansion coefficients, results in a Eigen value problem for the Hamiltonian matrix defined over all the determinants. The matrix elements of Hamiltonian between any two Slater determinants are evaluated by using Slater-Condon rules [6]. Inclusion of all the possible excited determinants within a given basis set is referred to as the Full-CI (FCI) method. While, the lowest Eigen value and Eigen vector of FCI Hamiltonian matrix correspond to the ground state, rest of the Eigen values and Eigen vectors correspond to various excited states. This gives exact results in a specified basis set. Since, FCI is not feasible even for the small and medium sized molecules in any meaningful basis; we require approximation like truncated expansions in a CI wave function. Truncating the CI space only up to singly and doubly excited determinants along with the reference HF determinant leads to CISD approximation. It is also well known that any approximate or truncated form of CI, is generally not size-extensive and does not separate into appropriate fragments.

The inability of CI to account for the dynamic correlation effects in a proper manner, is responsible for the lack of size-extensivity of truncated CI. It has been shown by Sinanoglu [59] in the context of pair correlation theory, that simultaneous but independent doubly excited processes are also important. This leads to quadruply, hextuply etc configurations with amplitudes as appropriate products of doubly excited amplitudes. Similar physical effects take place involving higher excited determinants. Any truncation based on a preset degree of excitation cannot account for such effects and thus, truncated CI suffers from loss of size-extensivity.

1.2.3.2 Many body perturbation theory

Many body perturbation theory (MBPT) [10-12,60-62] presents an alternative route for systematic incorporation of dynamic correlation effects and produces size-extensive energy at every order of the theory. In this approach, the exact Hamiltonian is partitioned into two parts, a zeroth order part whose solutions are usually known and a perturbation part, which is assumed to be very small when compared to the zeroth order part. There are two different kinds of perturbation series, namely, the Rayleigh Schrödinger (RSPT) [10,12,60] and the other is Brillouin Wigner perturbation theory (BWPT) [12]. Both the perturbation series, have the wave function expressed as a power series, in the region of the solutions of the zeroth order Hamiltonian. Corrections to the wave function at every order is stated in terms of the Eigen functions of the zeroth order Hamiltonian. In the Brillouin Wigner theory, the energy expression depends on the energy itself hence, an iterative procedure needs to be adapted to generate the energy. Each successive iteration produces energy at a higher order, which is not size-extensive. So, BWPT is rarely used to obtain the correlation energy. The properties of RSPT, however, depend upon the exact scheme exploited for its solution. Depending on the partitioning technique of the Hamiltonian, there are two variants of RSPT; Moller-Plessette (MP) PT and Epstien-Nesbet PT. The use of Fock operator as the core Hamiltonian leads to MP partitioning. It can also be shown that MP partitioning within a RSPT framework, leads to a perturbation series, which scales correctly with number of electrons (say N). This size extensive series (due to the presence of explicit linked diagrams) is often known as many body perturbation theory (MBPT). Goldstone [64] devised a diagrammatic approach to show that the terms which have incorrect scaling can be represented by unlinked diagrams. He also proved that such unlinked diagrams cancel each order at each order of perturbation, thus leading to only linked diagrams. The application of the diagrammatic approach to atoms was first done by Kelly [64]. In MBPT, the zeroth order Hamiltonian is constructed as the sum of Fock operators and the perturbation (V) is the full electron-electron repulsion term without the spherical average part.

In modern times, the accuracy of any many-body method can be measured in terms of the such a perturbative order. So, MBPT can be used as an efficient tool to calibrate the accuracy of measurement, of not only the energy but also the wave

functions. MP based RSPT is commonly used for correlated calculations of atoms and molecules. The acronyms MP2, MP4, MBPT (n), etc. have become very popular because of the accuracy and relative simplicity of the method.

In Epstein-Nesbet (EN) partitioning the diagonal part of the Hamiltonian [4] is used as the zeroth order Hamiltonian *(H_0)* and this leads to a perturbation expansion, in which the denominator contains the difference of the diagonal matrix element of the full Hamiltonian. In this case, the perturbation expansion can also be obtained as a result of infinite-order summation of certain classes of terms within the MP series. Unlike the case of MP, Epstein-Nesbet expansion is not invariant under orbital rotations. So, even though MBPT gives size-extensive results at each order, the slow convergence of the perturbation series is its drawback. In conclusion, to avoid the convergence problems, non-perturbative methods are more desirable. In the next subsections we will discuss some methods, which are neither strictly perturbative nor variational but they transcend both the perturbative and variational type of approaches.

1.3 Coupled cluster method

Coupled cluster method (CCM) is perhaps the most popular method among the present class of many body theories. First introduced in the area of nuclear physics by Coester and Kummel, CCM has its conceptual origin in the pair theories of Sinanoglo [54,65] and Nesbet [66]. Cizek and Paldus [67-69] were the pioneers who introduced it into the circle of quantum chemistry practitioners in its present standard form. In CCM, the wave function is described by the action of an exponential wave operator acting on a suitable reference function, which is generally, but not necessarily, a Hartree-Fock determinant. The wave function is denoted as,

$$\left|\Psi_{cc}\right\rangle = e^{T}\left|\Phi_0\right\rangle \tag{1.1}$$

where, $\left|\Phi_0\right\rangle$ is the reference state and *'T'* is known as the excitation or cluster operator. The cluster operators are expressed as a sum of electron excitation operators, *viz*, one-electron, two-electron, etc. (hence, the alternate nomenclature of excitation operator)

$$T = T_1 + T_2 + T_3 + ... + T_N \tag{1.2}$$

The cluster operators can be expressed in terms of second quantized notation as given below,

$$T_1 = \sum_{i,a} t_i^a a_a^\dagger a_i$$
$$T_2 = \sum_{\substack{i>j \\ a>b}} t_{ij}^{ab} a_a^\dagger a_b^\dagger a_j a_i \qquad (1.3)$$
$$\cdots\cdots\cdots\cdots$$
$$T_N = \sum_{\substack{i>j>k.... \\ a>b>c....}} t_{ijk..}^{abc..} a_a^\dagger a_b^\dagger a_c^\dagger a_k a_j a_i$$

where, the $t_{ij...}^{ab...}$ coefficients are also known as the cluster amplitudes. An *N*-body cluster operator, T_N acting on the reference/vacuum state, $|\Phi_0\rangle$ generates *N*-tuply excited hole-particle determinant. The use of a single reference determinant to generate the CC wave function is the reason for its nomenclature as single reference coupled cluster (SRCC) method. In the limit of all possible excitations i.e. when *N* equals the total no of electrons, CC theory must be equal to full CI. There is a straightforward connection of the cluster operators with the CI operators. The relationship between CI and CC coefficients are given below.

$$C_1 = T$$
$$C_2 = T_2 + \frac{1}{2!}T_1^2$$
$$C_3 = T_3 + T_1T_2 + \frac{1}{3!}T_1^3 \qquad (1.4)$$
$$C_4 = T_4 + T_1T_3 + \frac{1}{2!}T_2^2 + \frac{1}{4!}T_1^4$$

The coupled cluster equations are generally solved by the method of projection. Substituting Equation (1.1) into the Schrödinger equation with normal ordered Hamiltonian leads to:

$$H_N e^T |\Phi_0\rangle = E e^T |\Phi_0\rangle \qquad (1.5)$$

On left projection of equation (1.5) by $|\Phi_0\rangle$ we obtain an equation for the correlation energy.

$$\langle\Phi_0| H_N e^T |\Phi_0\rangle = E \langle\Phi_0| e^T |\Phi_0\rangle = E \qquad (1.6)$$

where, the concept of intermediate normalization holds true and the overlap between the reference function and the CC wave function is set to unity.

$$\langle\Phi_0|\Psi_{CC}\rangle = 1 \qquad (1.7)$$

Using Wick's theorem along with the fact that *exp(T)* is normal-ordered, the above equations (1.6) can be diagrammatically represented by a set of closed connected diagrams in which each cluster operator is connected to the Hamiltonian vertex. In order to determine the cluster amplitudes, equation (1.5) is left projected by the excited state determinants, which are generated by the action of the *T*-operator on the reference function. Projection by a particular excited determinant generates the cluster operator of that excitation level. e.g. T_2 can be obtained from the following equation.

$$\left\langle \Phi_{ij}^{ab} \left| H_N e^T \right| \Phi_0 \right\rangle = E \left\langle \Phi_{ij}^{ab} \left| e^T \right| \Phi_0 \right\rangle \tag{1.8}$$

The left and right hand side of the above equation have connected as well as disconnected terms. Nonetheless, presence of the exponential *T* term guarantees mutual cancellation of unlinked terms from both sides of equation (1.8). Thus only the connected, open terms survive in the above equation, leading to completely connected CC equations. Thus, Eqs. (1.6) and (1.8) can be rewritten as,

$$\begin{aligned} \left\langle \Phi_0 \left| H_N e^T \right| \Phi_0 \right\rangle_{closed,connected} &= E \\ \left\langle \Phi^* \left| H_N e^T \right| \Phi_0 \right\rangle_{open,linked} &= 0 \end{aligned} \tag{1.9}$$

where, $\left\langle \Phi^* \right|$ are the set of excited determinants. Mutual contraction among the cluster operators do not occur due to commutation relation. Since the Hamiltonian operator includes one and two particle operators, it can connect to a maximum of four cluster operators thus naturally truncating the exponential series. This renders the CC equations to be algebraic, non-linear equations in the unknown cluster amplitudes and are at most of quatric power. The above discussed CC equations can also be derived by left projection of equation (1.5) with e^{-T}. Thus equation (1.5) can be rewritten as,

$$e^{-T} H_N e^T \left| \Phi_0 \right\rangle = E \left| \Phi_0 \right\rangle \tag{1.10}$$

Equation (1.10) can also be viewed as an Eigen value equation for the similarity transformed Hamiltonian, $\bar{H}$ given as

$$\bar{H} = e^{-T} H_N e^T \tag{1.11}$$

Since, similarity transformation of any operator does not change the Eigen values of the operator, equation set (1.9) can be derived in a similar manner as shown above, giving rise to the following set of equations.

$$\begin{aligned}\left\langle \Phi_0 \left| e^{-T} H_N e^{T} \right| \Phi_0 \right\rangle &= E \\ \left\langle \Phi^* \left| e^{-T} H_N e^{T} \right| \Phi_0 \right\rangle &= 0\end{aligned} \tag{1.12}$$

It is to be noticed that the introduction of the *exp(-T)* opertaor, cancels out its *exp(T)* counterpart in the amplitude equation. This guarantees that the right hand side of the energy expression in equation (1.12) vanishes, taking with it any dependence of the amplitudes on the energy. The similarity transformed Hamiltonian (as stated above) is not Hermitian, therefore, the energy equation does not satisfy any variational condition. Using the Baker-Campbell-Hausdroff (BCH) expansion formula, $e^{-T} H_N e^{T}$ can be expanded [27,61] as,

$$\begin{aligned}\bar{H} = e^{-T} H_N e^{T} = H_N + \left[H_N, T\right] + \frac{1}{2!}\left[\left[H_N, T\right], T\right] + \\ \frac{1}{3!}\left[\left[\left[H_N, T\right], T\right], T\right] + \frac{1}{4!}\left[\left[\left[\left[H_N, T\right], T\right], T\right], T\right] + ...\end{aligned} \tag{1.13}$$

Due to the two body nature of H_N and commutative nature of cluster operator, this series can be shown to be terminated after four fold commutations. The connected nature of the correlation energy and cluster amplitudes are explicitly revealed by the presence of these commutators.

The amplitude expression (see equation 1.9) leads to a set of coupled nonlinear equations, which are generally solved iteratively to obtain the cluster amplitudes. Perturbation analysis of the iterative procedure show that, at every iteration, the functional gains correction from various orders of perturbation. After the self-consistency and numerical accuracy is attained, the correlation energy is obtained using the energy expression of equation (1.9). If T contains all possible excitation operators i.e. up to T_N for a N-electron system, then the method is called full CC (FCC), which is equivalent to FCI. Obviously, the number of cluster operators will be the same as CI operators. However, for practical application one needs to truncate at a finite order. The most commonly used truncation is the singles and doubles truncation, where $T = T_1 + T_2$ [71,72]. Unlike truncated CI, CC method continues to be size-consistent, for at any order of truncation. This is because of the exponential nature of the wave operator, which includes higher excitations through the products of cluster amplitudes. The CCSD anasatz can be further improved by perturbative or complete inclusion of triples (partial and full) [17,73], quadrupoles (CCSDT(Q) and

CCSDTQ) [74], etc. These anasatz are seen to further accelerate the convergence towards exactness.

1.4 EOM-CC Method

The equation of motion coupled cluster (EOM-CC) method [75-78] is a single-reference approach, where the excited state wave functions are generated by the action of a linear CI like operator on the correlated reference wave function. The Schrödinger equation for the reference state and the excited state (be it an electron attached or ionized state) can be described by the following equations,

$$\hat{H}\Psi_0 = E_0\Psi_0 \tag{1.14}$$

$$\hat{H}\Psi_k = E_k\Psi_k \tag{1.15}$$

where, the subscript *'0'* and *'k'* refer to the reference state and any excited state respectively. The excited state wave function Ψ_k is related to the reference state wave function by the following relation,

$$\Psi_k = \hat{\Omega}_k\Psi_0 \tag{1.16}$$

Left multiplying equation (1.14) with $\hat{\Omega}_k$ and subtracting it from equation 1.15, we can arrive at the following expression after some manipulation

$$\left[\hat{H},\hat{\Omega}\right]\Psi_0 = \omega_k\Omega_k\Psi_0 \tag{1.17}$$

where $\omega_k = E_k - E_0$. The form of Ω_k describes the particular EOM method corresponding to the target state.

For the specific case of ionization,

$$\Omega_k^{IP} = \sum_a R_i(k)i + \sum_{a>b,\,j} R_{ij}^a(k)\hat{a}^\dagger\hat{j}\hat{i} + \text{.....} \tag{1.18}$$

For the specific case of electron attachment

$$\Omega_k^{EA} = \sum_a R^a(k)\hat{a}^\dagger + \sum_{a>b,\,j} R_j^{ba}(k)\hat{b}^\dagger\hat{j}\hat{a}^\dagger + \text{.....} \tag{1.19}$$

and for the excitation energy problem

$$\Omega_k^{EE} = R_0(k) + \sum_a R_i^a(k)\hat{a}^\dagger i + \sum_{a>b,i>j} R_{ij}^{ab}(k)\hat{a}^\dagger\hat{b}^\dagger ij + \ldots\ldots \quad (1.20)$$

The expressions given above are for any general EOM approach. Coupled cluster theory is introduced through generation of the correlated wave function by the action of an exponential operator on a Slater determinant, which is generally, but not necessarily the Hartree-Fock determinant, i.e.

$$\Psi_0 = e^{\hat{T}}\left|\Phi_0\right\rangle \quad (1.21)$$

where, $\hat{T} = \hat{T}_1 + \hat{T}_2 + \ldots\ldots$ and $\hat{T}_1 = \sum_{ia} t_i^a\left\{a_a^\dagger a_i\right\}$, $\hat{T}_2 = \frac{1}{4}\sum_{ijab} t_{ij}^{ab}\left\{a_a^\dagger a_b^\dagger a_j a_i\right\}$ …

Since, $\hat{\Omega}$ and $\hat{T}$ commutes with each other, we can rewrite equation (1.17) as,

$$\left[\bar{H},\hat{\Omega}\right]\Phi_0 = \left(\bar{H}\hat{\Omega}\right)_c = \omega_k\hat{\Omega}_k\Phi_0 \quad (1.22)$$

Where, $\bar{H} = e^{-\hat{T}}He^{\hat{T}}$, and c denotes the connectedness of $\bar{H}$ and $\hat{\Omega}$

Since $\bar{H}$ is non Hermitian in nature, there exist different right (R) and left (L) Eigen vectors which are bi-orthogonal and can be normalized to satisfy the following condition,

$$L_k R_l = \delta_{kl} \quad (1.23)$$

$\bar{H}$ is diagonalized in the 1h and 2h1p sub space to generate the IP, whereas EA values are obtained through diagonalization of the same in the 1p and 2p1h sub space. EOMCC have been studied for calculation of molecular energies, structure and properties.

1.5 Multi-reference coupled cluster methods

In contrast to the SRCC theory, which mainly evolved from its correspondence with the single reference MBPT, the evolution of multi-reference coupled-cluster (MRCC) theories has been more or less independent of the underlying

perturbative structure. An MRCC theory is obtained by finding an exponentially parameterized ansatz for the wave-operator Ω, and formulating a scheme for unambiguous determination of these parameters. The motivation for exponential parameterization comes from the possibility of obtaining size-extensive results, along with the usual high accuracy stemming from partial infinite-order summation nature of CC theory.

Contrasting with SRCC where, there is only one way to parameterize the wave function, several possibilities open up for the multi-reference case. However, they can be classified into two broad categories: the first one describes a specific root, known as the state specific MRCC and other is the multi root description by effective Hamiltonian approach. Effective Hamiltonian based theories are further subdivided into two main subclasses: Hilbert space (HS) method and Fock Space (FS) method. In both the approaches, the energies are obtained by diagonalization of the effective Hamiltonian defined within a pre-chosen model space, and both approaches are fully size extensive. The HS-MRCC approach [79,80] uses a state universal operator with different cluster operators for each determinant in the model space. The FS-MRCC approach, on the other hand, uses a common vacuum and a valence universal wave operator, which correlates the model space with the virtual space. The HSMRCC method is more suitable for the calculation of potential energy surface. On the other hand, FSMRCC [81-84] method is more suited for direct difference of energy calculations such as ionization potential, electron affinity, and excitation energies. Since, we are essentially interested in treatment of excited state properties, FSMRCC is our method of choice. The next section discusses the theory of FSMRCC within the *(1,1)* valence rank with explicit equations for solving the Lagrange equations in the same sector.

1.6 General description of FSMRCC theory

Generally, a closed shell HF single determinant is selected as the vacuum or reference state with respect to which we define our holes and particles. A further subdivision (of the particle-hole orbitals) into active and inactive holes and particles are made, which will introduce the multi-reference flavour of the theory. By, taking an appropriate linear combination of the various determinants generated by different occupation of the active orbitals constitutes the model space. If we choose to have *'p'*

active particles and *'h'* active holes, then with the help of the $P^{(p,h)}$ projection operator, which projects onto the model space and $Q^{(p,h)}$ which projects onto the model space, a model space with *(p,h)* particle-hole rank will be generated. Each such model space actually describes a particular type of state within the Fock-space where, (0,0) is the ground state, (0,1) model space describes the single ionized states, (1,0) singly electron attached states and finally the (1,1) model space denotes the singly excited states. The choice of active and inactive group of orbitals is governed by the various energy spectrum of interest. Among the different model spaces mentioned above, (0,0), (0,1) and (1,0) are complete model space as they include all possible occupancies of electrons in the chosen active orbitals. The (1,1) model space is incomplete in the same respect, as it excludes all the doubly, triply etc. excited determinants. However, a simplification to this incompleteness can be achieved by assuming that it is complete with respect to a single occupancy in the active particles and single vacancy in the active holes. Hence, the (1,1) model space is termed as a quasi-complete model space. The zero[th] order wave function of (p,h) sector in Fock-space comprises a linear combinations of the model space functions

$$\left|\Psi_{(0)\mu}^{(p,h)}\right\rangle = \sum_i C_{\mu i}^{(p,h)} \left|\Phi_i^{(p,h)}\right\rangle \tag{1.24}$$

The main idea of effective Hamiltonian theory is to extract some selective eigen values of Hamiltonian from the whole eigen value spectrum. To fulfill this purpose, the configuration space is partitioned into a model space and an orthogonal space. The projection operator for the model space is defined as,

$$P^{(p,h)} = \sum_i \left|\Phi_i^{(p,h)}\right\rangle \left\langle\Phi_i^{(p.h)}\right| \tag{1.25}$$

The projection operator in the complimentary space is given by,

$$Q^{(p,h)} = 1 - P^{(p,h)} \tag{1.26}$$

The diagonalization of the effective Hamiltonian takes care of the non-dynamic correlation arising due to the interactions of the model space configurations. The dynamic correlation occurs due to the interactions of the model space configurations with the virtual space. This interaction is introduced through a universal wave operator Ω, which is parameterized such that it generates the exact wave function by acting on the model space. To generate the exact states for the (p,h) valence system,

the wave operator must be able to generate all the valid excitations from the model space. The valence universal wave operator Ω has the form

$$\Omega = \left\{ e^{S^{(p,h)}} \right\} \tag{1.27}$$

where, the curly braces denote normal ordering of the cluster operators with respect to the reference function. $S^{(p,h)}$ is defined as following

$$S^{(p,h)} = \sum_{k=0}^{p} \sum_{l=0}^{h} T^{(k,l)} \tag{1.28}$$

The cluster operator $T^{(k,l)}$ is capable of destroying exactly *k* active particles and *l* active holes, in addition to creation of holes and particles. The $S^{(p,h)}$ subsumes all lower valence Fock space $T^{(k,l)}$ operators, where the $T^{(0,0)}$ cluster amplitude corresponds to standard single-reference coupled cluster amplitudes.

The Schrödinger equation for the manifold of quasi-degenerate states can be written as

$$H \left| \Psi_{\mu}^{(p,h)} \right\rangle = E_{\mu} \left| \Psi_{\mu}^{(p,h)} \right\rangle \tag{1.29}$$

where, the correlated μ^{th} wave function in can be written as

$$\left| \Psi_{\mu}^{(p,h)} \right\rangle = \Omega \left| \Psi_{(0)\mu}^{(p,h)} \right\rangle$$

(1.30)

Substitution of equation (1.24) and (1.30) into equation (1.29) gives,

$$H\Omega \left(\sum_{i} C_{\mu i}^{(p,h)} \phi_{i}^{(p,h)} \right) = E_{\mu} \Omega \left(\sum_{i} C_{\mu i}^{(p,h)} \phi_{i}^{(p,h)} \right) \tag{1.31}$$

The effective Hamiltonian for the *(p,h)* valence rank system can be defined as

$$\sum_{j} \left(\hat{H}_{eff}^{(p,h)} \right)_{ij} C_{j\mu} = E_{\mu} C_{\mu i} \tag{1.32}$$

where the effective Hamiltonian can be defined as,

$$\left(\hat{H}_{eff}^{(p,h)}\right)_{ij} = \left\langle \phi_i^{(p,h)} \middle| \Omega^{-1}\hat{H}\Omega \middle| \phi_j^{(p,h)} \right\rangle \tag{1.33}$$

The above equation can be rewritten in terms of the model space as,

$$\hat{H}_{eff} = P^{(p,h)}\Omega^{-1}\hat{H}\Omega P^{(p,h)} \tag{1.34}$$

Equation (1.34) requires an explicit description of Ω^{-1}. But there can arise situations where Ω^{-1} may not exist [82]. In order to avoid the usage of Ω^{-1} while defining the effective Hamiltonian, Bloch and Lindgren formulated another set of equation commonly known as the Bloch equation, which is given as,

$$H\Omega P = \Omega H_{eff} P \tag{1.35}$$

The above equation is solved by left projection with P and Q opertaors respectively, giving rise to the following set of equations :

$$\begin{aligned} P^{(k,l)}\left[H\Omega - \Omega H_{eff}\right]P^{(k,l)} &= 0 \\ Q^{(k,l)}\left[H\Omega - \Omega H_{eff}\right]P^{(k,l)} &= 0 \end{aligned} \qquad \forall k = 0,.....p; l = 0,.....h \tag{1.36}$$

To solve the above equation set, an additional normalization is imposed through parameterization of Ω. In case of CMS, this is generally performed by imposing the intermediate normalization condition $P\Omega P = P$. However, the situation is a little bit different in case of incomplete model space. Mukherjee [85] has shown that in case of incomplete model space, the valence universality of the wave operator is sufficient to guarantee linked-cluster theorem; but one needs to relax the intermediate normalization. Pal *et. al* [84] have shown that for the special case of quasi-complete model space in (1,1) sector, the intermediate normalization can be used without any loss of generality.

In general, the equations for Ω and H_{eff} are coupled to each other through the equation set (1.36). Hence, H_{eff} cannot be explicitly expressed in terms of Ω. However, when intermediate normalization is imposed, H_{eff} can be directly written as a function of Ω.

$$P^{(p,h)}H\Omega P^{(p,h)} = P^{(p,h)}H_{eff}^{(p,h)}P^{(p,h)} \tag{1.37}$$

After solving for Ω and H_{eff}, diagonalization of the effective Hamiltonian within the *P* space gives the energies of the corresponding states and the left and the right eigen vectors.

$$\begin{aligned} H_{eff}^{(p,h)} C^{(p,h)} &= C^{(p,h)} E \\ \tilde{C}^{(p,h)} H_{eff}^{(p,h)} &= E \tilde{C}^{(p,h)} \\ \tilde{C}^{(p,h)} C^{(p,h)} &= C^{(p,h)} \tilde{C}^{(p,h)} = 1 \end{aligned} \tag{1.38}$$

The contractions amongst different cluster operators within the exponential are avoided due to the normal ordering, leading to partial hierarchical decoupling of the cluster equations, i.e. after solving the lower valence amplitude equations of a particular sector in Fock space, it appears as a known parameter in the equations for the higher valence rank. This is commonly referred to as sub-system embedding condition (SEC) [84]. The lower valence cluster equations are decoupled from the higher valence cluster equations, because of the SEC. Hence, the Bloch equations are solved progressively from the lowest valence *(0,0)* sector upwards up to (p, h) valence sector.

1.6.1 FSMRCC for excited states

The general theory for Fock-space MRCC is already stated in the previous section. In this section we will detail out the relevant working equations for the *(1,1)* sector and formulate CVA from this viewpoint. The valence universal wave operator for the specific problem of excitation energy is given by,

$$\Omega = \left\{ e^{T^{(0,0)}} + e^{T^{(0,1)}} + e^{T^{(1,0)}} + e^{T^{(1,1)}} \right\} \tag{1.39}$$

Under the singles and doubles scheme, the cluster operator for each sector contains, only one and two body parts. Matrix elements of the effective Hamiltonian for this sector can be written as,

$$\left(\tilde{H}_{eff} \right)_{(\mu\alpha,\nu\beta)}^{(1,1)} = \left(H_{eff} \right)_{(\mu\alpha,\nu\beta)}^{(1,1)} + \left(H_{eff} \right)_{(\alpha,\beta)}^{(1,0)} \delta_{\mu,\nu} + \left(H_{eff} \right)_{(\mu,\nu)}^{(0,1)} \delta_{\alpha,\beta} + H_{eff}^{(0,0)} \tag{1.40}$$

where, μ,ν and α,β corresponds to indices for active holes and active particles respectively. The Bloch equations for this sector is given by,

$$P^{(k,l)}\left[H\Omega-\Omega H_{eff}\right]P^{(k,l)}=0$$
$$Q^{(k,l)}\left[H\Omega-\Omega H_{eff}\right]P^{(k,l)}=0 \qquad \forall k=0,.....1; l=0,.....1 \tag{1.41}$$

Normal ordering of the cluster amplitudes leads to SEC that results in the decoupling of the lower valence sector equations from the higher valence ones. It has been shown by Mukherjee that if one abandons the requirement of intermediate normalization then the linked nature of the effective Hamiltonian and cluster operators can be ensured. The effective Hamiltonian in the model space for the (1,1) sector can be written as:

$$P^{(1,1)}\tilde{H}_{eff}^{(1,1)}P^{(1,1)}=P^{(1,1)}H\Omega P^{(1,1)} \tag{1.42}$$

The equations of all the cluster amplitudes (i.e. $T_2^{(1,1)}$ and the one and two body cluster operators of the lower valence sectors) as well as the effective Hamiltonian are independent of $T_1^{(1,1)}$ amplitudes. Although the excited state wave function in FSMRCCSD consists of the $T_1^{(1,1)}$ amplitudes, these are not explicitly required for evaluation of excitation energies. Thus, under singles and doubles approximation, we effectively have only two-body cluster amplitudes of the *(1,1)* sector. Due to spin adaptation two different types of $H_{eff}^{(1,1)}$ and $T_2^{(1,1)}$ exist. We indicate them as $\left(H_{eff}^{A}\right)^{(1,1)}$ and $\left(H_{eff}^{B}\right)^{(1,1)}$, $T_2^{A(1,1)}$ and $T_2^{B(1,1)}$ respectively. The equations for the effective Hamiltonian and excited state amplitudes, as depicted by the superscript 'A' are completely decoupled from the equations of the type-B quantities. However, the equations for type-B depends on the quantities of type-A. Thus, in addition to SEC, there is a further decoupling among the two types of blocks. The final expressions of the effective Hamiltonian (in matrix equation form) after spin adaptation can be written as,

$$\left(H_{eff}^{S}\right)_{(\mu\alpha,\nu\beta)}^{(1,1)}=\left(H_{eff}^{A}\right)_{(\mu\alpha,\nu\beta)}^{(1,1)}-2\left(H_{eff}^{B}\right)_{(\mu\alpha,\nu\beta)}^{(1,1)}+\left(H_{eff}\right)_{(\alpha,\beta)}^{(1,0)}\delta_{\mu,\nu}+\left(H_{eff}\right)_{(\mu,\nu)}^{(0,1)}\delta_{\alpha,\beta}+H_{eff}^{(0,0)} \tag{1.43}$$

and

$$\left(H_{eff}^{T}\right)_{(\mu\alpha,\nu\beta)}^{(1,1)}=\left(H_{eff}^{A}\right)_{(\mu\alpha,\nu\beta)}^{(1,1)}+\left(H_{eff}\right)_{(\alpha,\beta)}^{(1,0)}\delta_{\mu,\nu}+\left(H_{eff}\right)_{(\mu,\nu)}^{(0,1)}\delta_{\alpha,\beta}+H_{eff}^{(0,0)} \tag{1.44}$$

where, the superscript 'S' and 'T' denote the singlet and triplet effective Hamiltonian respectively. The indices $\{\mu,\nu,\alpha,\beta\}$ means the same as given in equation (1.40). As

can be seen from the above expression, that the triplet excitation energies are completely decoupled from the singlet energy. Hence, they can be obtained by solving for the type-A Bloch equations of the (1,1) sector. Calculation of singlet excitation energy is more complicated, as this requires the knowledge of both types of Bloch equations. If the closed connected part of the ground state effective Hamiltonian is dropped off from the calculation, we end up with the direct difference of energy of the corresponding state.

1.6.2 CVA for (1,1) sector in FSMRCC

The constrained variation approach [86] in the FSMRCC was pursued by Pal and co-workers [87-92] Similar simplifications of the $\Lambda^{(1,1)}$ amplitudes holds true as that of the excitation amplitudes in the same sector, i.e. $\Lambda_1^{(1,1)}$ amplitudes do not occur in the expression for energy even though they are contained in the wave function equations. Also, the construction of the Lagrangian for a specific state depends on the spin multiplicity of that state. Hence, the triplet excitation energies are completely decoupled from the singlet ones. Singlet energy of a particular, μ^{th} state in is given by,

$$E_\mu^S = \sum_{ij} \tilde{C}_{\mu i}^{S(1,1)} \left(H_{eff}^S \right)_{ij}^{(1,1)} C_{j\mu}^{S(1,1)} \tag{1.45}$$

The Lagrangian for the above mentioned state is constructed as given below,

$$\begin{aligned}
\pounds = & \sum_{ij} \tilde{C}_{\mu i}^{S(1,1)} \left(H_{eff}^S \right)_{ij}^{(1,1)} C_{j\mu}^{S(1,1)} \\
& + P^{(1,1)} \Lambda^{B(1,1)} \left[H\Omega - \Omega H_{eff}^{S(1,1)} \right]^B P^{(1,1)} \\
& + P^{(1,1)} \Lambda^{A(1,1)} \left[H\Omega - \Omega H_{eff}^{S(1,1)} \right]^A P^{(1,1)} \\
& + P^{(0,1)} \Lambda^{(0,1)} \left[H\Omega - \Omega H_{eff}^{(0,1)} \right] P^{(0,1)} \\
& + P^{(1,0)} \Lambda^{(1,0)} \left[H\Omega - \Omega H_{eff}^{(1,0)} \right] P^{(1,0)} \\
& + P^{(0,0)} \Lambda^{(0,0)} \left[H\Omega - \Omega H_{eff}^{(0,0)} \right] P^{(0,0)} \\
& - E_\mu^S \left(\sum_{ij} \tilde{C}_{\mu i}^{S(1,1)} C_{j\mu}^{S(1,1)} - 1 \right)
\end{aligned} \tag{1.46}$$

The Λ vectors and the cluster amplitudes are obtained by making the Lagrangian stationary with respect to the cluster amplitudes and Λ amplitudes respectively. The Eigen vectors are also obtained variationally. Thus, the cluster amplitudes are completely decoupled from the de-excitation amplitudes. As stated in section 1.7, the

cluster amplitudes follow the SEC. For the Λ vectors, there is a reverse decoupling. That is the higher valence de-excitation operators are solved first followed by the lower valence ones. Also, the decoupling in terms of the type-A and B amplitudes are also reversed. In case of $T_2^{(1,1)}$ amplitudes, the B-type amplitudes are solved after the type-A ones. In case of Λ vectors, we start solving from the $\Lambda_2^{B(1,1)}$ amplitudes and then move down towards the lower valence amplitudes till the vacuum sector. In case of evaluating the de-excitation amplitudes for the triplet sector, a different Lagrangian needs to be constructed. The triplet states are obtained by diagonalizing the triplet effective Hamiltonian. The triplet energy for a particular μ[th] state is given by,

$$E_\mu^T = \sum_{ij} \tilde{C}_{\mu i}^{T(1,1)} \left(H_{eff}^T \right)_{ij}^{(1,1)} C_{j\mu}^{T(1,1)} \tag{1.47}$$

The Lagrangian for the triplet state is constructed as shown below,

$$\begin{aligned} £ = & \sum_{ij} \tilde{C}_{\mu i}^{T(1,1)} \left(H_{eff}^T \right)_{ij}^{(1,1)} C_{j\mu}^{T(1,1)} \\ & + P^{(1,1)} \Lambda^{A(1,1)} \left[H\Omega - \Omega H_{eff}^{S(1,1)} \right]^A P^{(1,1)} \\ & + P^{(0,1)} \Lambda^{(0,1)} \left[H\Omega - \Omega H_{eff}^{(0,1)} \right] P^{(0,1)} \\ & + P^{(1,0)} \Lambda^{(1,0)} \left[H\Omega - \Omega H_{eff}^{(1,0)} \right] P^{(1,0)} \\ & + P^{(0,0)} \Lambda^{(0,0)} \left[H\Omega - \Omega H_{eff}^{(0,0)} \right] P^{(0,0)} \\ & - E_\mu^T \left(\sum_{ij} \tilde{C}_{\mu i}^{T(1,1)} C_{j\mu}^{T(1,1)} - 1 \right) \end{aligned} \tag{1.48}$$

It is important to note that the type-A amplitudes as stated in equation (1.48) is different from the type-A amplitudes of equation (1.46) due to the coupling of the type-A and type-B amplitudes in the singlet sector and also due to the difference of the effective Hamiltonian of the type-A and type-B respectively.

In this thesis we will be using only the singlet Λ vectors for construction of the excited state wave function to evaluate transition dipole moments.

1.7 Objective of this thesis

The main objective is to develop methods within FSMRCC formulation to calculate transition dipole moments. We will be using the exponential ansatz of the FSCC and the Λ-vectors, as described in this chapter to construct the different wave

functions and calculate the relevant off diagonal matrix elements of the dipole operator to finally evaluate the transition moments. All method developments will be presented under the singles and doubles scheme within FSMRCC. New approximate approaches will also be developed that can facilitate calculation of larger molecular systems for difference energies as well as properties arising from the difference energy calculations. The thesis is concluded with the future scope and certain ongoing projects associated with the work presented in this thesis.

References

[1] P. O. Lowdin, Int. J. Quantum Chem. **2**, 867 (1968)

[2] P. O. Löwdin, Adv. Chem. Phys. **2**, 207 (1958)

[3] O. Sinanoglu and I. Oksuz, Phys. Rev. **181**, 42 (1969)

[4] I. Shavitt and R. J. Bartlett, in Many body methods in chemistry and physics: MBPT and coupled cluster theory: Cambridge University Press, (2009)

[5] O. Sinanoglu and P. Westhaus, Phys. Rev. **183**, 56 (1969)

[6] A. Szabo and N. S. Ostlund, Modern Quantum Chemistry, (McGraw-Hill, New York, 1989)

[7] W. A. Goddard III, Phys. Rev. **157**, 73 (1967)

[8] I. Shavitt; in Methods in Electronic Structure Theory, edited by H. F. Schaefer III, (Plenum, New York, 1977), p 189

[9] J. Karwowski; in Methods in Computational Molecular Physics, NATO ASI Series B: Physics, Vol. **293**, edited by S.Wilson and G. H. F. Dierksen, (Plenum, New York, 1992), p 65

[10] S. Raimes; Many-Electron Theory, (North-Holland, Amsterdam, 1972).

[11] R. Manne; Int. J. Quant. Chem. **S11**, 175 (1977).

[12] I. Lindgren, J. Morrison; Atomic Many-Body Theory, (Springer-Verlag,

[13] Berlin, 1982)

[14] M. Urban, I. Huba˘c, V. Kell¨o, J. Noga; J. Chem. Phys. **72**, 3378 (1980)

[15] (a) J. Cizek, J. Chem. Phys. **45**, 4256 (1966). (b) ibid. Adv. Quant. Chem.**14**, 35 (1969).

[16] (a) R. J. Bartlett; J. Chem. Phys. **93**, 1697 (1989). (b) ibid. in "Modern Electronic Structure Theory, Part II", Advanced Series in Physical Chemistry - Vol. 2, edited by D. R. Yarkony, (World Scientific, Singapore, 1995), p 1047.

[17] J. Noga, R.J. Bartlett; J. Chem. Phys. **86**, 7041 (1987).

[18] G.W. Trucks, J. Noga, R. J. Bartlett; Chem. Phys. Lett. **145**, 548 (1988).

[19] J. Noga, P. Valiron; Chem. Phys. Lett. **324**, 166 (2000).

[20] P. Knowles, M. Schutz, and H. J. Werner in Modern Methods and Algorithms of Quantum Chemistry, Proceedings, Second Edition, Edited by J. Grotendorst, (Neumann Institute of Computing Series, Volume **3**, Julich, 2000)

[21] L. Adamowicz, J. P. Malrieu; in Multi-Reference Self-Consistant Size-Extensive Con_guration Interaction (CI) - A Bridge Between The Coupled-

Cluster Method And The CI Method., Recent Advances in Computational Chemistry - Vol. **3**: .Recent Advances in Coupled cluster methods., edited by R.J. Bartlett (World Scienti_c, Singapore, 1997), p 307

[22] K. Andersson, B. O. Roos; in .Modern Electronic Structure Theory, Part I., *Advanced Series in Physical Chemistry* - Vol. **2**, edited by D. R. Yarkony, (World Scienti_c, Singapore, 1995), p 55.

[23] B. O. Roos, K. Anderson, M. P. Fulscher, P. A. Malmqvist, L. S. Andres, K. Pierloot, M. Merchan; Adv. Chem. Phys. **93** (1996)

[24] H. Nakano, N. Otsuka, K. Hirao; in .Analytic energy gradients for second-order multireference perturbation theory. Recent Advances in Computational Chemistry - Vol. **4**: .Recent Advances in Multireference methods., edited by K. Hirao (World Scientific, Singapore, 1999), p 131.

[25] M. R. Hoffmann; in .Modern Electronic Structure Theory, Part II., Advanced Series in Physical Chemistry - Vol. **2**, edited by D. R. Yarkony, (World Scientific, Singapore, 1995), p 1166

[26] H. Nakano, J. Nakatani, K. Hirao; J. Chem. Phys. **114** (2001) 1133

[27] J. Paldus, in Methods in Computational Molecular Physics, NATO ASI Series B Vol. **293**, edited by S. Wilson and G. H. F. Dierckson (Plenum, New York, 1992).

[28] D. Mukherjee, Pramana **12**, 203 (1979)

[29] D. Mukherjee and I. Lindgren, Phys. Rep. **151**, 93 (1987).

[30] D. Mukherjee and S. Pal, Adv. Quantum Chem. **20**, 291 (1989).

[31] B. Jezioroski and H. J. Monkhorst, Phys. Rev. A **24**, 1668 (1981)

[32] F. A. Evangelista, W. D. Allen, H.F. Schaefer III; *J. Chem. Phys.* **125** 154113 (2006)

[33] L. Horny, H.F. Schaefer III, I. Hubac, S. Pal; Chem. Phys. **315,** 240 (2005)

[34] D. Mukhopadhyay, B. Datta, D. Mukherjee; Chem. Phys. Lett. **197,** 236 (1992)

[35] U.S. Mahapatra, B. Datta, D. Mukherjee; in .A State-Speci_c Multi-Reference Coupled Cluster Approach for Treating Quasi-Degeneracy., Recent Advances in Computational Chemistry - Vol. **3**: .Recent Advances in Coupled-cluster methods; edited by R.J. Bartlett (World Scienti_c, Singapore, 1997), p 155

[36] U.S. Mahapatra, B. Datta, B. Bandopadhyay, D. Mukherjee; Adv. Quant. Chem. **30,** 163 (1998)

[37] P. Durand, J. P. Malrieu, Adv. Chem. Phys. **67**, 321 (1987)

[38] N. Vaval, K. B. Ghose, S. Pal and D.Mukherjee, Chem. Phys. Lett. **209**, 292-298 (1993)

[39] S. Pal, M. Rittby, R. J. Bartlett, D. Sinha, and D. Mukherjee, J. Chem. Phys.**, 88**, 4357 (1988)

[40] U. Kaldor and A. Haque, Chem. Phys. Lett. **128**, 45 (1986)

[41] N. Vaval, S. Pal, D. Mukherjee, Theor. Chem. Acc. **99**, 100 (1998)

[42] M. Nooijen and R. J. Bartlett, J. Chem. Phys. **102**, 3629 (1995)

[43] H. Sekino and R. J. Bartlett, Int. J. Quantum Chem. **26**, 255 (1984)

[44] A. I. Krylov, Chem. Phys. Lett. **338**, 375 (2001)

[45] J. F. Stanton and R. J. Bartlett, J. Chem. Phys. **98**, 7029 (1993)

[46] K. Kowalski and P. Piecuch, J. Chem. Phys. **115**, 643 (2001)

[47] J. F. Stanton and J. Gauss, J. Chem. Phys. **101**, 8938 (1994)

[48] S. V. Levchenko, T. Wang and A. I. Krylov, J. Chem. Phys. **122**, 224106 (2005)

[49] J. F. Stanton, J. Chem. Phys. **99**, 8840 (1993)

[50] M. Kállay and J. Gauss, J. Chem. Phys. **121**, 9257 (2004)

[51] D. R. Hartree; Math. Proc. Cambridge Phil. Soc. **24**, 89, (1928).

[52] V. Fock; Zeitschrift fur. Physik **61**, 126 (1930).

[53] J. C. Slater; Phys. Rev. **35**, 210 (1930)

[54] (a) C. C. J. Roothan; Rev. Mod. Phys. **23**, 69 (1951). (b) ibid. **32**, 179 (1960)

[55] J. A. Pople, J. S. Binkley and R. Seeger; Int. J. Quant. Chem. Symp. **10**, 1 (1976).

[56] R. J. Bartlett; Annu. Rev. Phys. Chem. **32**, 359 (1981).

[57] R. Chaudhary, D. Mukherjee and M. D. Prasad, Lecture notes in chemistry, **50**, 3 (1950)

[58] H. Primas, Modern quantum chemistry: Action of light and organic crystals; Academic Press, vol - **2**, (1965)

[59] O. Sinanoglu, J. Chem. Phys. **36**, 706 (1962)

[60] M. Urban, V. Kello, and G. H. F. Diercksen, J. Mol. Struct.: THEOCHEM **219**, 547 (2001)

[61] F. E. Harris, H. J.Monkhorst and D. L. Freeman; Algebraic and Diagrammatic Methods in Many-Fermion Theory Oxford Press, New York, 1992

[62] S. A. Kucharski and R. J. Bartlett Adv. Quant. Chem. **18**, 281 (1986)

[63] J. Goldstone; Proc. Roy. Soc. London Ser. A **239**, 267 (1957)

[64] H. P. Kelly; Phys.Rev. **131**, 684 (1963)

[65] O. Sinanoglu, Adv. Chem. Phys. **6**, 315 (1964)

[66] R. K. Nesbet; Adv. Chem. Phys. **9**, 321 (1965)

[67] J. Cizek, Adv. Quantum Chem. **14**, 35 (1969);

[68] J. Cizek , J. Chem. Phys. **45**, 4256 (1966);

[69] J. Cizek and J. Paldus, Int. J. Quantum Chem. **5**, 359 (1971)

[70] J. Paldus, in Methods in Computational Molecular Physics, Edited by S. Wilson and G. H. F. Dierksen, (NATO ASI Series B: Physics, Volume **293**, Plenum, New York, 1992), p 99

[71] R. J. Bartlett, G. D. Purvis III, Int. J. Quant. Chem. **14,** 561(1978)

[72] J. A. Pople, R. Krishnan, H. B. Schlegel, J. S. Binkley, Int. J. Quant. Chem. **14** (1978) 546

[73] R. Krishnan, G. W. Trucks, J. A. Pople and M. Head-Gordon, Chem. Phys. Lett. **157**, 479 (1989)

[74] S. A. Kucharski, R. J. Bartlett, J. Chem. Phys. **97** (1992) 4282

[75] M. Nooijen and R. J. Bartlett, J. Chem. Phys. **102**, 3629 (1995)

[76] M. Nooijen and R. J. Bartlett, J. Chem. Phys. **102**, 6735 (1995)

[77] J. F. Stanton and J. Gauss, J. Chem. Phys. **101**, 8938 (1994)

[78] J. F. Stanton and R. J. Bartlett, J. Chem. Phys. **98**, 7029 (1993)

[79] A. Balkova, S. A. Kucharski, L. Meissner, R.J. Bartlett, J. Chem. Phys. **95**, 4311 (1991)

[80] A. Balkova and R. J. Bartlett, J. Chem. Phys. **101**, 8972 (1994)

[81] S. Pal, Mol. Phys. **108**, 3033 (2010)

[82] D. Mukherjee, S. Pal, Adv. Quantum Chem. **20**, 291 (1989)

[83] D. Mukherjee, R. K. Moitre, A. Mukhopadhyay, Mol. Phys. **30**, 1861 (1975)

[84] S. Pal, M. Rittby, R.J. Bartlett, D. Sinha, D. Mukherjee, J. Chem. Phys. **88**, 4357 (1988)

[85] D.Mukherjee Int. J. Quantum Chem. **30**, 409 (1986)

[86] P. Szalay, Int. J. Quantum Chem. **55**, 151 (1995).

[87] K. R. Shamasundar, S. Asokan, and S. Pal, J. Chem. Phys. **120**, 6381 (2004).

[88] K. R. Shamasundar and S. Pal, J. Chem. Phys. **114**, 1981 (2001); **115**, 1979 (2001).

[89] P. U. Manohar, N. Vaval, and S. Pal, J. Mol. Struct.: THEOCHEM **768**, 91 (2006); P. U. Manohar and S. Pal, Chem. Phys. Lett. **438**, 321 (2007).

[90] P. U. Manohar and S. Pal, AIP Conf. Proc. **963**, 337 (2007).

[91] A. Bag, P. U. Manohar, and S. Pal, Comput. Lett. **3**, 351 (2007).

[92] A. Bag, P. U. Manohar, N. Vaval, and S. Pal, J. Chem. Phys. **131**, 024102 (2009).

Chapter 2

Formulation of transition dipole moment within Fock-space multi-reference coupled cluster theory

---

This chapter introduces the formulation of transition moment within FSMRCC methodology. We present two different ways, to calculate these transition moments. In the first method, we construct the ground and excited state wave functions with the normal exponential ansatz of Fock-space coupled cluster method and then calculate the relevant off-diagonal matrix elements. This is called the expectation value method. In the second approach, we linearize the exponential form of the wave operator which will generate the left vector, by use of Lagrangian formulation. The right vector is still obtained from the exponential ansatz. This is identified as the bi-orthogonal approach. The given formulation is general in nature and can be extended to evaluate transition moments for ground/excited to excited states of closed, as well as open shell systems.

In order to relate transition moments to oscillator strengths, excitation energies have to be evaluated. The excitation energies are obtained from the Fock-space multi-reference coupled cluster theory as discussed in the previous chapter. A brief review of the FSMRCC wave equations is also presented in this chapter.

2.1 Introduction to transition dipole moment

Transition dipole moments (TDM) are of great general interest as they determine the transition rates (along with the rotational-vibrational levels to calculate Einstein transition probabilities) [1] and the probability of photon or electric field induced atomic and molecular state changes. It is a good test for assessing the validity and accuracy of *ab-initio* calculations. A calculation of transition dipole moment can be helpful in understanding the energy transfer rates; provides a basis for calculating extinction coefficients and fluorescence lifetimes etc. [2,3] The electronic transition dipole moment (ETDM) is an important prerequisite for understanding optical spectra. The probabilities per unit time for absorption induced emissions and spontaneous emissions (as derived from the first order, time-dependent perturbation theory in the dipole length approximation) are proportional to the square of the TDM between the two chosen states of interest. [4] For any transition from a state '*p*' to state '*q*', the TDM in the dipole length form is expressed as –

$$d_{pq} = \left\langle \psi_p \middle| \mu \middle| \psi_q \right\rangle \tag{2.1}$$

In order to understand and characterize radiative processes, we have to relate it to experimental observables (such as oscillator strength). The oscillator strength in the dipole length approximation is given by, [5]

$$f_{pq} = \frac{2}{3} \Delta E \left| d_{pq} \right|^2 \quad \text{where } \Delta E = E_q - E_p \tag{2.2}$$

Given the importance of transition moments, computing them and relating them to experimental observables is not very straightforward. This is due to the sensitivity of d_{pq} towards the quality of the wave function. [6] As stated previously, the calculation of TDM represents a different test altogether for any *ab-initio* method as there can be considerable redistribution of charge in a molecular situation without substantial change in the energy. Hence, calculation of TDM demands an accurate description of the wave function.

Single reference coupled cluster theory [7-10] is known to accurately describe the ground state wavefunction. However, it has been realized that a high level of correlated wave function is necessary for an adequate description of the excited states.

Multi-reference coupled cluster (MRCC) [11-23] theory, in the Fock-space version, has been known to be an accurate method of choice in that, it includes a combination of dynamic and static correlation arising from the multi-configurational nature of reference space. Using restricted Hartree Fock determinant of ground closed shell as vacuum, a suitable one particle–one hole (*1,1* sector) determinant set, constructed within an active set of holes and particles, serves as a suitable reference space for low-lying excited states.

A Fock-space coupled cluster (FSCC) [11-20] theory using such a reference has been well developed for excitation energies. Though in principle, the theory provides the excited state wave function, its use in the calculation of transition dipole moment has been scarce, mainly because of the description of the conjugate (left) vector of not just the ground state but also the excited state. Once the wave functions have been constructed, it is straightforward to generate the one-electron dipole induced matrix elements.

2.2. Previous and present developmental highlights

Calculation of excitation energies and electronic transition moments in multi-configuration linear response (MCLR) was done by Olsen *et al*. [24] Within the EOMCC formalism, Stanton and Bartlett [25] presented an idea to calculate the transition probabilities via a systematic bi-orthogonal approach. Size intensive transition moments from the coupled cluster singles and doubles linear response (CCSDLR) function was formulated by Jørgensen and co-workers. [26] A detailed description to calculate expectation values and transition elements by coupled cluster theory in general, was presented by Prasad. [27] Integral-direct frequency dependent polarizabilities and transition probabilities in the CC framework were implemented by Christiansen *et al*. [28] In the CC2 model, transition moments were computed using the resolution-of-the-identity approximation by Hättig and Köhn. [29] Later on Köhn and Pabst [30] implemented transition moments between excited states using the RI-CC2 approximation. In an early work by Stolarczyk and Monkhorst, [31] derivation of expectation value and transition moment was formulated within the generalized CC framework. The main idea was to define a new operator $\hat{W}$ and calculate the matrix elements of that operator. For an arbitrary n-particle operator- $\hat{V}$, the transition

moment was expressed as $V_X^Y = \left\langle \Psi^X \middle| \hat{V} \Psi^Y \right\rangle$ for $X \neq Y$. In order to calculate the transition moment, one had to know the operator- $\hat{W} = \hat{\Omega}^{-1} \hat{V} \hat{\Omega}$. Barysz *et al* [32,33] implemented the above mentioned scheme of Stolarczyk and Monkhorst in the FSCC framework to obtain the electronic transition moments and oscillator strength of certain molecules. They used the CCSD approximation and truncated the $\hat{W}$ operator at the quadratic level.

In this chapter, we formulate the electronic transition moment of the dipole operator between the ground or low lying excited states to a few other low lying excited states of some molecules in two different ways. We start by the initial formula of transition moment where the n-particle operator- $\hat{V}$, is chosen as the one-particle dipole moment operator. Instead of redefining another operator- $\hat{W}$, we calculate the expectation value of the dipole moment operator between the ground and the excited state wave functions. Hence, only $T^{(0,0)}$ amplitudes are sufficient to describe the ground state. The excited state is generated by the Fock-space exponential ansatz. In case of calculating TDM from excited to excited states, both the left and right Eigen states are described by the exponential ansatz. Thus, this method uses a straightforward conjugate of the ground and excited states and is called FSCC-T. In the other method, we take recourse to the constrained variation approach, where the matrix element is computed using a biorthogonal methodology. This involves solving an extra set of de-excitation Λ-amplitudes to describe the ground state and all other higher sector Λ-amplitudes to describe the excited state. This is abbreviated as FSCC-Λ.

2.3 Theory

2.3.1 Brief review of FSMRCC

The Fock-space method in the CC framework is well described and accounted for evaluation of ionization potential, electron affinity and excitation energies. [15,16] A brief review is presented here followed by the description of the transition moments within the same.

The basic assumption in the FSCC method is that of a common vacuum. The vacuum is commonly chosen to be the restricted Hartree-Fock solution of the N-electron state. Particles and holes are defined with respect to this vacuum. There is a further sub-division of the particles and holes into active and inactive particles and holes. The various sectors in Fock space are a representation of this active space. In general the number of active holes and particles are represented by the superscript of the wave function. A general model space consisting of '*p*' active particles and '*h*' active holes is given by –

$$\left|\Psi_{(0)\mu}^{(p,h)}\right\rangle = \sum_i C_{\mu i}^{(p,h)} \left|\Phi_i^{(p,h)}\right\rangle \tag{2.3}$$

where, $C_{\mu i}^{(p,h)}$ are the combination or model space coefficients of Φ_i. The correlated wave function for a particular μ^{th} state is given by,

$$\left|\Psi_{\mu}^{(p,h)}\right\rangle = \Omega \left|\Psi_{(0)\mu}^{(p,h)}\right\rangle \tag{2.4}$$

In the above equation - Ω is the universal wave operator. The universal wave operator will be generating states by its action on the reference wave function. Ω has the specific form

$$\Omega = \left\{ e^{S^{(p,h)}} \right\} \tag{2.5}$$

$$\text{where,} \quad S^{(p,h)} = \sum_{k=0}^{p} \sum_{l=0}^{h} T^{(k,l)} \quad \text{and} \quad T^{(k,l)} = T_1^{(k,l)} + T_2^{(k,l)} + T_3^{(k,l)} + \ldots \tag{2.6}$$

The superscript *(k,l)* denotes the exact number of '*k*' active particles and '*l*' active holes that can be annihilated in addition to creation of holes and particles. The curly braces in equation (2.5), denotes normal ordering of the wave operator with respect to the vacuum or reference state and '*T*' represents the cluster amplitude. The Schrödinger equation for quasi-degenerate states in the Fock-space formalism is given by,

$$H\left|\Psi_{\mu}^{(p,h)}\right\rangle = E_{\mu}\left|\Psi_{\mu}^{(p,h)}\right\rangle \tag{2.7}$$

On substituting the above equation with equations 2.3 and 2.4 gives,

$$H\Omega\left(\sum_i C_{\mu i}^{(p,h)}\left|\Phi_i^{(p,h)}\right\rangle\right)=E_\mu\Omega\left(\sum_i C_{\mu i}^{(p,h)}\left|\Phi_i^{(p,h)}\right\rangle\right) \tag{2.8}$$

The states generated by the action of the universal wave operator on the reference space are such that they satisfy the Bloch equations. With the help of the projection operator $P^{(k,l)}$ and $Q^{(k,l)}$

$$P^{(k,l)}=\sum_i\left|\phi_i^{(k,l)}\right\rangle\left\langle\phi_i^{(k,l)}\right|, \qquad Q^{(k,l)}=1-P^{(k,l)} \qquad \forall k=0,p \text{ and } \forall l=0,h \tag{2.9}$$

which projects onto the model space of *p*-active particles, *h*-active holes and its orthogonal complement respectively, an effective Hamiltonian is defined through the Bloch equations [34] as,

$$\begin{aligned} P^{(k,l)}(H\Omega-\Omega H_{eff}^{(k,l)})P^{(k,l)}=0 \\ Q^{(k,l)}(H\Omega-\Omega H_{eff}^{(k,l)})P^{(k,l)}=0 \end{aligned} \quad \text{for all } k=0,p \text{ and } l=0,q \tag{2.10}$$

Solving the above mentioned Bloch equations leads to a connected set of equations for each sector. The normal ordered wave operator ensures that contraction between different cluster operators in the exponential ansatz is avoided which leads to a partial decoupling of the various sector cluster equations. Higher sector amplitudes do not enter in the equations of lower sectors, due to the lack of contraction between the *T*-operators. Thus the equations 2.10 are solved starting from the lowest sector progressively upwards. This is known as subsystem embedding condition. [14] Diagonalizing the effective Hamiltonian within the *P*-space gives the energies of the corresponding states and the corresponding left and right eigenvectors $\tilde{C},C$ respectively.

$$H_{eff}C=CE,\ \tilde{C}H_{eff}=E\tilde{C} \text{ and } \tilde{C}C=C\tilde{C}=1 \tag{2.11}$$

2.3.2 Electronic Transition Moment and Dipole Strength

Generally, for any arbitrary Hermitian operator $\hat{O}$, the term

$$\hat{O}_M^N=\left\langle\Psi_M\left|\hat{O}\right|\Psi_N\right\rangle\Big/\left(\left\langle\Psi_M\middle|\Psi_M\right\rangle\left\langle\Psi_N\middle|\Psi_N\right\rangle\right)^{1/2} \tag{2.12}$$

is the expectation value of the operator $\hat{O}$ in the state Ψ_M, when $M=N$ and the

transition moment for the states Ψ_M and Ψ_N,when $M \neq N$. In FSCC methodology, the states Ψ_M and Ψ_N are the ortho-normal Eigen states of the effective Hamiltonian $\left(H_{eff}\right)$ which are defined through the Bloch equations (refer equation 2.10). Due to the non-Hermitian nature of H_{eff}, the transition moments are defined as the geometric mean of $\hat{O}_M^N$ and $\hat{O}_N^M$ as,

$$d_{MN} = \sqrt{\hat{O}_M^N \hat{O}_N^M} \tag{2.13}$$

where, $\hat{O}_M^N$ and $\hat{O}_N^M$ are referred to as 'left' and 'right' transition moments respectively. Replacing the arbitrary operator $\hat{O}$, with the one-electron dipole operator $\hat{\mu}$ in equation (2.12), the square of the transition dipole moment is defined as,

$$\left|d_{MN}\right|^2 = \frac{\left\langle \Psi_M \left|\hat{\mu}\right| \Psi_N \right\rangle \left\langle \Psi_N \left|\hat{\mu}\right| \Psi_M \right\rangle}{\left\langle \Psi_M \middle| \Psi_M \right\rangle \left\langle \Psi_N \middle| \Psi_N \right\rangle} \tag{2.14}$$

The dipole length oscillator strength is calculated from the following expression [5] -

$$f_{MN} = \frac{2}{3} \Delta E \left|d_{MN}\right|^2 \qquad \text{where, } \Delta E = E_N - E_M \tag{2.15}$$

Since, it is the square of the transition dipole moment absolute value that is related to the experimental observable, we will formulate and tabulate $\left|d_{MN}\right|^2$, which is commonly known as the dipole strength.

2.4 Dipole strength for ground to excited states of closed shell systems

Since we are now specifically defining our initial and final states to be a closed shell ground state and its corresponding low lying excited state respectively, the Ψ_M and Ψ_N states (as mentioned in the previous section) are defined as

$$\begin{aligned} \left|\Psi_M\right\rangle &= \left|\Psi_{gr}\right\rangle = \Omega_{gr} \left|\Psi_{HF}\right\rangle \\ \left|\Psi_N\right\rangle &= \left|\Psi_{ex}\right\rangle = \Omega_{ex} \left|\Psi_{N(0)}^{(1,1)}\right\rangle \end{aligned} \tag{2.16}$$

$$\text{where, } \Omega_{gr} = \exp\left(T^{(0,0)}\right) \text{ , } \Omega_{ex} = \exp\left\{T^{(0,0)} + T^{(0,1)} + T^{(1,0)} + T^{(1,1)}\right\} \tag{2.17}$$

The curly braces in the above equation denote normal ordering of the wave operator with respect to the reference state. The reference state mentioned in equation (2.16) is the restricted Hartree-Fock determinant and the model space wave function is given by

$$\left|\Psi_{N(0)}^{(1,1)}\right\rangle = \sum_i C_{Ni}^{(1,1)} \left|\phi_i^{(1,1)}\right\rangle \tag{2.18}$$

The next subsection will depict the relevant working equations for evaluation of dipole strength in the previously mentioned FSCC-T and FSCC-Λ methods. The formulation and representation of the conjugate (left) ground and excited states differentiate the FSCC-T and FSCC-Λ methods from each other. The right Eigen states in both the methods are constructed according to equation (2.16).

2.4.1. The expectation value method (FSCC-T)

In the expectation value approach the left conjugate states are constructed as the simple Hermitian conjugate of the right Eigen states. The linked cluster theorem holds true in this case and hence size consistency prevails [27]. This implies that the denominator, as shown in equation (2.14), cancels out the disconnected part of the numerator leaving behind only the connected part of the numerator. Thus, the expression for evaluating the square of transition dipole moment becomes,

$$\left|d_{MN}\right|^2 = \left\langle \Psi_M \left|\hat{\mu}\right| \Psi_N \right\rangle_C \left\langle \Psi_N \left|\hat{\mu}\right| \Psi_M \right\rangle_C \tag{2.19}$$

where the symbol '*C*' denotes a linked structure.

The conjugate ground state wave function in this FSCC-T formulation is expressed as,

$$\left\langle \Psi_M \right| = \left\langle \Psi_{HF} \left| \Omega_{gr}^{\dagger} \right.\right. \tag{2.20}$$

where the wave operator $\Omega_{gr}^{\dagger} = \exp(T^{\dagger(0,0)})$ acts on the Hartree Fock wave function to generate the left or conjugate ground state.

In a similar manner, the conjugate excited state wave function is given by,

$$\langle \Psi_N | = \sum_i \left\langle \phi_i^{(1,1)} \middle| \tilde{C}_{Ni}^{\dagger(1,1)} \Omega_{ex}^{\dagger} \right. \equiv \left\langle \Psi_{N(0)}^{(1,1)} \middle| \Omega_{ex}^{\dagger} \right. \tag{2.21}$$

where, $\Omega_{ex}^{\dagger} = \exp\left\{ T^{\dagger(0,0)} + T^{\dagger(0,1)} + T^{\dagger(1,0)} + T^{\dagger(1,1)} \right\}$ is the Hermitian conjugate of the normal wave operator Ω_{ex} and $\tilde{C}_{Ni}^{\dagger(1,1)}$ is the conjugate left Eigen vector of the effective Hamiltonian of the (*1,1*) sector. The conjugate wave operator $\Omega_{ex}^{\dagger}$ follows the same normal ordering as the normal cluster wave operator. The right ground and excited state wave functions are expressed in the normal exponential ansatz of FSCC theory as described in the previous subsection. Both the left and right transition moments are generated through connected diagrams arising from the contraction of $\Omega^{\dagger} \hat{\mu} \Omega$ terms giving rise to an overall linked structure. However, solving for the dipole strengths in this expectation value FSCC methodology, generates a non-terminating series, thus requiring a forced truncation. The final expression for dipole strength in the expectation value approach is,

$$|d_{MN}|^2 = \langle \Psi_{HF} | \left(\Omega_{gr}^{\dagger} \hat{\mu} \Omega_{ex} \right)_c \left| \Psi_{N(0)}^{(1,1)} \right\rangle \left\langle \Psi_{N(0)}^{(1,1)} \right| \left(\Omega_{ex}^{\dagger} \hat{\mu} \Omega_{gr} \right)_c | \Psi_{HF} \rangle \tag{2.22}$$

where $\left(\Omega_{gr}^{\dagger} \hat{\mu} \Omega_{ex} \right)_c$ and $\left(\Omega_{ex}^{\dagger} \hat{\mu} \Omega_{gr} \right)_c$ signifies that only connected terms arising from the contraction of the $T^{\dagger}$ and T-amplitudes through the one electron dipole operator is taken into consideration. Details of the actual implementation are given in the following chapter.

2.4.2 The bi-orthogonal formulation (FSCC-Λ)

This bi-orthogonal approach of evaluating dipole strength is based on the concept of linearizing the left vector through a linear superposition of the hole-particle states [27,35]. In this formalism, the ground state wave function for the quantity $\hat{O}_M^N$ is defined as follows,

$$\langle \Psi_M | = \langle \Psi_{HF} | \left(1 + \Lambda^{(0,0)} \right) \Omega_{gr}^{-1} \ , \qquad \Omega_{gr}^{-1} = \exp(-T^{(0,0)}) \tag{2.23}$$

and the conjugate excited state for $\hat{O}_N^M$ expressed as

$$\langle \Psi_N | = \sum_i \langle \phi_i^{(1,1)} | \tilde{C}_{Ni}^{(1,1)} \left(1+\tilde{\Lambda}\right)\Omega_{ex}^{-1} \tag{2.24}$$

$$\equiv \langle \Psi_{N(0)}^{(1,1)} | \left(1+\tilde{\Lambda}\right)\Omega_{ex}^{-1}$$

where, $\tilde{\Lambda} = \Lambda^{(0,0)} + \Lambda^{(0,1)} + \Lambda^{(1,0)} + \Lambda^{(1,1)}$ and $\Omega_{ex}^{-1} = \left\{ e^{-T(1,1)} e^{-T(1,0)} e^{-T(0,1)} e^{-T(0,0)} \right\}$

A knowledge of $\Lambda^{(0,0)}$ amplitudes along with the $T^{(0,0)}$ amplitudes can describe the conjugate ground state completely. The $\Lambda^{(0,0)}$ amplitudes are obtained from the constrained variation approach (CVA) by solving the Lagrangian for the ground state. The CVA was first pursued by Jorgensen and co-workers [36] wherein, the advantage of z-vector technique [37] was automatically incorporated. The basic concept of CVA involves, construction of a new functional with Lagrange undetermined multipliers. In single reference coupled cluster framework, the functional can be written as,

$$\zeta = \langle \phi_0 | e^{-T} \hat{H} e^{T} | \phi_0 \rangle + \sum_{j \neq 0} \lambda_j \langle \phi_j | e^{-T} \hat{H} e^{T} | \phi_0 \rangle \tag{2.25}$$

The first term on the right hand side of the above equation is the expression for energy. The second term is the constraint for single reference CC. The Lagrange multipliers are optimized with the cluster equations as the constraint. Once the Lagrange equation is solved, the λ-amplitudes are obtained. Similarly, a constrained variation approach (CVA) within the FSCC methodology [38,39] is used to evaluate the various higher sector de-excitation Λ-amplitudes. After the generation of *T*-amplitudes up to the one hole-one particle sector, the Λ-amplitude equations are solved. These Λ-equations are also partially decoupled. However, the decoupling is reverse to that of the cluster amplitudes - *T*. The higher sector de-excitation operators are solved first. Once these are generated, they appear as constant entities while solving the Λ-amplitudes of the lower sectors [39]. Thus, the entire process of generating the excitation and de-excitation amplitudes is a time consuming one. However, the linearization of the conjugate left vector achieves a natural termination of the series. The right ground and excited states are constructed as shown in equation (2.16). It has been shown independently by Barysz *et al* [32,33] and Prasad [27] that the expression of $\hat{O}_M^N$ (as given in equation 2.12) contains only the connected part of the numerator and hence, the dipole strength expression can be written as,

$$
\begin{aligned}
\left|d_{MN}\right|^2 &= \left\langle \Psi_{HF} \middle| \left[\left(1+\Lambda^{(0,0)}\right) \Omega_{gr}^{-1} \hat{\mu} \Omega_{ex} \right]_C \middle| \Psi_{N(0)}^{(1,1)} \right\rangle \left\langle \Psi_{N(0)}^{(1,1)} \middle| \left[\left(1+\tilde{\Lambda}\right) \Omega_{ex}^{-1} \hat{\mu} \Omega_{gr} \right]_C \middle| \Psi_{HF} \right\rangle \\
&\equiv \left\langle \Psi_{HF} \middle| \left[(1+\Lambda) \bar{\mu} e^{\tilde{S}} \right]_C \middle| \Psi_{N(0)}^{(1,1)} \right\rangle \left\langle \Psi_{N(0)}^{(1,1)} \middle| \left[\left(1+\tilde{\Lambda}\right) e^{-\tilde{S}} \bar{\mu} \right]_C \middle| \Psi_{HF} \right\rangle
\end{aligned} \tag{2.26}
$$

Where, $e^{\tilde{S}} = \exp\left\{T^{(0,1)} + T^{(1,0)} + T^{(1,1)}\right\}$ and $e^{-\tilde{S}} = \exp\left\{-T^{(0,1)} - T^{(1,0)} - T^{(1,1)}\right\}$

Due to valence universality, all the cluster operators (*T*-operators) of Ω are linearly independent. Hence, $e^{-\tilde{S}}$ exists [13]. '$\bar{\mu}$', which is $e^{-T^{(0,0)}} \hat{\mu} e^{T^{(0,0)}}$, is connected due to Baker-Campbell-Hausdorff (BCH) expansion. The various possible $\bar{\mu}$ terms are stored separately and later contracted with the de-excitation Λ-amplitudes, to yield all possible linked diagrams.

2.5 Dipole strength for doublet radical systems

This section will highlight the working formulae for the specific case of doublet radical. In the Fock-space methodology the doublet radicals are expressed in either two ways, as a case of electron attachment i.e. (*1,0*) sector or a case of electron detachment i.e. (*0,1*) sector. Under these conditions of electron attachment or detachment even the ground state of the radical system under study has to be expressed in terms of a multi-determinantal reference as opposed to a single reference function of closed shell ground state. For a particular case of electron detachment the Ψ_M and Ψ_N states (as mentioned in sub-section 2.3.2) are defined as

$$
\begin{aligned}
\left|\Psi_M\right\rangle &= \Omega \left|\Psi_{M(0)}^{(0,1)}\right\rangle \\
\left|\Psi_N\right\rangle &= \Omega \left|\Psi_{N(0)}^{(0,1)}\right\rangle
\end{aligned} \tag{2.27}
$$

where, the wave operator Ω is given by,

$$
\Omega = \exp\left\{T^{(0,0)} + T^{(0,1)}\right\} \tag{2.28}
$$

and
$$
\begin{aligned}
\left|\Psi_{M(0)}^{(0,1)}\right\rangle &= \sum_i C_{Mi}^{(0,1)} \left|\phi_i^{(0,1)}\right\rangle \\
\left|\Psi_{N(0)}^{(0,1)}\right\rangle &= \sum_j C_{Nj}^{(0,1)} \left|\phi_j^{(0,1)}\right\rangle
\end{aligned} \tag{2.29}
$$

The curly braces in equation (2.28) denote normal ordering of the wave operator with respect to the reference function. Depending on the choice of *'M'* and *'N'* the ground

or excited states can be conveniently defined. Equation (2.29) shows that the basic defining structure for both the ground and excited states of such radical systems are the same. Similar to the previously discussed case of transition moments from ground to excited states of closed shell molecules, the next subsection will describe the relevant working equations for evaluation of dipole strength in FSCC-T and FSCC-Λ methods. The formulation and representation of the conjugate (left) ground and excited states differentiate the FSCC-T and FSCC-Λ methods from each other. The right Eigen states in both the methods are constructed according to equation (2.27).

2.5.1. The expectation value method (FSCC-T)

The basic concept of this approach is the same as that described in sub-section 2.4.1. The left Eigen states are defined and constructed as the conjugate of the right Eigen states. The linked cluster theorem holds true in this case also and we get a completely connected set of equations for evaluating transition moments.

The conjugate left Eigen states are expressed as,

$$\begin{aligned}\left\langle \Psi_N \right| &= \sum_j \left\langle \phi_j^{(0,1)} \right| \tilde{C}_{Nj}^{\dagger(0,1)} \Omega^\dagger \equiv \left\langle \Psi_{N(0)}^{(0,1)} \right| \Omega^\dagger \\ \left\langle \Psi_M \right| &= \sum_i \left\langle \phi_i^{(0,1)} \right| \tilde{C}_{Mi}^{\dagger(0,1)} \Omega^\dagger \equiv \left\langle \Psi_{M(0)}^{(0,1)} \right| \Omega^\dagger \end{aligned} \tag{2.30}$$

where, the wave operator is the conjugate of the normal wave operator given in equation (2.28) and can be represented as

$$\Omega^\dagger = \exp\left\{ T^{\dagger(0,0)} + T^{\dagger(0,1)} \right\} \tag{2.31}$$

It is interesting to note that depending on the particular choice of state, one might end up calculating transition moment from the ground state to excited state as well as excited to excited state with the same code. This is an attractive aspect of Fock-space wherein, solutions of multiple roots are possible in one attempt. The final expression for evaluating dipole strength is given by,

$$\left| d_{MN} \right|^2 = \left[\left\langle \Psi_{M(0)}^{(0,1)} \right| \left(\Omega^\dagger \hat{\mu} \Omega \right)_c \left| \Psi_{N(0)}^{(0,1)} \right\rangle \left\langle \Psi_{N(0)}^{(0,1)} \right| \left(\Omega^\dagger \hat{\mu} \Omega \right)_c \left| \Psi_{M(0)}^{(0,1)} \right\rangle \right] \tag{2.32}$$

where $\left(\Omega^{\dagger}\hat{\mu}\Omega\right)_c$ and $\left(\Omega^{\dagger}\hat{\mu}\Omega\right)_c$ signifies that only connected terms arising from the contraction of the $T^{\dagger}$ and T-amplitudes through the one electron dipole operator is taken into consideration.

2.5.2 The bi-orthogonal formulation (FSCC-Λ)

Similar to the FSCC-Λ method described in sub-section 2.4.2, the bi-orthogonal approach uses an extra set of de-excitation amplitudes to generate the energy functional given by,

$$\begin{aligned} F(t,\lambda) &= \left\langle \Phi_o \left| (1+\Lambda) e^{-T} H e^{T} \right| \Phi_0 \right\rangle \\ &= \left\langle \Phi_o \left| e^{-T} H e^{T} \right| \Phi_0 \right\rangle + \sum_{q\neq 0} \lambda_q \left\langle \Phi_q \left| e^{-T} H e^{T} \right| \Phi_0 \right\rangle \end{aligned} \tag{2.33}$$

where, $\lambda_q^{'}s$ are the de-excitation amplitude parameters of the conjugate ground state. To calculate the first order property, we replace the Hamiltonian in the above expression with its explicit first derivative and solve the above set of equations. It is worthwhile to point out, that we can arrive at the above set of equations by linearizing the left vector of the extended coupled cluster (ECC) [35,36] functional also. For the particular case of doublet radicals, the lambda amplitudes have to be solved for the ground state and any one of the (*0,1*) or (*1,0*) sector as per the choice of reference state. Reverse decoupling signifies that the higher sector amplitude equations will be solved first, followed by the ground state lambda amplitudes. The left Eigen states are now given by,

$$\begin{aligned} \left\langle \Psi_M \right| &= \sum_i \left\langle \phi^{(0,1)} \left| \tilde{C}_{Mi}^{(0,1)} \left(1+\tilde{\Lambda}\right)\Omega^{-1} \equiv \left\langle \Psi_{M(0)}^{(0,1)} \right| \left(1+\tilde{\Lambda}\right)\Omega^{-1} \right. \right. \\ \left\langle \Psi_N \right| &= \sum_j \left\langle \phi^{(0,1)} \left| \tilde{C}_{Nj}^{(0,1)} \left(1+\tilde{\Lambda}\right)\Omega^{-1} \equiv \left\langle \Psi_{N(0)}^{(0,1)} \right| \left(1+\tilde{\Lambda}\right)\Omega^{-1} \right. \right. \end{aligned} \tag{2.34}$$

where, $\tilde{\Lambda} = \Lambda^{(0,0)} + \Lambda^{(0,1)}$ and $\Omega^{-1} = \left\{ e^{-T(0,1)} e^{-T(0,0)} \right\}$ (2.35)

Ω^{-1} also follows the same normal ordering with respect to the reference states. The dipole strength can now be evaluated from the following expression-

$$\begin{aligned} \left| d_{MN} \right|^2 &= \left\langle \Psi_{M(0)}^{(0,1)} \right| \left[\left(1+\tilde{\Lambda}\right)\Omega^{-1}\hat{\mu}\Omega \right]_C \left| \Psi_{N(0)}^{(0,1)} \right\rangle \left\langle \Psi_{N(0)}^{(0,1)} \right| \left[\left(1+\tilde{\Lambda}\right)\Omega^{-1}\hat{\mu}\Omega \right]_C \left| \Psi_{M(0)}^{(0,1)} \right\rangle \\ &\equiv \left\langle \Psi_{M(0)}^{(0,1)} \right| \left[\left(1+\tilde{\Lambda}\right)\tilde{\mu} \right]_C \left| \Psi_{N(0)}^{(0,1)} \right\rangle \left\langle \Psi_{N(0)}^{(0,1)} \right| \left[\left(1+\tilde{\Lambda}\right)\tilde{\mu} \right]_C \left| \Psi_{M(0)}^{(0,1)} \right\rangle \end{aligned} \tag{2.36}$$

where, the subscript *'c'* depicts the connectedness of the above equations. The term $\tilde{\mu}$ also represents a completely connected part which is shown below.

$$\tilde{\mu} = e^{-S}\bar{\mu}e^{S} \equiv e^{-S}e^{-T^{(0,0)}}\mu e^{T^{(0,0)}}e^{S} \tag{2.37}$$

The *'S'* amplitude in the above equation is the cluster amplitude of the (0,1) sector. By making use of the Baker-Campbell-Hausdorff (BCH) formula for $e^{-B}Ae^{B}$, the dipole moment operator can be represented as, $\bar{\mu} = \left(\mu e^{T^{(0,0)}}\right)_C$ and hence, $\tilde{\mu}$ is also connected. In terms of practical coding, all possible $\bar{\mu}$ terms are constructed first and stored separately. They are then connected to the *S* amplitudes to finally give the connected form of $\tilde{\mu}$.

The structure of the above equation sets in section 2.5 will remain the same even for the case of electron attachment. The superscript (0,1) will just be replaced by (1,0) denoting the EA sector of FSMRCC. Once the amplitudes till the Fock-space sector in question are generated, the relevant off-diagonal matrix elements can be calculated from the final equations as given in the above sections to tabulate dipole strength.

References

[1] R. C. Hilborn, Am. J. Phys. **50**, 982 (1982)

[2] G. Scholes, Annu. Rev. Phys. Chem. **54**, 57 (2003)

[3] D. Toptygin, J. Fluores. **13**, 201 (2003)

[4] See, L. I. Schiff, Quantum Mechanics, 3rd ed. (McGraw-Hill, New York, 1968), Chaps. 11 and 14.

[5] H. Okabe, Photochemistry of Small Molecules (Wiley-Interscience, New York, 1978).

[6] R. Crossley, Phys. Scr. **T8**, 117 (1984).

[7] J. Cizek, Adv. Quant. Chem. **14**, 35 (1969)

[8] R. J. Bartlett, Annu. Rev. Phys. Chem. **32**, 359 (1981)

[9] J. Noga and R. J. Bartlett, J. Chem. Phys. **86**, 7041 (1987)

[10] R. J. Bartlett, J. Chem. Phys. **93**, 1697 (1989)

[11] W. Kutzelnigg, J. Chem. Phys. **77**, 3081 (1982)

[12] I. Lindgren, Int. J. Quantum Chem. **S 12**, 33 (1978)

[13] I. Lindgren, D. Mukherjee, Phys. Rep. **151**, 93 (1987)

[14] D. Mukherjee, Pramana **12**, 203 (1979)

[15] A. Haque, U. Kaldor, Chem. Phys. Lett. **117**, 347 (1985)

[16] S. Pal, M. Rittby, R.J. Bartlett, D. Sinha, D. Mukherjee, J. Chem. Phys. **88**, 4357 (1988)

[17] U. Kaldor, Theo. Chim. Acta. **80**, 427 (1991)

[18] D. Mukherjee, S. Pal, Adv. Quantum Chem. **20**, 291 (1989)

[19] D. Mukherjee, R. K. Moitre, A. Mukhopadhyay, Mol. Phys. **30**, 1861 (1975)

[20] S. Pal, Mol. Phys. **108**, 3033 (2010)

[21] B. Jeziorski, H. J. Monkhorst, Phys. Rev. A, **24**, 1668 (1981)

[22] A. Banerjee, J. Simons, Int. J. Quantum Chem. **19**, 207 (1981)

[23] A. Balkova, S. A. Kucharski, L. Meissner, R.J. Bartlett, J. Chem. Phys. **95**, 4311 (1991)

[24] J. Olsen, A.M. S. de Marás, H.J.A. Jensen and P. Jørgensen, Chem. Phys. Lett. **154**, 380 (1989)

[25] J.F. Stanton and R.J. Bartlett, J. Chem. Phys. **98**, 7029 (1993)

[26] H. Koch, R. Kobayashi, A.M.S. de Marás and P. Jørgensen, J. Chem. Phys. **100**, 4393 (1994)

[27] M. D. Prasad, Theo. Chim. Acta **88**, 383 (1994)

[28] O. Christiansen, A. Halkier, H. Koch, T. Helgaker and P. Jorgensen, J. Chem. Phys. **108**, 2801 (1998)

[29] C. Hättig and A. Köhn, J. Chem. Phys. **117**, 6939 (2002)

[30] M. Pabst and A. Kohn, J. Chem. Phys. **129**, 214101 (2008)

[31] L.Z. Stolarczyk and H.J. Monkhorst, Phys. Rev. A **37**, 3926 (1988)

[32] M. Barysz, M. Rittby and R.J. Bartlett, Chem. Phys. Lett **193**, 373 (1992)

[33] M. Barysz, Theo. Chim. Acta **90**, 257 (1995)

[34] H. J. Monkhorst, Int. J. Quantum Chem., Symp. **11**, 421 (1977); E. Dalgaard and H. J. Monkhorst, Phys. Rev. A **28**, 1217 (1983)

[35] E. A. Salter, G. W. Trucks, R.J. Bartlett, J. Chem. Phys. **90**, 1752 (1989)

[36] P. Jorgensen, T. Helgaker, J. Chem. Phys. **89**, 1560 (1988)

[37] N. C. Handy, H.F. Schaefer III, J. Chem. Phys. **81**, 5031 (1984)

[38] P. G. Szalay Int. J. Quantum Chem. **55**, 151 (1995)

[39] K. R. Shamasunder, S. Asokan, S. Pal, J. Chem. Phys. **120**, 6381 (2004)

[40] J. Arponen, Ann. Phys. (N.Y) **151**, 311 (1983); J. Arponen, R. F. Bishop and E. Pajanne, Phys. Rev. A. **36**, 2519 (1987); *ibid* 2539 (1987)

[41] R. F. Bishop, J. Arponen and E. Pajanne in Aspects of many-body effects in molecules and extended systems, Lecture notes in Chemistry, edited by D. Mukherjee (Springer-Verlag) **50**, 78 (1989); N. Vaval, K. B. Ghose and S. Pal, J. Chem. Phys. **101**, 4914 (1994)

Chapter 3

Transition dipole moment and oscillator strength for ground to excited states of closed shell molecules

---

Within the Fock-space multi-reference coupled cluster framework, we have evaluated the electronic transition dipole moments, which determine absorption intensities. These depend on matrix elements between two different wave functions (e.g. ground state to the excited state). The transition dipole moments from the closed shell ground state to a few excited states, together with the oscillator strengths of a few molecules, are presented. A new hybrid semi-bi-orthogonal method is formulated, compared and tested against the previously developed expectation value and bi-orthogonal approach for various molecular transitions. A check for size intensivity of transition dipole moments in the two methods are also performed and tabulated.

3.1 A semi-bi-orthogonal approach : FSCC-ΛT

The second chapter emphasized the basic concepts and relevant working equations involved in the expectation value and bi-orthogonal approaches for calculation of dipole strength. This chapter will tabulate the transition moment and oscillator strength of a few test molecules for the two methods described previously, i.e. singlet ground state to a few low lying singlet excited states. The first method mentioned above, involves a non-terminating series in the context of coupled cluster method, thus requiring a forced truncation. The second approach linearizes the conjugate states and hence is naturally terminating. However, this suffers from the fact that additional amplitudes have to be calculated. In the context of FSCC, this implies the evaluation of these amplitudes till the Fock-space sector in question, in this case, one particle-one hole sector. Thus, both the approaches have their merits and demerits.

In this present chapter, we also formulate a new semi-bi-orthogonal approach. This is a hybrid of the expectation value (FSCC-T) and the bi-orthogonal (FSCC-Λ) approaches and differ from the two in a manner the conjugate states are defined. The ground state left vector is defined in a bi-orthogonal approach while the conjugate excited wave function is described in the straightforward exponential ansatz. This makes the left transition moment a naturally terminating series while the right transition moment is not so. However, unlike FSCC-Λ, now the de-excitation amplitudes have to be evaluated only for the ground state wave function, which in FSCC nomenclature is the *(0,0)* sector. We abbreviate this semi-bi-orthogonal approach as the FSCC-ΛT method.

The term $\hat{O}_M^N$ (refer equation 2.13) is calculated from the FSCC-Λ formulation (left transition moment of equation 2.26), while the $\hat{O}_N^M$ term is calculated from the FSCC-T formulation (right transition moment of equation 2.22). Thus, the final expression of dipole strength is given by

$$\left|d_{MN}\right|^2 = \left\langle \Psi_{HF} \right| \left[\left(1+\Lambda^{(0,0)}\right) \bar{\mu} e^{\tilde{s}} \right]_C \left| \Psi_{N(0)}^{(1,1)} \right\rangle \left\langle \Psi_{N(0)}^{(1,1)} \right| \left(\Omega_{ex}^{\dagger} \hat{\mu} \Omega_{gr} \right)_c \left| \Psi_{HF} \right\rangle \tag{3.1}$$

This makes the left transition moment a naturally terminating series. Unlike the bi-orthogonal approach, this FSCC-ΛT method does not require solving the higher sector

Λ-amplitudes. Once the $\Lambda^{(0,0)}$ - amplitudes are generated, the dipole strengths can be easily calculated as the matrix elements of the dipole operator (as given in equation 3.1).

3.2 Computational Attributes

Generally, a large number of optically allowed transitions arising from the ground state to electronically excited states are singlet in nature. We have evaluated a few such optically allowed transitions and their oscillator strengths for a number of molecules. The Hartree-Fock determinant for the ground state is assumed to be the reference function, which is treated as a vacuum for the Fock-space calculations. The model space is formed by subsequent addition and/or removal of electrons to/from certain orbitals known as active orbitals. The various Fock-space sectors and model space is represented in the particle-hole formalism. An effective Hamiltonian is constructed whose diagonalization imparts the energies of the corresponding states. The excitation energies are obtained directly as the energy difference of the two states of choice. In the solution of Bloch equations, $\bar{H}$ is constructed as $\left(He^{T}\right)_{C}$. This $\bar{H}$ is then contracted with Fock-space cluster amplitudes. Within CCSD approximation, $\bar{H}$ is truncated up to three body terms. For the excited state wave function, we have chosen a set of single active particle-hole *(1,1)* determinant as the model space. We have used GAMESS-US [1] to obtain the two-electron integrals. During the entire set of calculations, we have not frozen any of the occupied or virtual core orbitals.

As stated in the previous chapter, there is a drawback of the expectation value formulation (FSCC-T). Equation (2.22) leads to a non-terminating series. For the practical application of evaluating transition dipole moments, we have truncated it at an overall cubic level with respect to the $T^{\dagger}$ and T amplitudes. Under the CCSD approximation, $T^{\dagger} = T_1^{\dagger} + T_2^{\dagger}$ where, $T_1^{\dagger}$ and $T_2^{\dagger}$ represent the conjugate of singles and doubles excitation operator respectively. The same approximation holds true for the normal Fock-space *T*-amplitudes. Once the amplitudes are generated, we calculate the transition dipole moments from the matrix elements as mentioned in (2.22). Similar truncation scheme is followed for the right transition moment of FSCC-ΛT method under singles and doubles approximation.

Excited states of all the molecules were treated at the equilibrium geometry. Hence, the transition moments are calculated under the Frank Condon principle of fixed nuclear co-ordinates. The calculated excitation energies (EE) are the vertical EE. These calculations scale as N^6. We have tested our method against various molecules/molecular ion like: methylidyne cation, water, formaldehyde, ammonia, and acetone. To test the accuracy of electronic transition dipole moments obtained from the FSCC-T approach mentioned earlier (see section 2.4.1), we chose the CH^+ molecular ion. A comparison between expectation value approach and bi-orthogonal approach is presented for the formaldehyde molecule. Assessment of the newly formulated FSCC-ΛT is made against FSCC-T and FSCC-Λ for the water molecule in cc-pVTZ and cc-pVQZ basis sets. Other calculations of transition moments and oscillator strengths in FSCC-T and FSCC-ΛT are presented for ammonia and acetone for a few optically allowed transitions.

A comparison of all the FSCC methods against EOMCC method is tabulated for some of the transitions. The EOMCC results were obtained from ACES-II [2] software package. Experimental results have been presented wherever available. In order to test the size-intensivity, we have studied the variation of transition moments from the FSCC-T and FSCC-Λ approaches for the water monomer, water dimer and water trimer at non-interacting distance. This is presented in a separate table in the following section.

3.3 Results and discussions

3.3.1 CH^+ Molecule

The CH^+ molecule was chosen as a test molecule because extensive results were available from other *ab-initio* calculations. The ground state electronic configuration of CH^+ is $1\sigma^2 2\sigma^2 3\sigma^2$ which is chosen as vacuum. There is a large non-dynamical correlation in the ground electronic state itself, arising from the interaction of $1\sigma^2 2\sigma^2 3\sigma^2$ and $1\sigma^2 2\sigma^2 1\pi^2$ electronic configurations. Due to this configuration mixing, some of the low lying states will have appreciable double excitation character. Reference [3] lists the approximate excitation levels (AEL) for some of the low-lying states of CH^+. It was shown, that the state with the excitation energy close to 3.2 eV is dominated by single hole-particle excited determinants within a set of

active orbitals- 3σ and 1π. We report transition moment for this particular transition and some other excited states dominated by the single hole-particle excitation.

In the present calculation, the inter-nuclear distance was taken to be 2.13713a.u. The calculations were performed with the basis set as given in the reference [3]. We chose this particular basis because full configurational-interaction (FCI) and other theoretical results were available for this basis. A split valence basis, augmented with two diffuse *s* and *p* functions and one *d* polarization function was used for the carbon atom. The hydrogen atom was augmented with one diffuse 's' function and one 'p' polarization function. Table 3.1 presents the transition energies, electronic transition dipole moment, dipole strength and the oscillator strength of CH^+ molecule in the basis mentioned above.

On comparing the reported values in Table 3.1, we find that the transition moment, transition energy and hence the oscillator strength values (within the given basis) as obtained from FSCC-T method are close to the FCI results. The Fock-space active space that we have chosen is **4σ 2π**. We have also reported FSMRCC results- as calculated and tabulated by Barysz, [4] following the formulation of Stolarczyk and Monkhorst [5] for the 3σ to 1π transition.

A comparison with the EOMCC method has been made for the transitions arising from 3σ to 4σ and 3σ to 5σ. FSCC-T transition moment agrees well with the EOMCC transition moment for the higher excitations as well. The EOMCC result reported for these transitions has been obtained from ACES-II [2] package. Transition dipole moments have also been reported for transitions arising from the 3σ to 6σ state.

Table 3.1: Transition energies, transition moments, dipole strengths and oscillator strengths of CH^+ molecule from its ground state to a few excited states are tabulated. EE stands for excitation energy. TDM is transition dipole moments, DS is dipole strength and OS is the oscillator strength. All reported values are in atomic units. The basis set and geometry is given in text.

CH^+	State-1				State-2		State-3		State-4
	FSCC-T[a]	EOMCC[b]	FCI[c]	FSCC[d]	FSCC-T[a]	EOMCC[b]	FSCC-T[a]	EOMCC[b]	FSCC-T[a]
EE	0.1196	0.1198	0.1187	0.1191	0.5067	0.4990	0.6571	0.6544	0.6835
TDM	0.296	0.306	0.299	0.243	0.971	1.036	0.198	0.176	1.293
DS	0.088	0.095	0.089	0.059	0.943	1.073	0.039	0.031	1.672
OS	0.0069	0.0076	0.0070	0.0046	0.3187	0.3571	0.0173	0.0135	0.7618

[a] Our Method (refer equation 2.22), [b] Obtained from ACES-II package, see reference [2], [c] see reference [3] , [d] see reference [4]

State 1: $3\sigma \to 1\pi$, State 2: $3\sigma \to 4\sigma$, State 3: $3\sigma \to 5\sigma$, State 4: $3\sigma \to 6\sigma$

3.3.2 H_2CO Molecule

As a check for the developed FSCC-T and FSCC-Λ methods, we chose the formaldehyde molecule. Table 3.2 present the excitation energies, transition moments, dipole strengths and oscillator strengths for nine transitions in cc-pVDZ basis. Together with the results obtained from both the FSCC approaches, we also report values obtained from EOMCC method, for comparison. The C-O and C-H bond distance was taken to be 1.20838Å and 1.116351Å. The H-C=O bond angle is 121.75 degrees.

For formaldehyde, the ground state restricted Hartree-Fock determinant is chosen as the vacuum which is given by,

$$\psi_{HF} = 1a_1 2a_1 3a_1 4a_1 1b_2 5a_1 1b_1 2b_2$$

We chose four active holes and four active particles as the model space. Hence, $1b_2$, $5a_1$, $1b_1$ and $2b_2$ are chosen as active holes. $2b_1$, $6a_1$, $3b_2$ and $7a_1$ are chosen as the active particles. The FSCC-T method of evaluating transition dipole moments, generate higher values as compared to the transition moment obtained from FSCC-Λ

method in almost all the reported transitions. In certain transitions, the EOMCC method evaluate transition dipoles that agree very well with FSCC-Λ, while in some transitions it agrees better with FSCC-T formulation. Both FSCC-T and FSCC-Λ generate transition moments that are comparable with each other.

Table 3.2: Excitation energies, transition moments, dipole strengths and oscillator strengths in cc-pVDZ basis for the formaldehyde molecule is tabulated. EE is the excitation energy, TDM is transition dipole moment, DS is dipole strength and OS is oscillator strength. All the reported values are in atomic units. The C-O and C-H bond distances are 1.20838Å and 1.116351Å. The H-C=O bond angle is 121.75 degrees.

cc-pVDZ basis		State1	State2	State3	State4	State5	State6	State7	State8	State9
EE	FSCC	0.3106	0.4115	0.4194	0.5689	0.3415	0.5149	0.6252	0.5409	0.6743
	EOMCC[a]	0.3145	0.4180	0.4235	-	0.3494	0.5197	0.6268	0.5476	-
TDM	FSCC-T	0.849	1.482	0.299	0.528	0.125	0.567	0.886	1.100	0.580
	FSCC-Λ	0.782	1.399	0.256	0.541	0.119	0.512	0.873	1.008	0.609
	EOMCC[a]	0.813	1.338	0.295	-	0.091	0.505	0.876	0.997	-
DS	FSCC-T	0.722	2.197	0.089	0.278	0.016	0.321	0.785	1.210	0.337
	FSCC-Λ	0.612	1.958	0.065	0.292	0.014	0.262	0.762	1.016	0.371
	EOMCC[a]	0.661	1.791	0.086	-	0.008	0.255	0.768	0.994	-
OS	FSCC-T	0.1494	0.6029	0.0250	0.1056	0.0036	0.1102	0.3274	0.4363	0.1517
	FSCC-Λ	0.1267	0.5372	0.0183	0.1108	0.0032	0.0900	0.3176	0.3664	0.1670
	EOMCC[a]	0.1385	0.4993	0.0245	-	0.0019	0.0885	0.3210	0.3632	-

State 1: $2b_2 \rightarrow 6a_1$, State 2: $2b_2 \rightarrow 3b_2$, State 3: $2b_2 \rightarrow 7a_1$, State 4: $1b_1 \rightarrow 7a_1$,
State 5: $5a_1 \rightarrow 2b_1$, State 6: $5a_1 \rightarrow 6a_1$, State 7: $5a_1 \rightarrow 7a_1$, State 8: $1b_2 \rightarrow 6a_1$,
State 9: $1b_2 \rightarrow 7a_1$ [a] Obtained from ACES-II package, see reference [2].

3.3.3 H_2O Molecule

The water molecule in cc-pVTZ and cc-pVQZ basis sets is used as a test molecule to check the newly developed FSCC-ΛT method against the previously developed FSCC-T and FSCC-Λ methods. The ground state electronic configuration

of water, $1a_1^2 2a_1^2 1b_1^2 3a_1^2 1b_2^2$ is chosen as the vacuum. $1b_1$, $3a_1$ and $1b_2$ states are the chosen model space active holes, while $4a_1$ and $2b_1$ are chosen to be the active particles from the virtual space. The calculations were performed at the ground state equilibrium geometry of water, at a bond length of 0.957 atomic units and bond angle of 104.5^o. All possible optically active transitions arising from any of the model space states are tabulated in table 3.3.

The dipole strength in state 1, as calculated from the FSCC-ΛT formulation agrees with that of the other FSCC methods. In fact, its value lies approximately in between that obtained from the FSCC-T and FSCC-Λ methods, thus bringing it closer to the EOMCC dipole strengths. The experimental oscillator strength is also reported for this particular transition. The oscillator strength calculated from the FSCC-ΛT, converges towards the experimental value on going from cc-pVTZ to cc-pVQZ basis.

A general trend that can be observed on moving from state 1 to state 5 is that, the dipole strengths obtained from FSCC-ΛT, always lie in between those of FSCC-T and FSCC-Λ methods. The FSCC-T dipole strengths are always higher in value than the FSCC-ΛT dipole strengths. On inspecting the general trend of oscillator strengths, we find that it is similar to that of the dipole strengths. Oscillator strengths obtained from FSCC-ΛT is closer to the EOMCC values and lie between the two FSCC methods. Results obtained in the cc-pVTZ basis, show a slight aberration in the dipole strengths of states 2 and 3. In state 3, the FSCC-Λ method produces the same value of dipole strength as the EOMCC method, as opposed to all other states. While in state 2, the dipole strength is nearly constant when we compare it against the same in state 1. Although EOMCC shows some variation in these two transitions, dipole strength evaluated from both the FSCC methods, do not change significantly to reflect in the result. If we look at the symmetry of these states, then these transitions are taking place between orbitals of the same symmetry. The other three transitions, that is, state 1, 4 and 5 have different initial and final symmetries. But no concrete conclusion can be inferred from these behavioural patterns connected with their symmetry. The aberrations obtained in the triple zeta basis, is no longer found in the cc-pVQZ basis. On inspecting the results obtained from cc-pVQZ basis set, we find that the dipole strengths as well as oscillator strengths obtained from FSCC-ΛT method agree very well with FSCC-T, FSCC-Λ and EOMCC methods.

Table 3.3: Excitation energies, dipole strengths and oscillator strengths of a few allowed transitions for the water molecule in cc-pVTZ and cc-pVQZ basis are presented. All results are in atomic units. The geometry of the molecule is given in the text.

H_2O in cc-pVTZ basis		Excitation energy	Dipole Strength	Oscillator Strength
	FSCC-ΛT		0.181	0.0355
1 [b]	FSCC-T	0.2952	0.197	0.0389
$1b_2 \rightarrow 4a_1$	FSCC-Λ		0.157	0.0309
	EOMCC[a]	0.2964	0.177	0.0351
	FSCC-ΛT		0.181	0.0761
2	FSCC-T	0.6321	0.199	0.0841
$1b_1 \rightarrow 2b_1$	FSCC-Λ		0.156	0.0657
	EOMCC[a]	0.6302	0.189	0.0795
	FSCC-ΛT		0.431	0.1110
3	FSCC-T	0.3864	0.468	0.1206
$3a_1 \rightarrow 4a_1$	FSCC-Λ		0.406	0.1047
	EOMCC[a]	0.3879	0.406	0.1050
	FSCC-ΛT		0.210	0.0650
4	FSCC-T	0.4649	0.219	0.0678
$3a_1 \rightarrow 2b_1$	FSCC-Λ		0.146	0.0453
	EOMCC[a]	0.4652	0.192	0.0597
	FSCC-ΛT		0.646	0.2291
5	FSCC-T	0.5310	0.683	0.2417
$3b_1 \rightarrow 4a_1$	FSCC-Λ		0.604	0.2138
	EOMCC[a]	0.5317	0.650	0.2304

H_2O in cc-pVQZ basis		Excitation energy	Dipole Strength	Oscillator Strength
	FSCC-ΛT		0.228	0.0446
1[b]	FSCC-T	0.2938	0.252	0.0493
$1b_2 \rightarrow 4a_1$	FSCC-Λ		0.182	0.0356
	EOMCC[a]	0.2934	0.216	0.0424
	FSCC-ΛT		0.125	0.0517
2	FSCC-T	0.6181	0.146	0.0604
$1b_1 \rightarrow 2b_1$	FSCC-Λ		0.102	0.0423
	EOMCC[a]	0.6070	0.104	0.0419
	FSCC-ΛT		0.461	0.1175
3	FSCC-T	0.3826	0.510	0.1301
$3a_1 \rightarrow 4a_1$	FSCC-Λ		0.450	0.1147
	EOMCC[a]	0.3827	0.422	0.1077
	FSCC-ΛT		0.169	0.0518
4	FSCC-T	0.4593	0.178	0.0546
$3a_1 \rightarrow 2b_1$	FSCC-Λ		0.139	0.0427
	EOMCC[a]	0.4574	0.157	0.0480
	FSCC-ΛT		0.578	0.2031
5	FSCC-T	0.5271	0.617	0.2169
$3b_1 \rightarrow 4a_1$	FSCC-Λ		0.484	0.1701
	EOMCC[a]	0.5260	0.561	0.1966

[a] Obtained from ACES-II package, see reference [2]

[b] Experimental oscillator strength [6] for the transition presented by State 1: 0.041 a.u.

3.3.4. NH_3 molecule

The ground state of ammonia molecule that is chosen as the vacuum is $1a_1^2 2a_1^2 1e^4 1a_2^2$. We have chosen $1e^4 1a_2^2$ as our active hole states and $3a_1 4a_1 2e$ as the active particles. Hence, the model space comprises six active holes and six active particles, in spin orbital notation. All the optically allowed transitions arising from the above states have been presented in table 3.4. A comparison with EOMCC method have also been shown with respect to some of these transitions. The results are tabulated against the correlation consistent basis sets of Dunning [7] cc-pVDZ and cc-pVTZ. Table 3.4 presents the excitation energies, dipole strength and oscillator strengths of the allowed transitions. The calculations are performed on the ground state equilibrium geometry of the molecule with the N-H bond distance being 1.008 $\mathring{A}$ and the H-N-H bond angle as 107 degrees.

On comparing the dipole strengths between the FSCC-T and FSCC-ΛT methods we find, that the new bi-orthogonal approach gives comparable results to that of the expectation value approach. For some of the transitions we have also compared the two approaches against EOMCC approach. Both FSCC-T and FSCC-ΛT methods perform well in this comparison too. On moving from cc-pVDZ to cc-pVTZ basis, the excitation energies of the respective states are seen to converge, as is expected. States 2 and 8 have similar dipole strength values for the FSCC-T and FSCC-ΛT methods. As opposed to the dipole strength values calculated for the water molecule, FSCC-ΛT dipole strengths for ammonia do not necessarily have lower value than the corresponding FSCC-T dipole strengths.

Table - 3.4: The excitation energies, dipole strengths and oscillator strengths of a few optically allowed transitions for the ammonia molecule in cc-pVDZ and cc-pVTZ basis are tabulated. The molecule is treated at the ground state equilibrium geometry of r = 1.008 Å and $\theta = 107^o$. *All the values presented are in atomic units.*

NH_3 in cc-pVDZ basis		Excitation energy	Dipole strength	Oscillator Strength
1	FSCC-ΛT	0.5393	1.057	0.3797
	FSCC-T		1.106	0.3983
2	EOMCC[a]	0.6507	0.012	0.0055
	FSCC-ΛT	0.6476	0.014	0.0061
	FSCC-T		0.014	0.0059
3	FSCC-ΛT	0.6221	0.269	0.1117
	FSCC-T		0.280	0.1165
4	FSCC-ΛT	0.4742	0.578	0.1825
	FSCC-T		0.607	0.1918
5	FSCC-ΛT	0.5612	0.022	0.0081
	FSCC-T		0.023	0.0086
6	EOMCC[a]	0.5793	0.531	0.2053
	FSCC-ΛT	0.5782	0.453	0.1748
	FSCC-T		0.474	0.1828
7	EOMCC[a]	0.2400	0.120	0.0193
	FSCC-ΛT	0.2379	0.115	0.0182
	FSCC-T		0.125	0.0198
8	EOMCC[a]	0.3157	0.007	0.0015
	FSCC-ΛT	0.3137	0.007	0.0014
	FSCC-T		0.007	0.0014

State 1: $1e \rightarrow 3a_1$ State 2: $1e \rightarrow 4a_1$ State 3: $1e \rightarrow 2e$ State 4: $1e \rightarrow 3a_1$ State 5: $1e \rightarrow 4a_1$

State 6: $1e \rightarrow 2e$ State 7: $1a_2 \rightarrow 3a_1$ State 8: $1a_2 \rightarrow 2e$

NH_3 in cc-pVTZ basis		Excitation energy	Dipole strength	Oscillator Strength
1	FSCC-ΛT	0.5205	0.880	0.3054
	FSCC-T		0.923	0.3204
2	EOMCC[a]	0.6025	0.041	0.0166
	FSCC-ΛT	0.6091	0.031	0.0126
	FSCC-T		0.030	0.0124
3	FSCC-ΛT	0.6058	0.185	0.0746
	FSCC-T		0.194	0.0785
4	FSCC-ΛT	0.4573	0.536	0.1635
	FSCC-T		0.562	0.1715
5	FSCC-ΛT	0.5409	0.009	0.0031
	FSCC-T		0.010	0.0035
6	EOMCC[a]	0.5519	0.316	0.1163
	FSCC-ΛT	0.5546	0.294	0.1085
	FSCC-T		0.319	0.1182
7	EOMCC[a]	0.2318	0.194	0.0299
	FSCC-ΛT	0.2307	0.188	0.0290
	FSCC-T		0.203	0.0313
8	EOMCC[a]	0.3078	0.006	0.0012
	FSCC-ΛT	0.3093	0.004	0.0008
	FSCC-T		0.004	0.0008

[a] Obtained from ACES-II package, see reference [2]

3.3.5 C_3H_6O Molecule

We have chosen the acetone molecule in order to test the performance of the semi-bi-orthogonal approach for a larger electron system. Acetone is a 32 electron system and we have chosen the active holes having $2a_1, 3b_1, 4b_2, 3a_1, 6a_2$ symmetry, while the active particles have $4a_1$ and $4b_1$ symmetry. Table 3.5 tabulates four such optically allowed transitions in cc-pVDZ basis. We have also compared the results obtained from FSCC-Λ and FSCC-T for one particular transition, against EOMCC method. The acetone molecule is treated at the ground state geometry of C=O bond distance of 1.235Å and C-C bond length of 1.495Å.

As seen from the table, the dipole strength obtained from FSCC-ΛT approach for the transition described in state 1, agrees well with FSCC-T as well as EOMCC dipole strength values. Due to comparable excitation energy of the same state, oscillator strength is also in good agreement. The other transitions described by the states 2, 3 and 4 show similar comparable results between the FSCC-ΛT and FSCC-T. This is also reflected in the oscillator strength values.

Table - 3.5: Excitation energies, dipole strengths and oscillator strengths of a few optically active transitions are presented for the acetone molecule in cc-pVDZ basis. The ground state geometry is 1.235Å for C=C and C-C bond length is 1.495Å

C_2H_6O in cc-pVDZ basis		Excitation energy	Dipole Strength	Oscillator Strength
1	FSCC-ΛT	0.2894	0.164	0.0317
	FSCC-T		0.109	0.0402
	EOMCC[a]	0.2968	0.146	0.0288
2	FSCC-ΛT	0.3926	0.233	0.0567
	FSCC-T		0.252	0.0659
3	FSCC-ΛT	0.4187	0.203	0.0598
	FSCC-T		0.194	0.0541
4	FSCC-ΛT	0.4401	0.183	0.0462
	FSCC-T		0.212	0.0624

[a] Obtained from ACES-II package, see reference [2]

3.4 Size Intensivity

Both FSCC-T and FSCC-Λ formulations were tested for size-intensivity of the transition dipole moments. We have calculated the transition dipoles for water monomer, dimer and trimer at non-interacting distances in FSCC-T and FSCC-Λ formulations. The water molecules are treated at the equilibrium ground state geometry in cc-pVZD basis. The results are presented in Table 3.6. We find that the transition moments are size-intensive in both the FSCC methods as the transition dipole remains constant with increase in water monomer unit. Since, the formulation of FSCC-ΛT also involves a connected form (equation 3.1), the dipole strengths evaluated in this method will also be size-intensive.

Table 3.6: Water monomer, dimer and trimer in cc-pVDZ basis. Experimental ground state geometry is, r = 0.957 and θ = 104.5˚. The monomer units were placed at non-interacting distance to check the size-intensivity of the FSCC-T and FSCC-Λ methods. TDM stands for transition dipole moments.

cc-pVDZ basis		H_2O monomer	H_2O Dimer	H_2O Trimer
TDM	FSCC-T	0.339	0.339	0.339
	FSCC-Λ	0.297	0.297	0.297

3.5 Inference

In this chapter, we have evaluated and tabulated electronic transition dipole moments within the Fock-space multi-reference coupled cluster framework. We report transition energies, transition moments and oscillator strengths for methylidyne cation (in FSCC-T method) and formaldehyde (FSCC-T and FSCC-Λ methods) molecules. We observe that both FSCC-T and FSCC-Λ provide transition dipole moments that are in close proximity of each other. Also, both these methods agree well with EOMCC transition moments. The newly developed FSCC-ΛT approach evaluates dipole strengths that agree well with those obtained from other FSCC-T and

FSCC-Λ methods, as tested for the water molecule. For the ammonia and acetone molecules, the dipole strengths obtained from FSCC-ΛT, are also in close proximity to EOMCC dipole strengths. EOMCC dipole strengths, as implemented in ACES-II [2] software package also use a similar linearized conjugate left vector for the left transition moment. This similarity in the theory is the main cause for the FSCC-ΛT and EOMCC dipole strengths to be similar in nature, although the treatment of the right transition moment is completely different. We have also mentioned in the previous section that FSCC-T and FSCC-Λ gives size-intensive transition dipole moments. Since, the formulation of FSCC-ΛT also involves a connected form (equation 3.1), the transition moments evaluated by this method will also be size-intensive. This is in contrast to EOMCC, where the left transition moment is not size-intensive, while the right transition moment is size-intensive.

As seen from table 3.3 for the water molecule, the results show that FSCC-ΛT method produces dipole strengths that lie in between the other two FSCC methods, namely FSCC-T and FSCC-Λ. This is expected, considering that FSCC-ΛT is a hybrid of the two other FSCC methods. The comparison with experimental oscillator strength for state-1 of the water molecule shows that the FSCC-ΛT method performs better than the FSCC-T and FSCC-Λ methods. Though in case of water, the FSCC-ΛT dipole strengths were always lower in magnitude than the FSCC-T dipole strengths, which was not the case for the other molecules. We have compared our results (obtained from FSCC-ΛT) against the FSCC-T method, as it is a straightforward way to generate dipole strengths without the use of any extra set of amplitudes. Though the FSCC-Λ formulation is a naturally terminating series, solving the higher sector Λ-amplitudes is a time consuming step. Hence, we have omitted testing FSCC-Λ method against FSCC-ΛT formulation barring the test water molecule. As seen from the results, FSCC-ΛT produces similar values and is computationally cheaper. It can thus be concluded that, FSCC-T and FSCC-ΛT formulations are the suitable methods to calculate singlet electronic dipole strengths and oscillator strengths in FSCC formalism.

References

[1] GAMESS: "General Atomic and Molecular Electronic Structure System" M.W.Schmidt, K.K.Baldridge, J.A.Boatz, S.T.Elbert, M.S.Gordon, J.H.Jensen, S.Koseki, N.Matsunaga, K.A.Nguyen, S.Su, T.L.Windus, M.Dupuis and J.A.Montgomery, J. Comput. Chem. **14**, 1347 (1993).

[2] J. F. Stanton, J. Gauss, S. A. Perera, J. D. Watts, A. D. Yau, N. Oliphant, P. G. Szalay, W. J. Lauderdale, S. R. Gwaltney, S. Beck, A. Balkova, M. Nooijen, H. Sekino, C. Huber, K. K. Baeck, D. E. Bernholdt, P. Rozyczko, J. Pittner, W. Cencek, D. Taylor , R. J. Bartlett, Integral packages included are VMOL (J. Almlöf, P. R. Taylor); VPROPS (P. Taylor); ABACUS (T. Helgaker, H. J. Aa. Jensen, P. Jørgensen, J. Olsen, P. R. Taylor); HONDO/GAMESS (M. W. Schimdt, K. K. Baldrige, J. A.Boatz, S.T.Elbert, M.S.Gordon, J.H.Jensen, S.Koseki, N.Matsunaga, K.A.Nguyen, S.Su, T.L.Windus, M.Dupuis, J.A.Montgomery). ACES II a program product of the Quantum Theory Project, University of Florida, 2006

[3] J. Olsen, A.M. S. de Marás, H.J.A. Jensen and P. Jørgensen, Chem. Phys. Lett. **154**, 380 (1989)

[4] M. Barysz, Theo. Chim. Acta **90**, 257 (1995)

[5] L.Z. Stolarczyk and H.J. Monkhorst, Phys. Rev. A **37**, 3926 (1988)

[6] A. H. Laufer, J. R. McNesby, Can. J. Chem. **43**, 3487 (1965)

[7] T. H. Dunning, Jr., J. Chem. Phys. **90**, 1007 (1989)

Chapter 4

Transition dipole moment and oscillator strength of doublet radicals

---

Electronic dipole strengths (square of transition moments) are evaluated for various transitions, arising from the ground/excited states to a few valence excited states for some doublet species. A brief review of the Fock-space multi-reference coupled cluster theory specifically, for the *(0,1)* valence rank is presented first. This is followed by the relevant equations for the solution of the de-excitation lambda operators through a constrained variation approach. A few pilot applications are presented for the expectation value and bi-orthogonal approaches for dipole strength and oscillator strength.

4.1 Fock-space theory for (0,1) valence sector

The general theory of FSMRCC [1-5] is already presented in the first chapter. We will briefly describe the working equations and energy expressions for the specific case of *(0,1)* valence sector which corresponds to the ionization potential problem and discuss the formulation of CVA [6-10] in this context. As mentioned previously, FSMRCC is based on the concept of a common vacuum. In the present scenario, the N-electron RHF configuration is chosen as the vacuum and holes and particles are defined with respect to this reference. A subset of active holes and particles are usually delineated around the fermi level whose varying occupancy gives rise to the model space. The model space determinant is denoted by $\left\{\phi_i^{(0,1)}\right\}$ and hence, the configurations of this CMS are given by,

$$\left|\Psi_{\mu(0)}^{(0,1)}\right\rangle = \sum_i C_{\mu i}^{(0,1)} \left|\phi_i^{(0,1)}\right\rangle \tag{4.1}$$

where, *'C's* are the model space coefficients. The comparatively weak interactions of the model space configurations with the virtual space configurations give rise to the dynamic electron correlation. This is brought in to effect through a universal wave operator Ω, which generates the correlated wave function by its action on the model space determinants.

$$\left|\Psi_{\mu}^{(0,1)}\right\rangle = \Omega \left|\Psi_{\mu(0)}^{(0,1)}\right\rangle \tag{4.2}$$

Specific form of this wave operator is given below,

$$\Omega = \left\{e^{\tilde{T}^{(0,1)}}\right\} \text{ , where } \tilde{T}^{(0,1)} = T^{(0,1)} + T^{(0,0)} \tag{4.3}$$

Curly brackets in equation (4.3) denotes normal ordering of the cluster amplitudes with respect to the reference function. The higher valence cluster operator subsumes the lower valence ones. Due to normal ordering the lower valence amplitude equations are decoupled from the higher valence ones. This means that we first solve for the $T^{(0,0)}$ amplitude equations and then these appear as constant entities while solving for the higher valence $T^{(0,1)}$ amplitudes. This is known as subsystem embedding condition. [3] As the *(0,1)* sector is a complete model space (CMS), intermediate normalization holds true, that is,

$$P^{(0,1)}\Omega P^{(0,1)} = P^{(0,1)} \tag{4.4}$$

The wave operator is parameterized such that the states generated by its action on the reference function satisfies the Bloch-Lindgren equation for effective Hamiltonian, which is the modified form of the Schrödinger equation. The Bloch equations for the *(0,1)* sector is given by,

$$\begin{aligned} P^{(0,1)}(H\Omega - \Omega H_{eff}^{(0,1)})P^{(0,1)} &= 0 \\ Q^{(0,1)}(H\Omega - \Omega H_{eff}^{(0,1)})P^{(0,1)} &= 0 \end{aligned} \tag{4.5}$$

Diagonalizing the effective Hamiltonian within the model space (as defined through the Bloch equation) will generate the energies of the corresponding states and the left and right Eigen vectors.

$$\begin{aligned} H_{eff}^{(0,1)}C^{(0,1)} &= C^{(0,1)}E \\ \tilde{C}^{(0,1)}H_{eff}^{(0,1)} &= E\tilde{C}^{(0,1)} \end{aligned} \tag{4.6}$$

4.2 CVA in the (0,1) sector

The energy of a specific $'\mu'^{\,th}$ state in the *(0,1)* sector can be rewritten from equation (4.5) as,

$$E_\mu = \sum_{ij} \tilde{C}_{\mu i}^{(0,1)} \left(H_{eff}\right)_{ij}^{(0,1)} C_{j\mu}^{(0,1)} \tag{4.7}$$

The basic assumption of the CVA [6,7] is to construct a Lagrangian that will minimise the energy expression given above with the constraint that the equation set (4.4) are satisfied for a specific μ^{th} state. The Lagrangian for the *(0,1)* sector is given by,

$$\begin{aligned} £ = \; & \sum_{ij} \tilde{C}_{\mu i}^{(0,1)} \left(H_{eff}\right)_{ij}^{(0,1)} C_{j\mu}^{(0,1)} \\ & + P^{(0,1)}\Lambda^{(0,1)}P^{(0,1)}P^{(0,1)}\left[H\Omega - \Omega H_{eff}^{(0,1)}\right]P^{(0,1)} \\ & + P^{(0,1)}\Lambda^{(0,1)}Q^{(0,1)}Q^{(0,1)}\left[H\Omega - \Omega H_{eff}^{(0,1)}\right]P^{(0,1)} \\ & + P^{(0,0)}\Lambda^{(0,0)}P^{(0,0)}P^{(0,0)}H\Omega P^{(0,0)} \\ & + P^{(0,0)}\Lambda^{(0,0)}Q^{(0,0)}Q^{(0,0)}H\Omega P^{(0,0)} \\ & - E_\mu\left(\sum_{ij} \tilde{C}_{\mu i}^{(0,1)} C_{j\mu}^{(0,1)} - 1\right) \end{aligned} \tag{4.8}$$

The Λ in equation (4.7) are the de-excitation amplitudes in terms of Fock-space formalism and are known as the Lagrange multipliers. The above equation can lead to a more simplified form, courtesy the CMS. The effective Hamiltonian of CMS can be represented explicitly through the cluster operators, as a result of which, the closed part of the Lagrange multiplier vanishes. [7,8] Thus equation (4.8) simplifies to

$$
\begin{aligned}
£ = \; & \sum_{ij} \tilde{C}_{\mu i}^{(0,1)} \left(H_{eff} \right)_{ij}^{(0,1)} C_{j\mu}^{(0,1)} \\
& + P^{(0,1)} \Lambda^{(0,1)} Q^{(0,1)} Q^{(0,1)} \left[H\Omega - \Omega H_{eff}^{(0,1)} \right] P^{(0,1)} \\
& + P^{(0,0)} \Lambda^{(0,0)} Q^{(0,0)} Q^{(0,0)} H\Omega P^{(0,0)} \\
& - E_{\mu} \left(\sum_{ij} \tilde{C}_{\mu i}^{(0,1)} C_{j\mu}^{(0,1)} - 1 \right)
\end{aligned}
\tag{4.9}
$$

Differentiating equation (4.9) with respect to the Λ-amplitudes, results in an expression for the cluster amplitudes. The cluster amplitudes (Ω) are decoupled from those of the de-excitation amplitudes. However, the reverse is not true. The Λ equations are coupled with the Ω amplitudes. After solving for Ω till the *(0,1)* sector, the Λ equations are solved by making them stationary with respect to the cluster amplitudes. There is a reverse de-coupling in these Λ equations. The higher valence $\Lambda^{(0,1)}$ amplitudes are solved first, followed by the lower valence de-excitation amplitudes. While solving for the higher valence amplitudes the lower valence Λ amplitudes do not occur. Once the higher valence Λ amplitudes are generated, they appear as constant entities in the lower valence sector.

4.3 Computational Details

The open shell molecules are treated in the Fock-space sector as a case of electron detachment (or attachment in case of *1,0* sector). We have started our calculations with the closed shell HF determinant as the reference and have removed an electron from a specific orbital of choice, to generate the doublet radical. We have used FSCC-T and FSCC-Λ methods for calculating the dipole strength and oscillator strength of a few test molecules. The dipole strengths were evaluated as the relevant off-diagonal matrix elements as stated in the equations, given in section 2.5 (refer equations 2.32 and 2.36). The FSCC-T method is an exponentially non-terminating series. Hence, for practical application we have included all terms up to cubic order in

cluster amplitudes. The FSCC-Λ method is a naturally terminating series and no approximation have been used for evaluation of dipole strength within this formulation.

In the FSCC-Λ formulation, the connected form of $\bar{\mu}$ terms were constructed first and stored separately to further connect with the higher valence cluster amplitudes. The connected form of $\tilde{\mu}$ (refer section 2.5.2) was then contracted with the de-excitation amplitudes which finally gave rise to a completely linked form of diagrams. We have used GAMESS [11] for generating the starting AO integrals and have not applied frozen core approximation anywhere. The codes used to generate the Fock-space ionization energies and dipole strengths are all in-house codes. Comparison with EOMCC data, wherever applicable have been obtained from Q-CHEM [12] software package. Our calculations were performed under the coupled cluster singles and doubles (CCSD) approximation and hence, scaled as N^6. The tables, given below, contain the difference in ionization potentials, dipole strengths and oscillator strengths in two methods: expectation value method, denoted by FSCC-T and the bi-orthogonal approach, denoted by FSCC-Λ. We have tested our method against radicals/radical ion like: OH, H_2O^+ and NO.

4.4 Pilot applications

4.4.1 H_2O^+ radical ion

The water molecule in cc-pVTZ basis is used as a test molecule to check the newly developed codes for FSCC-T and FSCC-Λ method against the EOM-IP as obtained from Q-CHEM [12] software package. The ground state electronic configuration of water, $1a_1^2 2a_1^2 1b_1^2 3a_1^2 1b_2^2$ is chosen as the vacuum. All the occupied orbitals were chosen as active holes. The transitions arising from removing an electron from either of the chosen active orbitals are presented in the table given below. The calculations were performed at the ground state equilibrium geometry of water, at a bond length of 0.957 atomic units and bond angle of 104.5^o. Table 4.1 as given later, lists the dipole strengths of a few transitions among the chosen active orbitals. A comparison with EOM-IP is also tabulated for the first transition depicted in the table. It can be clearly seen that dipole strengths obtained from both the

methods are in close proximity to each other. The EOM-IP oscillator strength also matches well with our value. The ΔE values are obtained by taking the absolute energy difference (difference in IP values) between the two states of transition under consideration.

Table 4.1: Difference energy, dipole strength and oscillator strength of H_2O^+ radical is given in cc-pVTZ basis for a few transitions. ΔE, DS and OS are the difference in energies, dipole strength and oscillator strength respectively. All results are in a.u.

States	ΔE	FSCC-T		FSCC-Λ		EOM-IP[a]	
		DS	OS	DS	OS	DS	OS
$3a_1 \leftrightarrow 1b_2$	0.0818	0.023	0.001	0.023	0.001	0.017	0.001
$2a_1 \leftrightarrow 1b_2$	0.7428	0.344	0.170	0.323	0.160		
$2a_1 \leftrightarrow 3a_1$	0.6609	0.302	0.133	0.290	0.128		
$1a_1 \leftrightarrow 1b_2$	19.4124	0.005	0.065	0.005	0.064		

[a] EOM-IP result was obtained from Q-CHEM software package [12]

4.4.2 NO radical

The closed shell ground state HF configuration for the NO^- anion is chosen as the vacuum. The removal of an electron from such an anionic state results in the generation of the radical species. The vacuum thus constitutes $1\sigma^2 2\sigma^2 3\sigma^2 4\sigma^2 5\sigma^2 6\sigma^2 7\sigma^2 8\sigma^2$ orbitals. Among the given orbitals, the $5\sigma^2 6\sigma^2 7\sigma^2 8\sigma^2$ orbitals were chosen as the active orbitals. Different excited states were obtained by removing an electron from any of the chosen active orbitals. The removal of an electron from the 8σ state results in the so called ground state of NO radical. Removal of an electron from any orbital other than 8σ will result in creation of various excited states for the NO radical. Different transitions were obtained by checking for the energy difference and dipole strengths between any two such states. Table 4.2 tabulates the difference energies, dipole strengths and oscillators strengths of a few such allowed transitions in cc-pVTZ basis. The N-O bond distance was taken to be 1.150Å. As can be seen from the table, the dipole strengths and oscillator

strengths from the FSCC-T and FSCC-Λ methods agree well with each other. The oscillator strength was calculated in the dipole length formulation as given by the equation (2.15). The transition occurring from the 5σ symmetry state and the $6\sigma \leftrightarrow 7\sigma$ transition, is being underestimated by the FSCC-Λ method as compared to the FSCC-T method. On the other hand, the dipole strength obtained from the transition $6\sigma \leftrightarrow 8\sigma$ shows good agreement between both the methods.

Table 4.2: Difference energy, dipole strength and oscillator strength of NO radical is given in cc-pVTZ basis for a few transitions. ΔE, DS and OS are the difference in energies, dipole strength and oscillator strength respectively. All results are in a.u.

States	ΔE	FSCC-T		FSCC-Λ	
		DS	OS	DS	OS
$5\sigma \leftrightarrow 6\sigma$	0.0005	0.338	0.001	0.306	0.001
$6\sigma \leftrightarrow 7\sigma$	0.0295	0.299	0.006	0.267	0.005
$6\sigma \leftrightarrow 8\sigma$	0.1461	0.297	0.029	0.298	0.029

4.4.3 OH radical

The OH radical was also treated in the same balance as that of the NO radical. The OH anion was chosen as the vacuum with respect to which holes and particles were defined. Since, we are interested in calculating transition moments of the *(0,1)* sector we will concentrate on transitions within the active hole space. The configuration for the vacuum is given by, $\psi_{HF} = 1\sigma^2 2\sigma^2 3\sigma^2 1\pi^2 2\pi^2$ out of which the $3\sigma 1\pi 2\pi$ states were chosen as the active orbitals. Various transitions occurring within this active space have been tabulated for the aug-cc-pVTZ basis in table 4.3. The O-H bond distance was chosen to be 0.9697 Å. As can be seen from the table, FSCC-T and FSCC-Λ methods give dipole strengths which agree with each other. Since the transition energy is also the same for the FSCC methods, the oscillator strength also agrees well.

Table 4.3: Difference energy, dipole strength and oscillator strength of OH radical is given in aug-cc-pVTZ basis for a few transitions. ΔE, DS and OS are the difference in energies, dipole strength and oscillator strength respectively. All results are in a.u.

States	ΔE	FSCC-T		FSCC-Λ	
		DS	OS	DS	OS
$1\sigma \leftrightarrow 1\pi$	0.6605	0.450	0.198	0.424	0.187
$2\sigma \leftrightarrow 1\pi$	0.1519	0.024	0.002	0.035	0.003

4.5 Conclusions

The square of transition moments, i.e. dipole strengths were tabulated for a few molecules together with the respective oscillator strengths. As can be seen from the tables, both FSCC-T and FSCC-Λ methods gave dipole strengths that agreed well with each other. We have depicted transitions only for the *(0,1)* sector and hence studied the case of electron detachment. These transitions occur within the space of occupied orbitals and we were able to treat a few excited state doublet transitions for the presented molecules. The methods were also compared with EOM-IP result wherever available. A more rigorous investigation remains to be performed for a larger test set following the initial success of these methods for the doublet species. It was seen from the test set that FSCC-Λ method generated transition moments that were mostly lower in magnitude than those obtained from FSCC-T method. But due to the limited test set depicted above, no concrete conclusion can be reached.

References

[1] D. Mukherjee, Pramana **12**, 203 (1979)

[2] I. Lindgren and D. Mukherjee, Phys. Rep. **151**, 93 (1987)

[3] S. Pal, M. Rittby, R. J. Bartlett, D. Sinha and D. Mukherjee, J. Chem. Phys. **88**, 4357 (1988)

[4] D. Mukherjee and S. Pal, Adv. Quant. Chem. **20**, 291 (1989)

[5] S. Pal, Phys. Rev. A, **39**, 39 (1989)

[6] P. Szalay, Int. J. Quantum. Chem. **55**, 151 (1995)

[7] K. R. Shamasundar, S. Asokan and S. Pal, J. Chem. Phys. **120**, 6381 (2004)

[8] K. R. Shamasundar and S. Pal, J. Chem. Phys. **114**, 1981 (2001); **115**, 1979 (2001)

[9] P.U. Manohar, N. Vaval and S. Pal, J. Mol. Struct. THEOCHEM **768**, 91 (2006); P. U. Manohar and S. Pal, Chem. Phys. Lett. **438**, 321 (2007)

[10] A. Bag, P. U. Manohar, N. Vaval and S. Pal, J. Chem. Phys. **131**, 024102 (2009)

[11] GAMESS: "General Atomic and Molecular Electronic Structure System" M.W.Schmidt, K.K.Baldridge, J.A.Boatz, S.T.Elbert, M.S.Gordon, J.H.Jensen, S.Koseki, N.Matsunaga, K.A.Nguyen, S.Su, T.L.Windus, M.Dupuis and J.A.Montgomery, J. Comput. Chem. **14**, 1347 (1993).

[12] Y. Shao, L. Fusti-Molnar, Y. Jung, J. Kussmann, C. Ochsenfeld, S. T. Brown, A. T. B. Gilbert, L. V. Slipchenko,S. V. Levchenko, D. P. O'Neill, R. A. DiStasio Jr., R. C. Lochan, T. Wang, G. J. O. Beran, N. A. Besley, J. M. Herbert, C. Y. Lin, T. Van Voorhis, S. H. Chien, A. Sodt, R. P. Steele, V. A. Rassolov, P. E. Maslen, P. P. Korambath, R. D. Adamson, B. Austin, J. Baker, E. F. C. Byrd, H. Dachsel, R. J. Doerksen, A. Dreuw, B. D. Dunietz, A. D. Dutoi, T. R. Furlani, S. R. Gwaltney, A. Heyden, S. Hirata, C.-P. Hsu, G. Kedziora, R. Z. Khaliullin, P. Klunzinger, A. M. Lee, M. S. Lee, W. Liang, I. Lotan, N. Nair, B. Peters, E. I. Proynov, P. A. Pieniazek, Y. M. Rhee, J. Ritchie, E. Rosta, C. D. Sherrill, A. C. Simmonett, J. E. Subotnik, H. L. Woodcock III, W. Zhang, A. T. Bell, A. K. Chakraborty, D. M. Chipman, F. J. Keil, A. Warshel, W. J. Hehre, H. F. Schaefer III, J. Kong, A. I. Krylov, P. M. W. Gill, M. Head-Gordon, A. Aspuru-Guzik, C. Chang, R. G. Edgar, E. Sundstrom, J. Parkhill, K. Lawler, M. Gordon, M. Schmidt, N. Shenvi, D.

Lambrecht, M. Goldey, R. Olivares-Amaya, Y. Bernard, L. Vogt, M. Watson, J. Liu, S. Yeganeh, B. Kaduk, O. Vydrov, X. Xu, I. Kaliman, K. Khistyaev, N. Russ, I.Y. Zhang, W.A. Goddard III, F. Liu, R. King , A. Landau, M. Wormit, A. Dreuw, M. Diedenhofen, A. Klamt, A.W. Lange, D. Ghosh, D. Kosenkov, T. Kus, A. Landau, D. Zuev, J. Deng, S.P. Mao, Y.C. Su, D. Small, L. D. Jacobson, Q-Chem, Version 4.0.1, Q-Chem, Inc., Pittsburgh, PA (2007)

Chapter 5

Perturbative order analysis of the similarity transformed Hamiltonian in Fock-space coupled cluster theory: Difference energy and electric response properties

---

In this chapter, a perturbative analysis of the ground state similarity transformed Hamiltonian and its effect on the various Fock-space coupled cluster (FSCC) sectors is presented through calculation of ionization potential, electron affinity, excitation energies and response properties. Various truncation schemes of the effective Hamiltonian are presented with explicit form of the defining equations. Based on such a truncation, the approximate methods are labelled as FSCC(n), where n represents the correlation energy of the ionized, electron attached or excited states corrected at least up to n^{th} order within coupled cluster singles and doubles scheme (CCSD). A lower scaling CC2 type of approach (abbreviated as FS-CC2) is compared against the group of FSCC(n) methods for energies. Electric response properties have been compared and contrasted for the two lower scaling methods: FSCC(2) and FS-CC2. The various truncated methods are tested for a number of small molecules. The results obtained from a range of truncated methods are compared against full FSCCSD calculations.

5.1 Introduction

Chemistry is governed by energy differences, e.g. thermodynamic properties of activation energy, free energy change, enthalpy change or spectroscopic properties like excitation energy (EE), ionization potential (IP) and electron affinity (EA) as direct difference of energies. In both cases, *ab-initio* calculation has emerged as a versatile tool for understanding and interpreting experimentally determined energy differences. Among the various methods available, the Fock space multi-reference coupled cluster (FSMRCC) [1-9] and the closely related equation of motion coupled cluster (EOM-CC) [10-17] analogue have emerged as the most accurate and systematic methods for determination of EE [10], IP [11,12] and EA [14]. Significant development has occurred in the context of both methods for generating codes capable of calculating energy differences, with accuracy within the fraction of eV with respect to experimental values. Both FSMRCC [3,6,9] and EOMCC [11,14,16] methods are generally used in singles and doubles approximations. However, inclusion of triples in the calculation gives enhanced accuracy at the expense of added computational cost [18-26]. The inclusion of partial as well as full triples has been tried within the framework of both EOMCC [27-33] and FSMRCC [34-39]. Significant development has also taken place in the context of analytic derivative calculation within the framework of EOMCC [40-44]. Similar realization is yet to be achieved in the context of FSMRCC. However, some breakthrough has been obtained in the context of property calculation within the FSMRCC framework, mainly by Pal and co-workers [45-48].

Inspite of having all other favourable characteristics, both FSMRCC and EOMCC, even in CCSD approximation, have the prohibitively high scaling of N^6 [12,17,49] (where N is the number of basis functions) and large storage requirements which restrict their use beyond molecules containing more than ten second row atoms in any reasonable basis set. So a lot of effort has been devoted to the development of lower scaling approximations for calculation of direct difference of energies like EE, IP and EA, mainly in the framework of EOMCC [49-57]. The coupled cluster method has an intriguing relationship with many body perturbation theory (MBPT) [58]. Various orders of MBPT can be recovered from the suitable lower order iteration of coupled cluster amplitude equations. For example, in the lowest order approximation to CCSD, T_2 amplitudes give rise to MBPT(2) method. So, most of the efforts towards

generation of lower scaling approximation to FSMRCCSD and EOM-CCSD are evolved around the perturbational truncation of the coupled cluster effective Hamiltonian [51,55,57].

Nooijen and Snijders [55] were the first to give the proposal to approximate the CCSD amplitudes by their MBPT(2) analogues. Later, Stanton and Gauss [57] generalized the idea and proposed a hierarchical approximation to EOMCCSD similarity transformed Hamiltonian. They have coined the term EOM-CCSD(n), where n denotes that the effective Hamiltonian contain terms up to n^{th} order in perturbation. At large values of n, the truncated similarity transformed Hamiltonian converges to full CCSD effective Hamiltonian and the corresponding EOM-CCSD(n) energy converges to standard EOM-CCSD energy. However, a second order approximation (n=2) leads to EOM-CCSD(2) method and provides significant advantage in terms of reducing the scaling as well as storage requirements [59]. Therefore, the EOMCCSD(2) approximation, in its original form as well as with further modifications, has been extensively used to generate lower computational scaling methods [49-52] for the calculation of ionization potential, electron affinity and excitation energy [55,57,60]. It has been shown to give excellent performance for potential energy surfaces, as well as other complex multi-reference situations, despite of its lower computational cost. Another elegant way to calculate difference energies and properties within the class of CC is the similarity transformed EOM-CCSD (STEOM-CCSD) as developed and advocated by Nooijen [61-66]. STEOM-CC is similar to the Fock-space formalism [63] and an extensive benchmark for valence excited states are available [66]. A perturbative analogue to STEOM (STEOM-PT) offers significant computational savings, as compared to the original method and is very well benchmarked [66]. The authors have shown significant improvement of results over EOM-CCSD and CASPT2 for singlet energies. However, triplet excited states were not described that accurately. In terms of property calculations, Pal and co-workers [67] have shown that the EOMIP-CCSD(2) method can be used to calculate geometry and IR frequency of large doublet radicals, with accuracy comparable to the standard EOMIP-CCSD method. However, no such benchmark studies are available for electric response properties. The same group later showed that although the method is very accurate for geometric properties, it is not so precise for calculation of ionization potential itself. To be specific, the EOMIP-CCSD(2) method significantly overestimates the ionization potentials, especially for the cases

where Hartree-Fock orbitals do not provide a correct zeroth order description of the ground state wave-function. Similar problems were reported by Dutta. *et. al.* [68] for spin-flip (SF) and electron attachment (EA) variants of EOM-CCSD(2).

It is obvious that the source of the error lies in the truncated form of the similarity transformed Hamiltonian. However, an in-depth understanding of the cause and possible remedy will require a detailed perturbational analysis of the similarity transformed Hamiltonian. Although Bartlett and co-workers [69] have performed some initial investigation along this line, they have restricted their study only to excitation energy case and benchmark values were reported only for two molecules in a single basis set. However, similar studies are required in the context of ionization potential and electron affinity problems also, where the reference and target states differ in the number of electrons, making the error analysis less straightforward than the excitation energy case. An in-depth analysis of the effect of perturbation truncation of similarity transformed Hamiltonian on various direct difference of energies like IP, EA and EE in the context of FSMRCC is presented in this chapter. This chapter also explores the behaviour of those methods for electric response properties like, dipole moment and polarizabilities. The Bloch equation framework of FSMRCC makes the perturbational analysis more straightforward than the CI like framework in EOMCC.

As the details of the FSMRCC theory is already discussed in chapter 1, the next section depicts an order analysis and truncation scheme for the ground state effective Hamiltonian. Computational attributes are stated in section 5.3. Numerical results and discussions on them follow in section 5.4. Section 5.5 comprises the concluding remarks.

5.2 Perturbational truncation of the ground state effective Hamiltonian

The effective Hamiltonian (also identified as similarity transformed Hamiltonian) for the ground state is defined as

$$H_{eff}^{(0,0)} \equiv \bar{H} = \Omega^{-1} H \Omega \equiv e^{-T} H e^{T} \tag{5.1}$$

Following the Campbell-Baker-Hausdorff expansion, the above equation is recasted as,

$$\bar{H} = \left(He^{T}\right)_{c,open} = \left(f + v\right)\left(1 + T + \frac{T^{2}}{2!} + ...\right) \tag{5.2}$$

Subscripts *c* and *open* refer to the open connected part of the above equation. The closed part of $\bar{H}$ is dropped off to facilitate direct calculation of correlation energy. The use of $\bar{H}$ anywhere else in this chapter will imply only the connected open parts. *'f'* and *'v'* denote the one and two body parts of the Hamiltonian. Expanding equation (5.2) and collecting terms in various perturbational order gives rise to a series of truncation schemes of $\bar{H}$ under the CCSD approximation. Contraction of $\bar{H}$ with higher valence cluster operators will generate the effective Hamiltonian of those sectors.

$$H_{eff}^{(n)} = \bar{H}^{(n)} + \left(\bar{H}^{(n)} S^{(k,l)}\right)_{c} \qquad \forall k,l = 0,1 \tag{5.3}$$

The various methods are abbreviated as FSCC(n), where n $\left(2 \le n \le 4\right)$ depicts that the correlation energy is correct at least up to nth order. At higher values of n, the FSCC(n) will converge towards the full FSCCSD energies. This truncation scheme is similar to the one proposed by Stanton and Gauss [57] with respect to EOM-CCSD and it is size extensive through all orders. It is important to point out, no truncation scheme has been applied to the higher sectors of FS. The effective Hamiltonian of *(0,1)*, *(1,0)* and *(1,1)* sectors are complete with respect to the truncated effective Hamiltonian of the ground state. The next subsection presents the hierarchy of FSCC(n) methods, explicitly stating the terms contributing to the effective Hamiltonian at each level of truncation and the working equations related to it.

5.2.1 FSCC(2)

Taking the canonical HF as the reference determinant, f is zeroth order, v and T_2 appear at first order and T_1 appears at second order in correlation. Expanding equation (5.2) and collecting all terms up to second order in perturbation we get

$$\bar{H}^{(2)} = v + \left(fT_2\right)_c + \left(vT_2\right)_c \tag{5.4}$$

where, normal ordering of the operators have been assumed. The T_2 amplitude equation is defined by the following expression.

$$\left\langle \phi_{ij}^{ab} \middle| v + \left(fT_2 \right)_c \middle| \phi_0 \right\rangle = 0 \tag{5.5}$$

Hence, the correlation energy is now given by,

$$E^{(2)} = \left\langle \phi_0 \middle| vT_2 \middle| \phi_0 \right\rangle \tag{5.6}$$

Thus FSCC(2) is similar to the MBPT(2) approximation and leads to identical results. This method scales as N^5 and is an attractive choice for study of difference energies for larger systems and also response properties.

5.2.2 FSCC(3)

Similar to the previous method, expanding equation (5.2) and collecting all terms that contribute up to third order in perturbation we have,

$$\bar{H}^{(3)} = \bar{H}^{(2)} + \frac{1}{2}\left(vT_2T_2 \right)_c + \left(vT_1 \right)_c \tag{5.7}$$

T_1 and T_2 amplitude equations are now given by,

$$\begin{aligned} &\left\langle \phi_{ij}^{ab} \middle| v + \left(fT_2 \right)_c + \left(vT_2 \right)_c \middle| \phi_0 \right\rangle = 0 \\ &\left\langle \phi_i^a \middle| \left(fT_1 \right)_c + \left(vT_2 \right)_c \middle| \phi_0 \right\rangle = 0 \end{aligned} \tag{5.8}$$

which is solved in an iterative manner. The final correlation energy is still given by equation (5.6).

5.2.3 FSCC(4)

The various terms contributing to the effective Hamiltonian up to the fourth order are

$$\bar{H}^{(4)} = \bar{H}^{(3)} + \left(vT_1T_2 \right)_c \tag{5.9}$$

Where the amplitude equations will be solved by the following sets of equations,

$$\begin{aligned} &\left\langle \phi_{ij}^{ab} \middle| v + \left(fT_2 \right)_c + \left(vT_2 \right)_c + \left(vT_1 \right)_c + \frac{1}{2}\left(vT_2T_2 \right)_c \middle| \phi_0 \right\rangle = 0 \\ &\left\langle \phi_i^a \middle| \left(fT_1 \right)_c + \left(vT_2 \right)_c + \left(vT_1 \right)_c \middle| \phi_0 \right\rangle = 0 \end{aligned} \tag{5.10}$$

The correlation energy is obtained from equation (5.6)

5.2.4 FS-CC2

The FSCC(3) and FSCC(4) methods scale as N^6 and hence does not provide any computational simplicity in terms of scaling as compared to the standard FSCCSD calculations. Another lower scaling method that has been extensively used for benchmarking energies and properties of molecules, is the CC2 approach. In the CC2 type of approach, T_2 amplitudes are kept at a minimum but solved for the entire set of T_1 equations. We have implemented a similar strategy for the ground state amplitudes and labelled the new method as FS-CC2. Contrary to the FSCC(2) method, FS-CC2 method solves for the singles amplitude equation completely at the cheaper doubles amplitude value. The ground state energy obtained from this method should be similar in nature to that obtained from the FSCC(2) method, as the energy is dominated by the doubles amplitude. However, it remains to be seen how this method will perform for the direct difference energies (IP, EA and EE) and electric response properties as compared to FSCC(2) method. The inclusion of T_1 amplitudes bring in a relaxation factor that was missing in the FSCC(2) method. Although it is not strictly under any perturbative truncation scheme, this method also reduces the computational cost due to its iterative N^5 scaling. In our present study we have incorporated this idea of solving for the T_1 amplitudes at a cheaper T_2 amplitude and used it as an extended approximation to the FSCC(2) method.

5.3 Computational details

In order to achieve computational simplicity we have started with the restricted HF determinant as our reference space, though in principle we can start with any other appropriate single determinant as has been shown by Stanton *et al* [70]. The one and two electron integrals, converged Hartree-Fock coefficients and Eigen values are taken from GAMESS-US [71] package. Calculations were performed at the ground state equilibrium geometry. Hence, all reported values are the vertical energies under the Frank-Condon principle. No frozen core approximation was used in any of the calculations. All the coupled cluster calculations were done using our in-house coupled cluster codes. The ground state cluster amplitudes were generated first, followed by the *(0,1), (1,0)* and *(1,1)* amplitudes. After the generation of T amplitudes, they were contracted with the normal ordered Hamiltonian and stored in the form of $\bar{H}$. All possible terms, up to three body is included in $\bar{H}$. Calculation of

difference energy is performed using the *aug-cc-pVTZ* basis which includes diffuse functions. The dipole moment and polarizabilities are calculated as energy derivatives and the *sadlej-pVTZ* basis set is used which has been optimised for evaluation of response properties.

The energies have been reported for FSCC(n) methods (n=2,3,4) and for the FS-CC2 type of approach. The FS-CC2 approach generates the singles amplitude (i.e. T_1 amplitudes) solving for a cheaper T_2 amplitude. Once the T-amplitudes have been generated for the ground state, we use these for the construction of higher valence excitation amplitudes in the various Fock-space sectors. The molecular set used for the energy comparison with full CCSD results are: ammonia, boron monohydride, hydrogen fluoride, carbon monoxide, hydrogen sulphide, water, methane and methylidyne cation.

Dipole moments and polarizabilities have been calculated using the finite difference method. Since, we have used the difference of energies for generating first and second order properties, our convergence criteria for energy values at all sectors of Fock-space was tightened to an order of 10^{-10}. An electric field value of 10^{-3} atomic units has been applied in the molecular axis direction and the orbitals were allowed to relax before starting off the CC calculations. Hence, all the reported dipole moments and polarizabilities are relaxed response properties. The properties are calculated and compared in FS-CC2 and FSCC(2) formulations. The other two FSCC(n) methods have been dropped off from these test calculations in order to achieve computational simplicity. The test set used for the response calculations include, ammonia, hydrogen fluoride, hydrogen sulphide, carbon monoxide, water, ozone, formaldehyde and methylidyne cation. As Sadlej basis set is not available for Boron atom, we were unable to check for the response properties for boron monohydride molecule.

It is pertinent to mention here that we have not studied the effect of active space dependence of the various approximated methods on the difference energies. Our comparison is only against full FSCCSD calculations within the same active space. Calculation of excitation energies in Fock-space methodology is active space dependent. An efficient way to remove this dependency would be to use Intermediate Hamiltonian technique (IH-FSMRCC) as extensively studied and implemented in the valence universal formalism by Meissner [72-74]. Since, we are comparing the

methods in the same active space, we believe that the general trends will still hold true even on changing the active space.

5.4 Illustrative calculations

The objective of this section is to highlight the changes of difference energy calculations and response properties obtained from the various approximate FSCC(n) and FS-CC2 methods against full FSCCSD. As previously mentioned, the order analysis is only with respect to the ground state similarity transformed Hamiltonian. In the first part of analysis we will discuss the effect of the truncation schemes on the difference energies like IP, EA and EE. The second part of the discussion focuses on the behaviour of the response properties for the various Fock-space sectors in the two lower scaling methods, FS-CC2 and FSCC(2).

5.4.1 Difference energy : IP

Table 5.1 presents the comparison of ionization potentials of the various approximate methods against the full FSCCSD calculation. The active space for the (0,1) sector of each molecule is given below.

Molecules	Active Space
Ammonia	1e, 2e, $3a_1$
Boron hydride	$2\sigma_g$, $3\sigma_g$
Hydrogen fluoride	$3\sigma_g$, 1π, 2π
Hydrogen sulphide	$2b_2$, $5a_1$, $2b_1$
Carbon monoxide	$4\sigma_g$, 1π, 2π, $5\sigma_g$
Water	$1b_2$, $3a_1$, $1b_1$
Methylidyne cation	$2\sigma_g$, $3\sigma_g$
Methane	$1T_2$, $2T_2$, $3T_2$

Table 5.1: Ionization potential tabulated in eV for all the molecules, computed at aug-cc-pVTZ basis

IP	States	FS-CC2	FSCC(2)	FSCC(3)	FSCC(4)	FSCCSD
NH_3	$3a_1$	9.891	9.931	9.994	9.922	9.908
	2e	16.039	16.052	16.165	16.125	16.107
	1e	17.766	17.781	17.889	17.847	17.830
BH	3σ	9.385	9.426	9.987	9.804	9.806
	2σ	17.056	17.116	17.446	17.295	17.308
HF	1π	16.120	16.004	15.953	16.073	16.052
	$3\sigma_g$	20.016	19.902	19.886	19.997	19.976
H_2S	$2b_1$	10.301	10.356	10.577	10.432	10.433
	$5a_1$	13.308	13.362	13.607	13.466	13.465
	$2b_2$	15.606	15.668	15.889	15.753	15.752
CO	$5\sigma_g$	14.047	14.301	14.512	14.181	14.200
	1π	17.237	17.197	17.111	17.148	17.103
	$4\sigma_g$	19.891	19.825	19.803	19.857	19.817
H_2O	$1b_1$	12.662	12.631	12.615	12.639	12.619
	$3a_1$	14.855	14.816	14.824	14.855	14.834
	$1b_2$	19.005	18.959	19.000	19.031	19.009
CH^+	3σ	23.704	23.741	24.346	24.172	24.173
	2σ	33.661	33.710	34.092	33.970	33.975
CH_4	$1T_2$	14.259	14.333	14.531	14.409	14.405

The ionization potential energies calculated at the various approximated methods are seen to converge towards the FSCCSD values on increasing the level of perturbation. A close look at the table will show that although FSCC(4) method gives

the energy difference nearly as good as that obtained from the FSCCSD calculations, this is not so for FSCC(3) over FSCC(2). One would expect that the FSCC(3) would have improved the results over FSCC(2) method, but this is clearly not the case. In case of ammonia molecule, the FSCC(2) method outperforms the FSCC(3) method for all the three states under consideration. Similar trend is followed by hydrogen fluoride, hydrogen sulphide, methane and the sigma state symmetries of carbon monoxide. Only the remaining three molecules i.e. water, methylidyne cation and boron hydride show the IP to be generated more accurately by the FSCC(3) method rather than FSCC(2). Although for the majority of states under consideration the FSCC(2) method does provide superior IP values over its immediate higher counterpart, no fixed trend can be predicted directly from the table without any error analysis. On comparing the FS-CC2 with the FSCC(2) method we find that although the latter does provide better IPs, the difference between them is small.

A general comparison of the plot of root mean squared deviation (rmsd) is shown in figure 5.1. It is evident from the chart that FSCC(4) outperforms all the other approximate methods when compared to the FSCCSD. This error analysis also shows that FSCC(3) does perform better than FSCC(2). In order to understand this point in detail, we have plotted the maximum deviation in eV in figure 5.2. This plot shows that even though in some cases the FSCC(2) method does perform better than FSCC(3), the maximum deviation is substantially higher for the FSCC(2) method for one particular state. Although, on an average the FSCC(3) method might perform better than FSCC(2), it cannot be safely concluded that for any particular IP it will provide better agreement than its perturbative lower counterpart. The two lower scaling methods, FSCC(2) and FS-CC2, follow similar trends in terms of rmsd values and maximum deviation.

Figure 5.1: Root mean squared deviation (rmsd) plot in eV for the ionization potential values as tabulated in table 5.1 for all the molecules

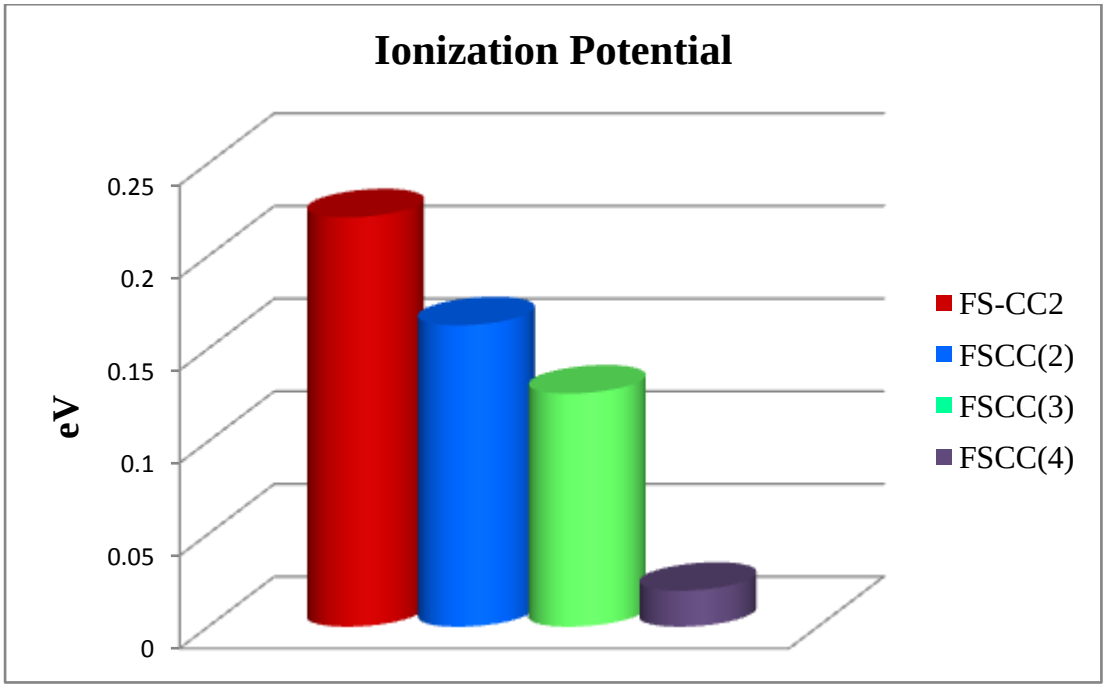

Figure 5.2: The maximum deviation from FSCCSD IP value in eV

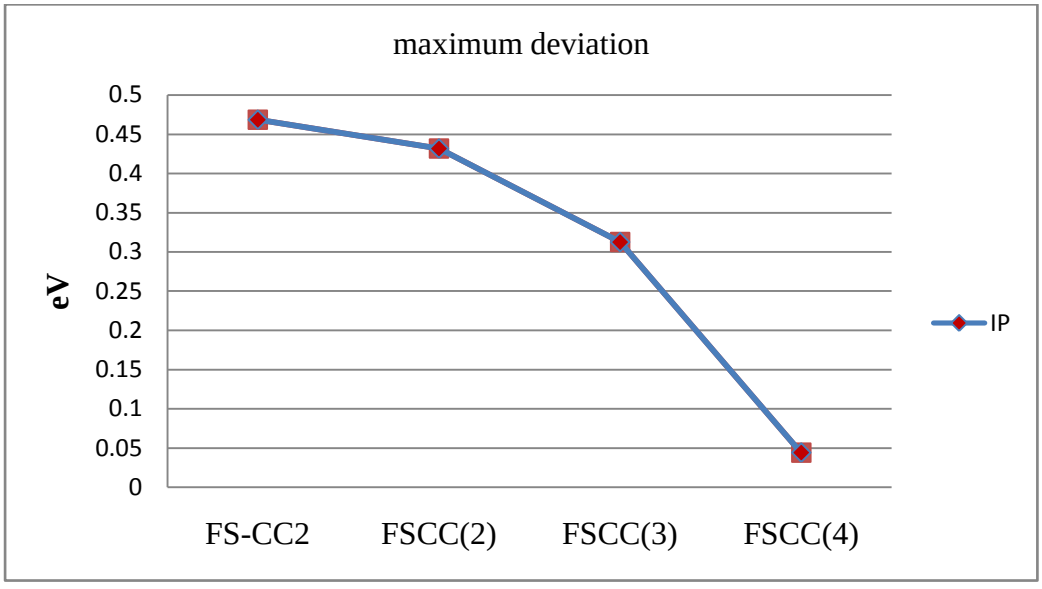

5.4.2 Difference energy : EA

Table 5.2 presents the comparison of electron affinity of the various approximate methods against the full FSCCSD calculation. The active space for the (1,0) sector of each molecule is given below.

Molecules	Active Space
Ammonia	$4a_1$, $5a_1$, $3e$
Boron hydride	1π, 2π, $4\sigma_g$, $5\sigma_g$, 3π, 4π, $6\sigma_g$
Hydrogen fluoride	$4\sigma_g$, $5\sigma_g$, $6\sigma_g$, 3π, 4π
Hydrogen sulphide	$6a_1$, $3b_2$
Carbon monoxide	3π, 4π, $6\sigma_g$, $7\sigma_g$
Water	$4a_1$, $2b_2$
Methylidyne cation	1π, 2π
Methane	$3a_1$, $4T_2$, $5T_2$, $6T_2$

Table 5.2: Electron affinity tabulated in eV for all the molecules, computed at aug-cc-pVTZ basis

EA	States	FS-CC2	FSCC(2)	FSCC(3)	FSCC(4)	FSCCSD
NH_3	$4a_1$	0.642	0.649	0.657	0.648	0.649
	$5a_1$	1.179	1.181	1.182	1.179	1.180
	3e	1.289	1.291	1.292	1.289	1.289
BH	1π	-0.233	-0.272	-0.038	-0.024	-0.032
	$4\sigma_g$	0.794	0.789	0.803	0.811	0.809
	$5\sigma_g$	1.343	1.346	1.353	1.344	1.346
	3π	1.625	1.613	1.687	1.696	1.693
	$6\sigma_g$	2.202	2.199	2.214	2.217	2.216
HF	$4\sigma_g$	0.671	0.678	0.682	0.675	0.675
	$5\sigma_g$	3.495	3.511	3.512	3.498	3.495
	$6\sigma_g$	4.688	4.716	4.728	4.699	4.696
	3π	5.142	5.164	5.152	5.140	5.137
H_2S	$6a_1$	0.516	0.513	0.529	0.528	0.528
	$3b_2$	1.223	1.221	1.228	1.229	1.229
CO	3π	1.574	1.554	1.574	1.594	1.583
	$6\sigma_g$	1.613	1.618	1.621	1.616	1.616
	$7\sigma_g$	1.919	1.910	1.913	1.923	1.920
H_2O	$4a_1$	0.618	0.627	0.632	0.622	0.623
	$2b_2$	1.234	1.235	1.235	1.233	1.234
CH^+	1π	-10.865	-10.906	-10.555	-10.558	-10.560
CH_4	$3a_1$	0.644	0.645	0.653	0.651	0.651
	$4T_2$	1.285	1.286	1.288	1.287	1.287

Similar to the IP case, electron affinity energies calculated at the various approximated methods are seen to converge towards the FSCCSD values on increasing the level of perturbation. As can be inferred from the table itself for the majority of states under consideration, FSCC(3) method performs better than FSCC(2), while FSCC(4) scores over FSCC(3). There are some states where the FSCC(2) method does perform better than FSCC(3) but the difference in EA value between the two methods in those particular states is very small. A comparison

between the two lower scaling methods, FS-CC2 and FSCC(2) show the CC2 type of approach (FS-CC2 method) to perform better for most of the states. In order to get a clear picture of the general trend, a plot of rmsd error bars are provided in figure 5.3.

Figure 5.3: Root mean squared deviation (rmsd) plot in eV for the electron affinity values as tabulated in table 5.2 for all the molecules

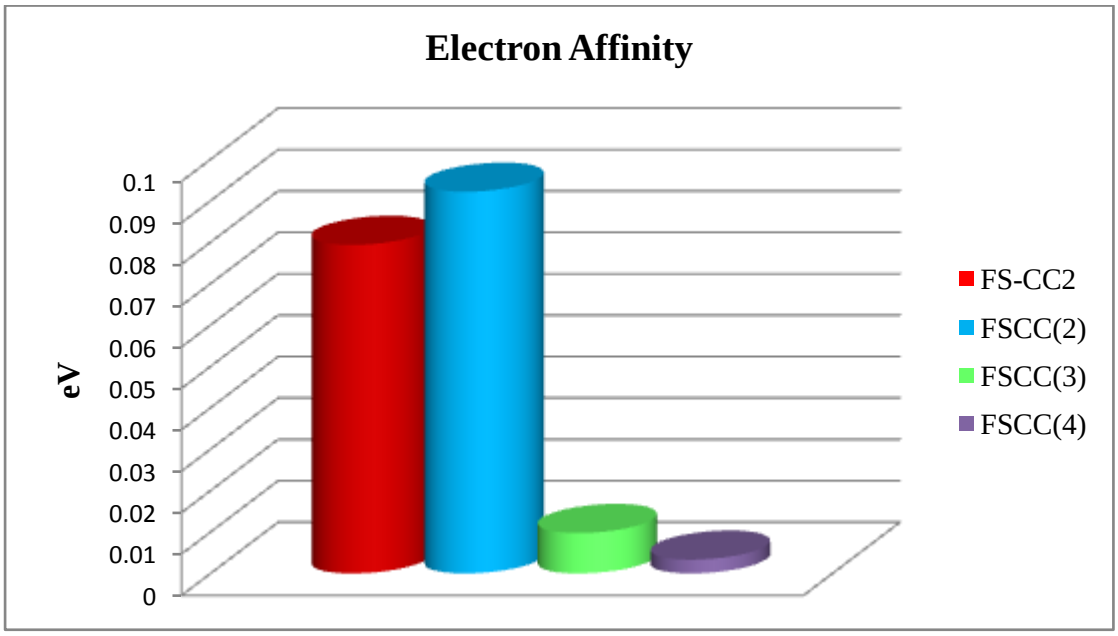

Figure 5.4: Maximum deviation from FSCCSD EA value in eV

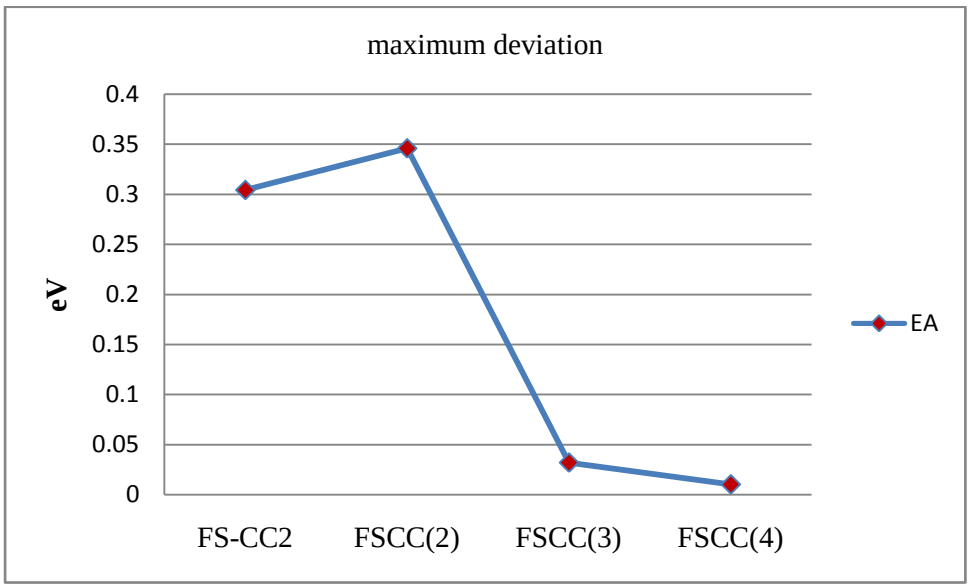

It is evident from the chart that FSCC(4) again outperforms its lower ordered perturbative counterparts by a large margin. The FSCC(3) method is also seen to perform substantially better than either FSCC(2) or FS-CC2. The FS-CC2 method

does also perform marginally better than the other lower scaling method. A plot of the maximum deviation also highlights the same trend as found in the rmsd plot. The FSCC(2) method is seen to deviate the most, while the deviation is negligible in case of FSCC(4)

In contrast with the previously tabulated IP values, it is seen that FS-CC2 method performs better for EA case, as compared with the FSCC(2) method. However, no far reaching conclusion can be drawn from the analysis of such a limited data set. Both the difference energy calculations show that the higher order perturbative approximate methods, FSCC(3) and FSCC(4) are superior to their lower order counterparts. The FSCC(4) method is already in close proximity to the full FSCCSD value for both IP and EA problems.

5.4.3 Difference energy : EE

The singlet excitation energies of all the molecules for a few low lying states are given below.

Table 5.3: Singlet excitation energies tabulated in eV for all the molecules, computed at aug-cc-pVTZ basis

Singlet Energies	States	FS-CC2	FSCC(2)	FSCC(3)	FSCC(4)	FSCCSD
NH_3	1e to $4a_1$	13.932	13.953	14.078	14.025	14.011
	1e to $5a_1$	15.256	15.271	15.381	15.337	15.321
	1e to 3e	15.383	15.402	15.513	15.466	15.450
	2e to $4a_1$	12.138	12.155	12.285	12.236	12.220
	2e to $5a_1$	13.491	13.505	13.620	13.578	13.561
	2e to 3e	13.686	13.699	13.815	13.772	13.755
	$3a_1$ to $4a_1$	6.054	6.097	6.180	6.100	6.088
	$3a_1$ to $5a_1$	7.386	7.427	7.495	7.420	7.407
	$3a_1$ to 3e	7.504	7.546	7.615	7.538	7.526
BH	$2\sigma_g$ to 1π	10.672	10.701	11.186	11.042	11.047
	$2\sigma_g$ to $4\sigma_g$	13.822	13.868	14.215	14.078	14.086
	$2\sigma_g$ to $5\sigma_g$	15.036	15.093	15.451	15.297	15.309
	$2\sigma_g$ to 3π	15.107	15.154	15.568	15.413	15.419
	$2\sigma_g$ to $6\sigma_g$	15.736	15.794	16.147	15.995	16.007

	$3\sigma_g$ to 1π	2.438	2.438	3.053	2.935	2.932
	$3\sigma_g$ to $4\sigma_g$	6.308	6.345	6.909	6.733	6.735
	$3\sigma_g$ to $5\sigma_g$	7.358	7.403	7.965	7.773	7.777
	$3\sigma_g$ to 3π	7.302	7.336	7.922	7.746	7.747
	$3\sigma_g$ to $6\sigma_g$	8.291	8.330	8.896	8.716	8.718
	$3\sigma_g$ to $4\sigma_g$	14.484	14.385	14.372	14.471	14.446
	$3\sigma_g$ to $5\sigma_g$	18.266	18.138	18.136	18.256	18.234
	$3\sigma_g$ to $6\sigma_g$	18.972	18.867	18.862	18.962	18.938
	$3\sigma_g$ to 3π	18.575	18.485	18.467	18.560	18.539
HF	1π to $4\sigma_g$	10.541	10.444	10.418	10.517	10.495
	1π to $5\sigma_g$	13.961	13.861	13.817	13.921	13.900
	1π to $6\sigma_g$	15.020	14.915	14.874	14.983	14.960
	1π to 3π	14.635	14.539	14.484	14.590	14.570
	1π to 4π	14.650	14.558	14.504	14.606	14.586
	$2b_2$ to $6a_1$	11.740	11.791	12.045	11.914	11.912
	$2b_2$ to $3b_2$	13.080	13.140	13.374	13.390	13.390
	$5a_1$ to $6a_1$	9.583	9.629	9.898	9.760	9.758
H_2S	$5a_1$ to $3b_2$	10.886	10.933	11.200	11.061	11.059
	$2b_1$ to $6a_1$	6.571	6.620	6.870	6.725	6.726
	$2b_1$ to $3b_2$	7.757	7.804	8.082	7.932	7.932
	$4\sigma_g$ to $6\sigma_g$	16.629	16.632	16.492	16.617	16.590
	$4\sigma_g$ to 3π	15.619	15.538	15.604	15.669	15.614
	$4\sigma_g$ to $7\sigma_g$	17.863	17.787	17.777	17.838	17.795
	1π to 3π	13.970	13.961	13.749	13.902	13.868
	1π to 4π	14.439	14.319	14.323	14.430	14.375
CO	1π to $6\sigma_g$	12.137	12.040	12.084	12.163	12.096
	1π to $7\sigma_g$	15.142	15.090	15.010	15.060	15.013
	$5\sigma_g$ to $6\sigma_g$	11.170	11.395	11.603	11.308	11.318
	$5\sigma_g$ to 3π	9.737	9.895	10.104	9.896	9.879
	$5\sigma_g$ to $7\sigma_g$	11.696	11.947	12.159	11.833	11.850
	$1b_2$ to $4a_1$	14.429	14.393	14.449	14.466	14.447
	$1b_2$ to $2b_2$	16.076	16.027	16.073	16.110	16.087
	$3a_1$ to $4a_1$	10.469	10.436	10.464	10.484	10.464
H_2O	$3a_1$ to $2b_2$	12.132	12.097	12.110	12.136	12.115
	$1b_1$ to $4a_1$	8.167	8.147	8.150	8.161	8.143
	$1b_1$ to $2b_2$	9.895	9.869	9.860	9.878	9.858

CH^+	$2\sigma_g$ to 1π	14.167	14.169	14.755	14.654	14.656
	$3\sigma_g$ to 1π	2.539	2.533	3.248	3.132	3.129
CH_4	$1T_2$ to $3a_1$	10.887	10.887	11.095	10.977	10.973
	$1T_2$ to $4T_2$	12.067	12.067	12.269	12.148	12.144
	$1T_2$ to $5T_2$	12.189	12.189	12.392	12.270	12.266
	$1T_2$ to $6T_2$	12.187	12.187	12.391	12.268	12.264
	$2T_2$ to $3a_1$	10.887	10.887	11.095	10.977	10.973
	$2T_2$ to $4T_2$	12.188	12.188	12.391	12.269	12.264
	$2T_2$ to $5T_2$	12.194	12.194	12.396	12.275	12.271
	$2T_2$ to $6T_2$	12.196	12.196	12.396	12.277	12.273
	$3T_2$ to $4T_2$	12.188	12.188	12.391	12.269	12.265
	$3T_2$ to $5T_2$	12.194	12.194	12.395	12.275	12.271
	$3T_2$ to $6T_2$	12.195	12.195	12.396	12.276	12.271

Table 5.3 gives the excitation energies for the singlet case. The detailed data set for triplet excitation energies can be found in the appendix A. As is seen from table 5.3, the singlet excitation energies also follow the same trend as the IP and EA case. The perturbative higher ordered methods outperform the lower ordered ones. This is also the case for triplet excitation energies. A comparison between the two lower order methods show that FSCC(2) performs better for both the singlet and triplet energy than the FS-CC2. A plot of rmsd error analysis for both singlet and triplet states clearly show the superiority of FSCC(4) and FSCC(3) over either of the two lower scaling ones. A close look at the rmsd plots between the singlet energies will show that the rmsd for singlet EE for all the methods are comparable to the triplet EE. In both the case the rmsd is around 0.2 eV, which is consistent with that reported by Nooijen in closely related STEOM-PT method [66]. Figures 5.7(a) and 5.7(b) depicts the maximum deviation of the singlet and triplet excitation energies for all the methods respectively. As seen in case of singlet and triplet EE, although the maximum deviation is slightly greater for the FSCC(2) method as compared with FS-CC2, on an average the FSCC(2) method outperforms the FS-CC2 method. The maximum deviation in case of FSCC(2) is greater for a particular transition in CH^+ ion. As can be seen in table 5.3, the $3\sigma_g$ to 1π transition of CH^+ molecule, accounts for the larger error in both the lower scaling methods. This is also seen in case of triplet excitation energy.

Figure 5.5: Root mean squared deviation (rmsd) plot in eV for the singlet excitation energies for all the molecules

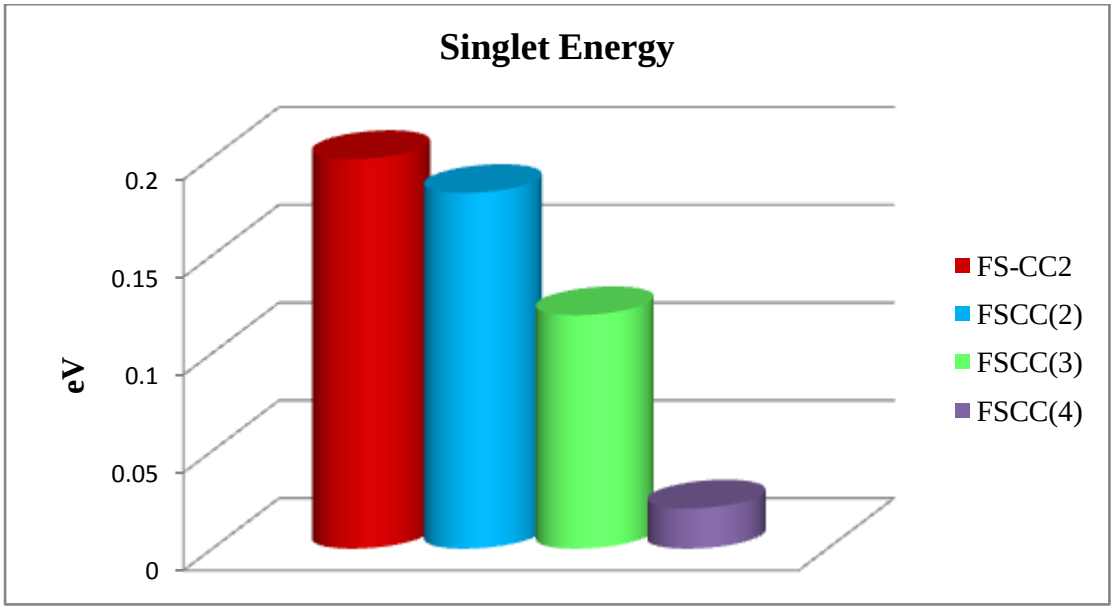

Figure 5.6: Root mean squared deviation (rmsd) plot in eV for the triplet excitation energies for all the molecules

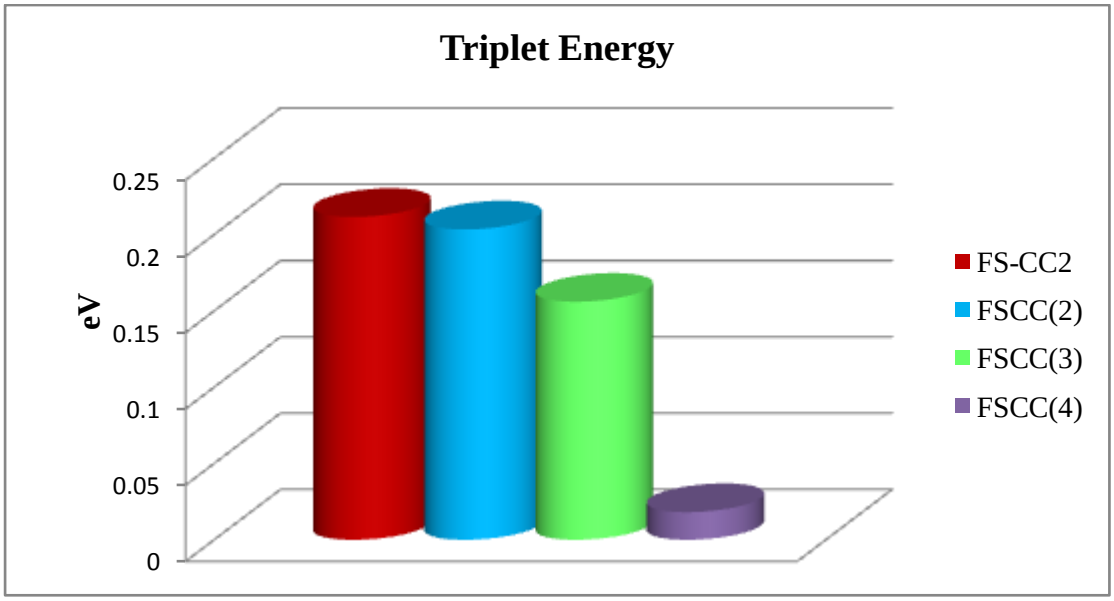

Figure 5.7(a): The maximum deviation from FSCCSD singlet EE values in eV

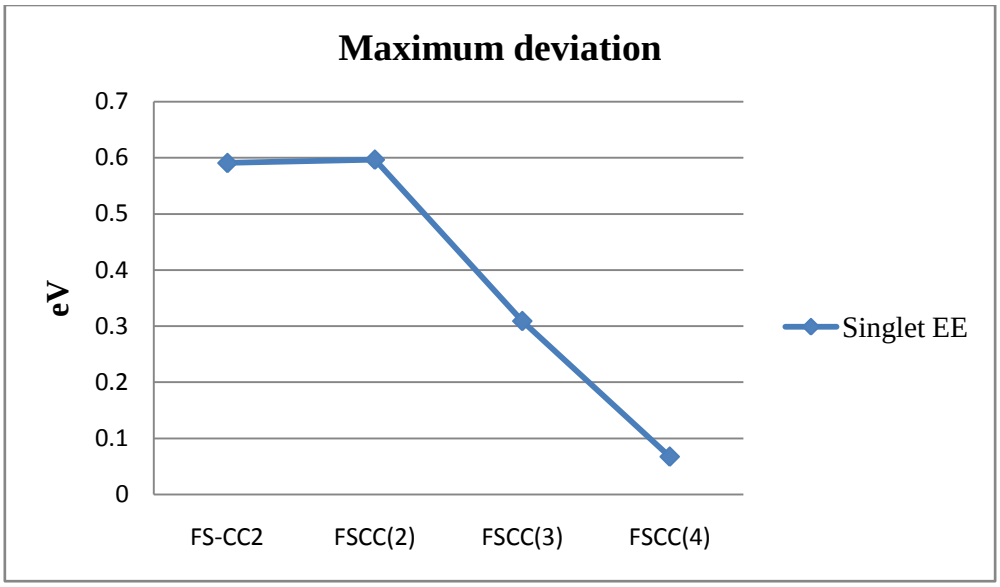

Figure 5.7(b): The maximum deviation from FSCCSD triplet EE values in eV

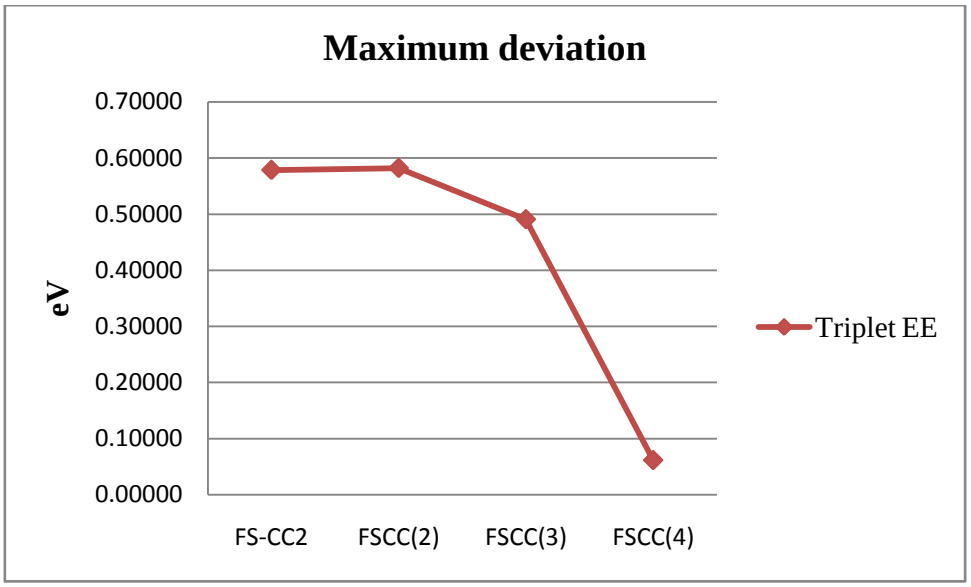

5.4.4. Response properties : Dipole moment and polarizability

5.4.4.1 (0,1) Sector

The response properties for the (0,1) sector is tabulated in table 5.4. All the calculated values are in atomic units. While reporting the dipole moments and polarizabilities, we have not included the SCF moments. So, the table below, reports the response properties for the correlated part only. Addition of the SCF moments will occur as a constant for each molecule and hence, the trend will still remain the same. Since, we have applied finite difference technique to calculate response properties, the direction of applied electric field is primarily the molecular direction for all the systems under study. The external field was applied in only one direction and the first and second order properties are calculated using the five point central difference method. The direction of applied field for ammonia is x-direction, for water it is the y-direction and z-direction for all other molecules. Only the two low scaling methods are checked against the full FSCCSD calculations. Even though FSCC(3) and FSCC(4) performed extremely well in case of difference energies, they have the same scaling as FSCCSD, thus providing no computational simplicity. The prime motivation of the study is to check for the behaviour of the FS-CC2 and FSCC(2) methods compared to full FSCCSD.

A mere look at the dipole values obtained from the low scaling methods is not sufficient to draw any meaningful comparison between the two. In some of the states, the FSCC(2) method performs slightly better than its fellow counterpart, while in some others FS-CC2 gives better results. In case of polarizability, the difference is quite clear. The FS-CC2 method outperforms the FSCC(2) method by a large extent. The same is clear from a rmsd plot as shown in figure 5.8. No conclusive evidence is obtained from the dipole moment viewpoint. Both FS-CC2 and FSCC(2) give comparable first order properties with respect to the FSCCSD calculations as is seen from the error bars, which is consistent with that reported by *Dutta. et. al.* for geometries of doublet radical [67].

Note: All the figures pertaining to response properties are given at the end of this section to facilitate comparison between them.

Table 5.4: Dipole moments and polarizabilities of the (0,1) sector, tabulated in atomic units for all the molecules, computed at Sadlej-pVTZ basis

Properties for (0,1) sector	States	Full CCSD		FS-CC2		FSCC(2)	
		Dipole	Polarizability	Dipole	Polarizability	Dipole	Polarizability
HF	1π	0.227	2.54	0.230	2.51	0.226	2.28
	$3\sigma_g$	0.248	2.64	0.247	2.60	0.248	2.41
CH^+	3σ	0.177	2.66	0.189	2.75	0.190	2.77
	2σ	0.420	2.19	0.493	2.14	0.498	2.18
H_2S	$2b_1$	0.275	8.22	0.289	8.03	0.283	7.77
	$5a_1$	0.169	8.59	0.170	8.36	0.165	8.18
	$2b_2$	0.598	7.72	0.610	7.42	0.605	7.21
H_2CO	$2b_2$	0.907	5.48	0.912	5.31	0.900	5.75
	$1b_1$	0.946	7.64	0.977	7.60	0.941	7.57
	$5a_1$	1.271	4.03	1.282	3.65	1.277	4.29
	$1b_2$	0.507	7.10	0.538	7.04	0.520	6.17
NH_3	$3a_1$	0.073	5.72	0.075	5.60	0.075	5.29
	2e	0.243	4.66	0.242	4.50	0.242	4.17
	1e	0.074	5.21	0.071	5.00	0.071	11.92
H_2O	$1b_1$	0.146	4.10	0.149	3.97	0.145	3.53
	$3a_1$	0.002	4.37	0.002	4.25	0.005	3.92
	$1b_2$	0.304	3.69	0.305	3.56	0.303	3.14
CO	$5\sigma_g$	0.304	2.53	0.323	2.47	0.323	1.81

	1π	1.171	4.97	1.237	4.88	1.232	4.86
	$4\sigma_g$	1.583	5.85	1.659	5.55	1.650	5.89
	$1a_2$	1.049	2.63	1.090	2.54	1.093	2.18
O_3	$6a_1$	1.149	2.36	1.181	2.24	1.171	1.89
	$4b_2$	1.066	2.45	1.103	2.35	1.094	1.93

5.4.4.2 (1,0) Sector

The dipole moments and polarizabilities of the (1,0) sector is presented below in table 5.5. Similar to the previous sector (section 5.4.4.1), the SCF moments have not been added to the final correlation calculations and hence, tabulated values are the correlated dipole moments and polarizabilities. The calculations are performed under similar conditions as done for the (0,1) sector, i.e. an external electric field was applied to all the molecules along their molecular axis as stated in the previous subsection.

A look at the behaviour of the dipole moments of each molecule show that both the approximate methods, give nearly exact dipole moments as that given by full FSCCSD method. The first order properties in this sector is thus well described by the two low scaling methods. In case of polarizability, the FS-CC2 method performs better than FSCC(2). This trend is similar to the one seen in (0,1) sector and we believe that the T_1 amplitudes included in the FS-CC2 calculations are responsible for its better performance over FSCC(2). Although the FS-CC2 method performs better, the maximum deviation is larger in this sector, as compared to the (0,1) sector. The FS-CC2 and FSCC(2) methods show a maximum deviation of 15 and 31 a.u. with respect to polarizability calculations. This affects the root mean squared deviation too and is seen in figure 5.9.

Table 5.5: Dipole moments and polarizabilities of the (1,0) sector, tabulated in atomic units for all the molecules, computed at Sadlej-pVTZ basis

Properties for EA	States	Full CCSD		FS-CC2		FSCC(2)	
		Dipole	Polarizability	Dipole	Polarizability	Dipole	Polarizability
HF	$4\sigma_g$	0.034	96.77	0.034	96.72	0.034	95.98
	$5\sigma_g$	0.017	21.76	0.017	21.62	0.017	20.25
CH^+	1π	0.003	8.33	0.002	8.34	0.002	8.30
H_2S	$6a_1$	0.013	492.98	0.013	486.30	0.013	487.56
	$3b_2$	0.040	175.51	0.040	168.18	0.040	169.38
	$4b_2$	0.012	360.08	0.013	350.76	0.013	352.82
	$7a_1$	0.013	73.37	0.013	58.77	0.013	62.45
	$3b_1$	0.003	58.15	0.003	58.69	0.003	58.49
H_2CO	$2b_1$	0.044	369.05	0.044	364.39	0.045	345.09
	$6a_1$	0.007	33.10	0.007	46.40	0.007	10.10
	$3b_2$	0.028	285.89	0.028	270.42	0.029	302.11
	$7a_1$	0.017	119.43	0.016	126.81	0.016	150.66
NH_3	$4a_1$	0.004	918.47	0.004	906.06	0.004	920.79
	$5a_1$	0.014	107.96	0.014	108.99	0.014	107.54
	3e	0.022	834.60	0.022	820.09	0.022	835.84
H_2O	$4a_1$	0.019	122.41	0.019	122.10	0.019	122.48
	$2b_2$	0.021	25.22	0.021	25.43	0.021	25.29
CO	3π	0.002	636.14	0.003	634.89	0.005	622.05
	$6\sigma_g$	0.006	58.45	0.007	56.53	0.007	56.33
	$7\sigma_g$	0.001	342.99	0.002	341.17	0.001	321.94
O_3	$2b_1$	0.012	8.89	0.012	8.99	0.012	8.09

5.4.4.3 (1,1) Sector

The singlet and triplet response properties are given as rmsd plots in figures 5.10 and 5.11. Due to the large number of data points for the excitation energy calculations, the details of the dipole moments and polarizabilities of the excited states are not included in this thesis. As can be seen from the rmsd plots, the FS-CC2 method, outperforms the FSCC(2) method for both dipole moment and polarizability in the singlet and triplet excited states. Although the FS-CC2 method does perform better for polarizability, the deviation from FSCCSD calculation for the same is quite large.

Figure 5.8: Root mean squared deviation (rmsd) plot in atomic units for the response properties of the (0,1) sector

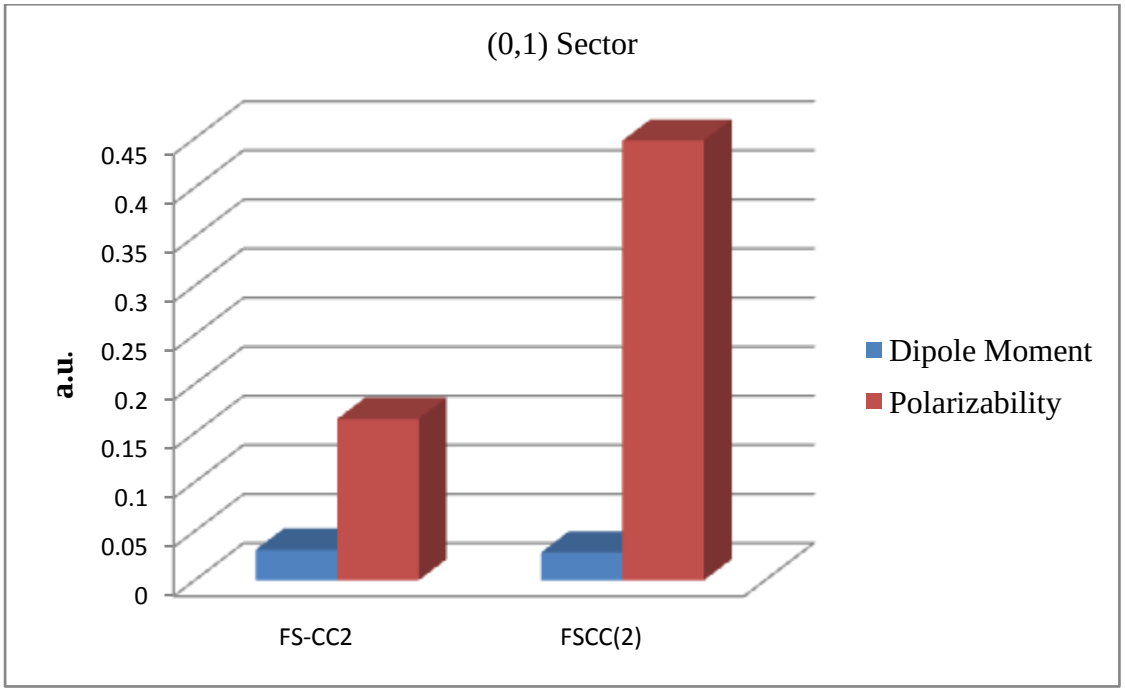

Figure 5.9: Root mean squared deviation (rmsd) plot in atomic units for the response properties of the (1,0) sector

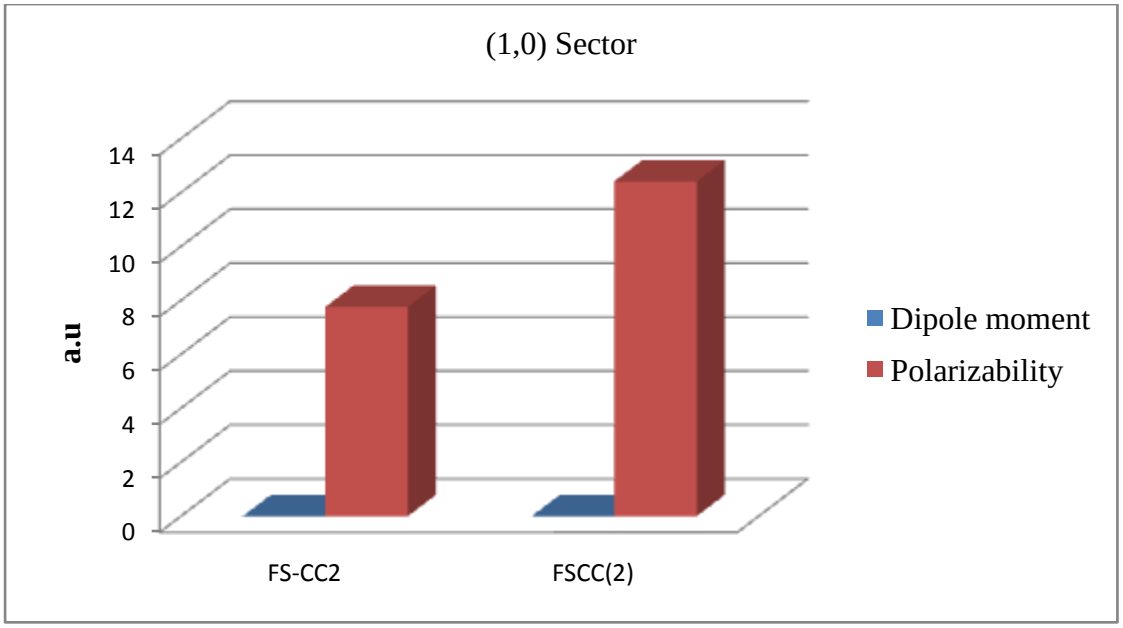

Figure 5.10: Root mean squared deviation (rmsd) plot in atomic units for the response properties of the (1,1) sector (both singlet and triplet dipole moments)

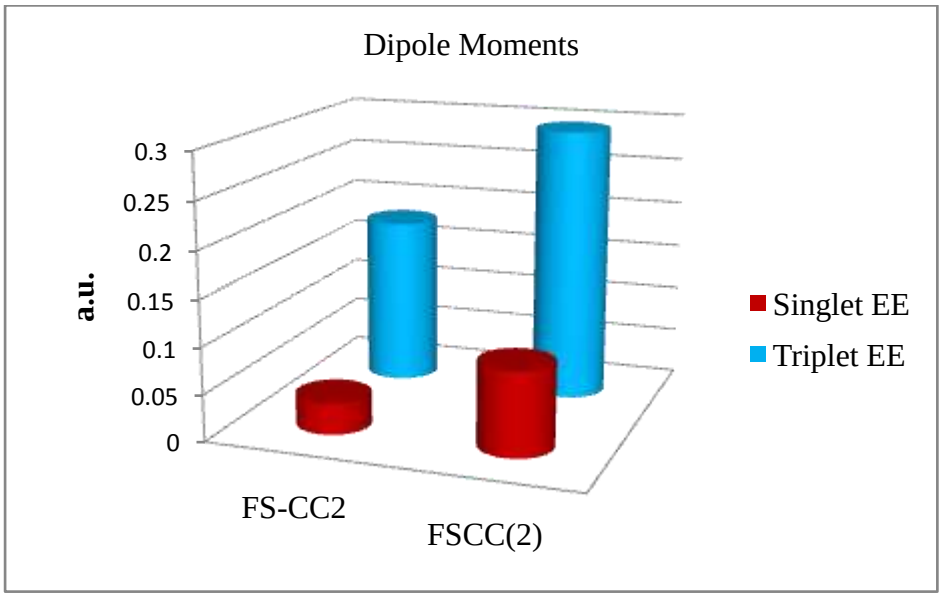

Figure 5.11: Root mean squared deviation (rmsd) plot in atomic units for the response properties of the (1,1) sector (both singlet and triplet polarizabilities)

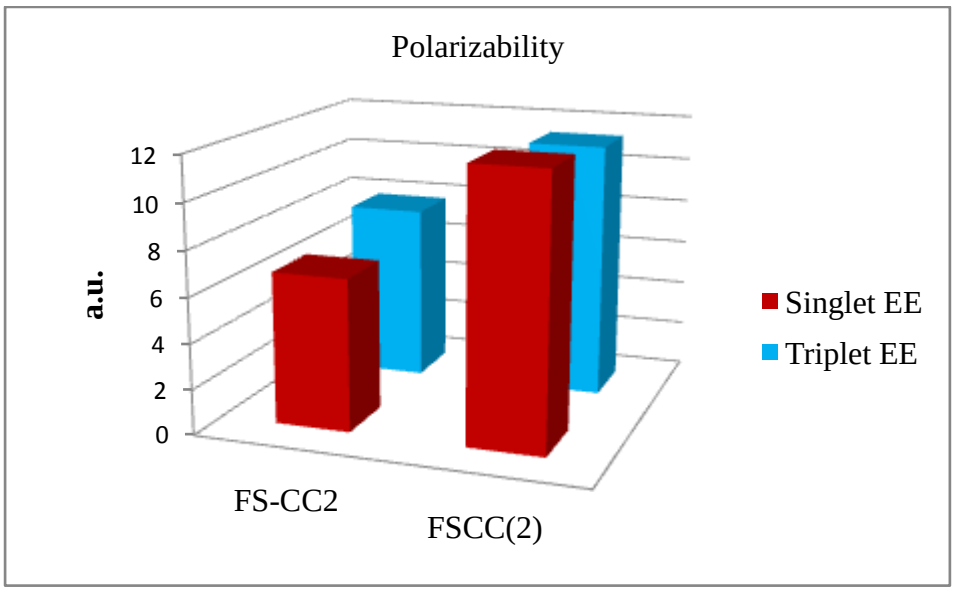

5.5 Concluding Remarks

Behaviour of the direct difference energies in all three approximate FSCC(n) methods show a gradual convergence towards the FSCCSD values. This is as expected from a theoretical viewpoint due to the perturbational nature of truncation. Although the IP, EA and EE values, converge smoothly towards FSCCSD on increasing the perturbational order, there is no guarantee that in each FSCC(n) method the value would converge from one end. As is seen in MBPT, FSCC(n) methods do not have a fixed upper or lower bound to the FSCCSD values. The FSCC(n) methods give fluctuating difference energies but the error deviation will keep on decreasing on increase in perturbational order, finally converging completely to FSCCSD values at a higher order. Among the various direct difference energies computed earlier, the singlet and triplet energies as well as the ionization energies show similar trend. Although the trend is a bit different for the electron affinity case, where FS-CC2 outperforms the FSCC(2). However, they always give comparable values. Therefore, it may be interesting to pursue FS-CC(2) for large scale excitation energy calculation as an alternative to more popular CC2 method.

The two low scaling methods, FS-CC2 and FSCC(2) were compared against standard FSCCSD to test their performance for electric response properties. It can be seen that FS-CC2 shows better performance than the FS-CC(2) method for dipole moment and polarizability. The betterment in result is more prominent in case of polarizability. It is well known that singles amplitudes contributes at least second order in perturbation. Therefore, inclusion on T_1 has a pronounced effect on polarizability (which is a second order property) than that in the first order property of dipole moment. The part of the missing second order perturbation effect, arising from second order T_2 terms in case of FS-CC2 and from second order T_1 and T_2 terms in case FS-CC(2), also explains the huge error in polarizability as compared to the full FSCCSD. The first order property dipole moment, however, is reproduced with reasonable accuracy in both the approximate versions.

In conclusion one can state that, as a further approximation to the FSCC(2) method, a CC2 type of approach gives reasonable energy differences as well as electric response properties, and this can be an attractive alternate method to study large molecular systems, where a N^6 scaling prohibits standard FSCCSD calculations.

References

[1] D. Mukherjee, Pramana 12, 203 (1979

[2] W. Kutzelnigg, J. Chem. Phys. **77**, 2081 (1982)

[3] D. Mukherjee, R. K. Moitre and A. Mukhopadhyay, Mol. Phys. **30,** 18

[4] I. Lindgren and D. Mukherjee, Phys. Rep. **151**, 93 (1987)

[5] A. Haque and U. Kaldor, Chem. Phys. Lett. **117**, 347 (1985)

[6] D. Mukherjee and S.Pal, Adv. Quantum Chem. **20**, 291 (1989)

[7] S. Pal, M. Rittby, R.J. Bartlett, D. Sinha and D. Mukherjee, J. Chem. Phys. **88**, 4357 (1988)

[8] U. Kaldor, Theor. Chim. Acta. **80**, 427 (1991)

[9] S.Pal, Mol. Phys. **108**, 3033 (2010)

[10] J. Geertsen, M. Rittby and R. J. Bartlett, J. Chem. Phys. Lett. **164**, 57 (1989)

[11] J. F. Stanton and R. J. Bartlett, J. Chem. Phys. **98**, 7029 (1993)

[12] R. J. Bartlett and J. F. Stanton, In Reviews in Computational Chemistry; Eds. L. B. Lipkowitz and D. B. Boyd. VCH: New York, Vol. **5**, p 65 (1994)

[13] P.A. Pieniazek, S. A. Arnstein, S. E. Bradforth, A. I. Krylov and C. D. Sherrill, J. Chem. Phys. **127**, 164110 (2007)

[14] M. Nooijen and R. J. Bartlett, J. Chem. Phys. **102**, 3629 (1995)

[15] K. Kowalski and P. Piecuch, Chem. Phys. Lett. **347**, 237 (2001)

[16] H. Sekino and R. J. Bartlett, Int. J. Quantum Chem. **26**, 255 (1984)

[17] A.I. Krylov, Annu. Rev. Phys. Chem. **59**, 433 (2008)

[18] G. D. Purvis and R. J. Bartlett, J.Chem. Phys. **76**, 1910 (1982)

[19] G. E. Scuseria and H. F. Schaefer, Chem. Phys. Lett. **146**, 23 (1988)

[20] G. E. Scuseria, Chem. Phys. Lett. **176**, 27 (1991)

[21] J. F. Stanton, Chem. Phys. Lett. **281**, 130 (1997)

[22] J. Noga and R. J. Bartlett, J. Chem. Phys. **86**, 7041 (1987)

[23] S. A. Kucharski and R. J. Bartlett, J. Chem. Phys. **108**, 5243 (1998)

[24] K. Raghavachari, G. W. Trucks, J. A. Pople and M. Head-Gordon, Chem. Phys. Lett. **157**, 479 (1989)

[25] R. J. Bartlett, J. D. Watts, S. A. Kucharski and J. Noga, J. Chem. Phys. Lett. **165**, 513 (1990)

[26] M. Urban, J. Noga, S. J. Cole and R. J. Bartlett, J. Chem. Phys. **123**, 054101 (2005)

[27] K. Kowalski and P. Piecuch, J. Chem. Phys. **115**, 8263 (2001)

[28] K. Kowalski and P. Piecuch, J. Chem. Phys. **113**, 8490 (2000)

[29] S. A. Kucharski, M. Wloch, M. Musial and R. J. Bartlett, J. Chem. Phys. **115**, 8263 (2001)

[30] P. U. Manohar, J. F. Stanton and A. I. Krylov, J. Chem. Phys. **131**, 114112 (2009)

[31] M. Kallay and J. Gauss, J. Chem. Phys. **121**, 9257 (2004)

[32] M. Musial, S. A. Kucharski and R. J. Bartlett, J. Chem. Phys. **118**, 1128 (2003)

[33] P.A. Pieniazek, S. E. Bradforth and A. I. Krylov, J. Chem. Phys. **129**, 074104 (2008)

[34] S. Pal, M. Rittby and R. J. Bartlett, J. Chem. Phys. Lett. **160**, 212 (1989)

[35] N. Vaval, K. B. Ghose, S. Pal and D. Mukherjee, Chem. Phys. Lett. **209**, 292 (1993)

[36] N. Vaval, S. Pal and D. Mukherjee, Theor. Chem. Acc. **99**, 100 (1998)

[37] M. Musial and R. J. Bartlett, J. Chem. Phys. **129**, 244111 (2008)

[38] M. Musial and R. J. Bartlett, J. Chem. Phys. **129**, 044101 (2008)

[39] M. Musial, S. A. Kucharski, P. Zerzucha, T. Kus and R. J. Bartlett, J. Chem. Phys. **131**, 194104 (2009)

[40] J. F. Stanton and J. Gauss, J. Chem. Phys. **101**, 8938 (1994)

[41] S. V. Levchenko, T. Wang and A. I. Krylov, J. Chem. Phys. **122**, 224106 (2005)

[42] J. F. Stanton, J. Chem. Phys. **99**, 8840 (1993)

[43] M. Kallay and J. Gauss, J. Chem. Phys. **121**, 9257 (2004)

[44] J. C. Saeh and J. F. Stanton, J. Chem. Phys. **111**, 8275 (1999)

[45] L. Ravichandran, N. Vaval and S. Pal, J. Chem. Theory Comput. **7**, 876 (2011)

[46] L. Ravichandra, D. Bhattacharya, N. Vaval and S. Pal, J. Chem. Sci. **124**, 223 (2012)

[47] D. Ajitha and S. Pal, J. Chem. Phys. **114**, 3380 (2001)

[48] K. R. Shamasundar, S. Asokan and S. Pal, J. Chem. Phys. **120**, 6381 (2004)

[49] R. J. Bartlett, Annu. Rev. Phys. Chem. **32**, 359 (1981)

[50] S. Hirata, M. Nooijen, I. Grabowski and R. J. Bartlett, J. Chem. Phys. **114**, 3919 (2001)

[51] M. Head-Gordon, R. J. Rico, M. Oumi and T. J. Lee, Chem. Phys. Lett. **219**, 21 (1994)

[52] S. R. Gwaltney and M. Head-Gordon, Chem. Phys. Lett. **323**, 21 (2000)

[53] M. Head-Gordon and co-workers have pursued several truncation schemes, which is similar to EOMCC. For more details, see reference 51 and the references therein.

[54] S. R. Gwaltney, E. F. C. Byrd, T. V. Voorhis and M. Head-Gordon, Chem. Phys. Lett. **353**, 359 (2002)

[55] M. Nooijen and J. G. Snijders, J. Chem. Phys. **102**, 1681 (1995)

[56] J. J. Eriksen, P. Jorgensen, J. Olsen and J. Gauss, J. Chem. Phys. **140**, 174114 (2014)

[57] J. F. Stanton and J. Gauss, J. Chem. Phys. **103**, 1064 (1995)

[58] S. A. Kucharski, R. J. Bartlett and L. Per-Olav, Fifth-order Many Body Perturbation Theory and it's relationaship to various Coupled Cluster Approaches. In Adv. Quantum Chem., Academic Press: 1986; Vol 18, p 281.

[59] In terms of scaling, the EOM-CCSD(2) method scales as N^5 for IP and EA EOMCC calculations. However, for calculation of EA the (ab|cd) integrals are required to be stored. Hence, the storage requirement is same as EOMEA-CCSD.

[60] A. K. Dutta, J. Gupta, H. Pathak, N. Vaval and S. Pal, J. Chem. Theory Comput, **10**, 1923 (2010)

[61] M. Nooijen and R.J. Bartlett, J. Chem. Phys. **106**, 6441 (1997).

[62] M. Nooijen and R.J. Bartlett, J. Chem. Phys. **106**, 6449 (1997).

[63] M. Nooijen and R.J. Bartlett, J. Chem. Phys. **107**, 6812 (1997).

[64] M. Nooijen, Spectrochim. Acta A, **55**, 539 (1999).

[65] Wladyslawski and M. Nooijen, Adv. Quantum Chem. **49**, 1 (2005)

[66] J. Sous , P. Goel and M. Nooijen, Mol. Phys, **112**, 5 (2014)

[67] A. K. Dutta, N. Vaval and S. Pal, J. Chem. Theory Comput. **9**, 4313 (2013)

[68] A. K. Dutta, S. Pal and D. Ghosh, J. Chem. Phys. **139**, 124116 (2013)

[69] S. R. Gwaltney, M. Nooijen and R. J. Bartlett, Chem. Phys. Lett. **248**, 189 (1996)

[70] J. F. Stanton, R. J. Bartlett and C. M. L. Rittby, J. Chem. Phys. **97**, 5560 (1992)

[71] M. W. Schmidt, K. K. Baldridge, J. A. Boatz, S. T. Elbert, M. S. Gordon, J. H. Jensen, S. Koseki, N. Matsunaga, K. A. Nguyen, S. Su,T. L. Windus, M. Dupuis, J. A. Montgomery, J. Comput. Chem. **14**, 1347 (1993)

[72] L. Meissner, J. Chem. Phys. **103**, 8014 (1998)

[73] L. Meissner and P. Malinowski, Phys. Rev. A, **61**, 062510 (2000)

[74] L. Meissner, P. Malinowski and A. Nowaczyk, Chem. Phys. Lett. **381**, 441 (2003)

Chapter 6

Lower scaling methods and their effect on transition moments

In the previous chapter, we evaluated the difference energies and electric response properties in a couple of lower scaling methods within the FSCCSD formulation. In this chapter, we compare the dipole strengths of a few molecules from their ground to low lying excited states. The comparison is performed with the two low scaling methods that has been formulated in the previous chapter, i.e. FSCC(2) and FS-CC2. The dipole strength obtained from these methods are compared against the dipole strength calculated from FSCCSD method.

6.1 Introduction

This chapter checks for the behaviour of the square of transition dipole moments from ground state to a few other singlet excited states for a number of small molecular systems. Driven by the success of treating electric response properties, especially dipole moments (where the root mean squared deviation was around 0.05 a.u. for the singlet transitions) as obtained from the two lower scaling methods, we have calculated and compared the dipole strengths in those two methods against the FSCCSD method. The theory pertaining to the two lower scaling methods are recapitulated first followed by the computational details. Results and discussions come later.

6.2 Theory

6.2.1 FSCC(2) method

Starting with the canonical HF as the reference determinant, the *f* occurs at zeroth order, *v* and T_2 emerge at first order and T_1 materializes at second order in correlation. Expanding $\bar{H}$ and assembling all those terms which contribute to second order in perturbation gives us,

$$\bar{H}^{(2)} = v + \left(fT_2 \right)_c + \left(vT_2 \right)_c \tag{6.1}$$

where, normal ordering of the operators have been assumed. The T_2 amplitude equation is given by the following expression.

$$\left\langle \phi_{ij}^{ab} \middle| v + \left(fT_2 \right)_c \middle| \phi_0 \right\rangle = 0 \tag{6.2}$$

Thus, correlation energy is now given by,

$$E^{(2)} = \left\langle \phi_0 \middle| vT_2 \middle| \phi_0 \right\rangle \tag{6.3}$$

This renders FSCC(2) similar to the MBPT(2) approximation and leads to identical results. This method scales as N^5 as the T_1 amplitudes have been completely neglected from the calculations. Solving for the lowest order of T_2 in the *(0,0)* sector, we use these generated amplitudes for further contraction with the higher valence cluster

amplitudes. No such approximation have been introduced in the higher valence cluster operators.

6.2.2 FS-CC2

Another lower scaling method that has been extensively used for benchmarking energies and properties of molecules, is the CC2 [1-5] approach. In the CC2 type of approach, T_2 amplitudes are kept at a minimum but solved for the entire set of T_1 equations. We have implemented a similar strategy for the ground state amplitudes and labelled the new method as FS-CC2. Contrary to the FSCC(2) method, FS-CC2 method solves for the singles amplitude equation completely at the cheaper doubles amplitude value. The ground state energy obtained from this method should be similar in nature to that obtained from the FSCC(2) method, as the energy is dominated by the doubles amplitude. The inclusion of T_1 amplitudes bring in a relaxation factor that was missing in the FSCC(2) method. Although it is not strictly under any perturbative truncation scheme, this method also reduces the computational cost due to its iterative N^5 scaling. In our present study we have incorporated this idea of solving for the T_1 amplitudes at a cheaper T_2 amplitude and used it as an extended approximation to the FSCC(2) method and tested them for calculation of electronic transition dipole moments.

6.3 Computational Details

In order to evaluate transition moments, we have described three different approaches within the FSCC formalism. Since, the main objective is to check for the variation of TDM in FSCC(2) and FS-CC2 methods, we have evaluated TDM from the expectation value approach (FSCC-T method). The other two methods namely, FSCC-Λ and FSCC-ΛT requires the use of de-excitation amplitudes. We have not truncated any of the Λ-amplitudes in the same manner as that of the similarity transformed Hamiltonian as shown in the previous chapter. Thus, any method that uses these de-excitation operators cannot be presently used to check for the variation of TDM in the two low scaling methods. We have tabulated the dipole strength for the following set of molecules: CO, HCN, HF, LiH, CH^+, NO^+ and H_2O. All the molecules were treated at the ground state equilibrium geometry.

6.4 Results and discussions

Table 6.1 presents the comparison of dipole strengths calculated from the expectation value method within the two approximate methods against the full FSCCSD calculation. The active space for the *(1,1)* sector of each molecule is given below. The active holes and particles are separated by a divider.

Molecules	Active space
CO	$5\sigma / 6\sigma 3\pi 4\pi 7\sigma$
HCN	$1\pi 2\pi / 6\sigma 7\sigma 3\pi 4\pi$
HF	$2\sigma 3\sigma 1\pi 2\pi / 4\sigma 5\sigma$
LiH	$1\sigma 2\sigma / 3\sigma$
CH^+	$2\sigma 3\sigma / 1\pi 2\pi$
NO^+	$4\sigma 1\pi 2\pi 5\sigma / 3\pi 4\pi 6\sigma 7\sigma 5\pi 6\pi 8\sigma$
H_2O	$1b_1 3a_1 1b_2 / 4a_1 2b_1$

Calculations pertaining to the set of molecules as mentioned in the previous section, is done on the ground state equilibrium geometry. The test set calculations was performed on Sadlej-pVTZ basis which has been optimised for property calculations. As can be clearly seen from the table, the FS-CC2 method gives better performance than the FSCC(2) method. This trend is similar to the one previously observed for the dipole moments in singlet sector. A plot of the root mean squared deviation also validates our observation. For most of the molecules, the FS-CC2 method actually gives comparable dipole strengths as that of FSCCSD. The inclusion of T_1 amplitudes in the FS-CC2 calculations introduces some relaxation effect in this approximate method rendering it suitable for such transition moment property calculations.

Table 6.1: Dipole strengths from the closed shell ground state to singlet excited states tabulated in atomic units for all the molecules, computed at Sadlej-pVTZ basis

Molecules	States	Full CCSD	FS-CC2	FSCC(2)
		Dipole Strength	Dipole Strength	Dipole Strength
HF	2σ to 4σ	0.042	0.044	0.054
	2σ to 5σ	0.003	0.004	0.003
	3σ to 4σ	0.431	0.451	0.414
	3σ to 5σ	0.003	0.003	0.002
	1π to 4σ	0.180	0.182	0.139
	1π to 5σ	0.070	0.071	0.061
NO^+	4σ to 3π	0.460	0.476	0.435
	4σ to 6σ	0.089	0.085	0.088
	4σ to 7σ	1.660	1.666	1.810
	5σ to 4π	0.227	0.211	0.197
	5σ to 6σ	0.142	0.155	0.162
	5σ to 8σ	0.394	0.402	0.361
LiH	1σ to 3σ	0.025	0.022	0.021
	2σ to 3σ	1.192	0.987	0.853
HCN	1π to 6σ	0.200	0.197	0.218
	1π to 7σ	0.212	0.222	0.264
	1π to3π	0.860	0.927	0.900
CH^+	2σ to 1π	0.334	0.395	0.392
	3σ to 1π	0.037	0.066	0.066
CO	5σ to 3π	0.712	0.764	0.967
	5σ to 6σ	0.014	0.012	0.032
	5σ to 7σ	0.575	0.572	0.469
H_2O	$1b_1$ to $4a_1$	0.427	0.455	0.440
	$1b_1$ to $2b_1$	0.040	0.042	0.047
	$3a_1$ to $4a_1$	0.448	0.462	0.380
	$1b_2$ to $4a_1$	0.054	0.058	0.049
	$1b_2$ to $2b_1$	0.369	0.372	0.285

Figure 6.1: Root mean squared deviation from FSCCSD dipole strength values in a.u.

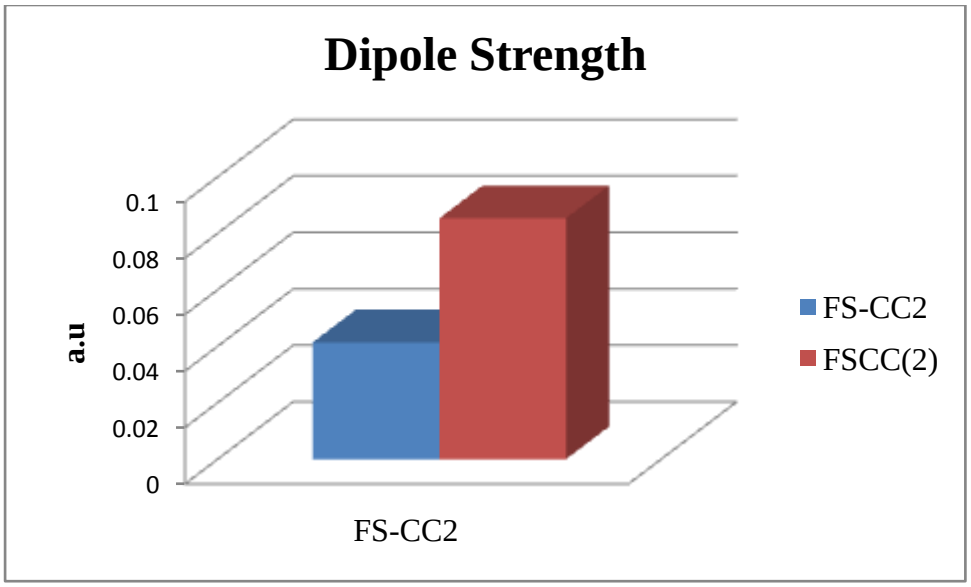

Figure 6.2: Maximum deviation from FSCCSD dipole strength value in a.u.

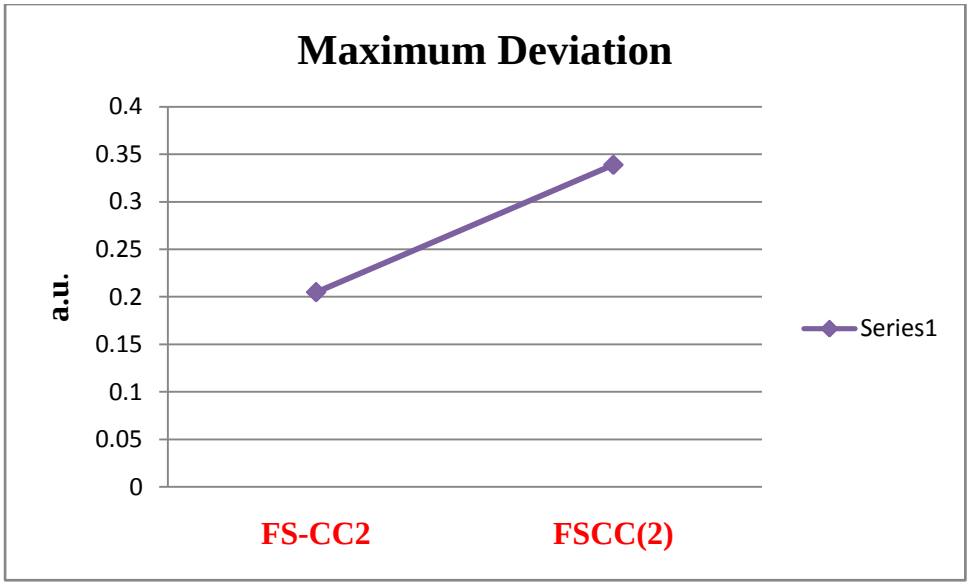

6.5 Concluding remarks

This chapter presented the behaviour of the electronic transition moments in a couple of low scaling methods. The behavioural pattern is similar to the other response properties as calculated and tabulated in the previous chapter. The general trend is very clear from the above test set calculations. Introduction of the T_1

amplitudes generates transition dipoles that are in close agreement with the full FSCCSD calculations. The root mean squared average value as plotted in figure 6.1 shows the mean deviation to be around 0.04 a.u. for the FS-CC2 method. The FSCC(2) approximation deviates more as compared to this. The plot of maximum deviation showcases a deviation of 0.2 a.u and 0.35 a.u. for FS-CC2 and FSCC(2) respectively. This large deviation corresponds to the single transition from the 2σ to 3σ for the LiH molecule. If we treat this particular transition as a 'bad apple' case and neglect it from our relative error calculations, then the rmsd values drop down to 0.025 a.u. and 0.04 a.u. for the FS-CC2 and FSCC(2) calculations. Thus, it can be concluded that FS-CC2 gives nearly comparable transition dipole moments as that of FSCCSD and this method can be further probed to be used for calculations pertaining to larger molecular systems. The FSCC(2) method may also be used for the same purpose but will provide a larger error bar.

References

[1] C. Hattig and F. Weigend, J. Chem. Phys. **113**, 5145 (2000)

[2] C. Hattig, J. Chem. Phys. **118**, 775 (2003)

[3] C. Hattig, Adv. Quantum Chem. **50**, 37 (2005)

[4] A. Hellweg, S. A. Grun and C. Hattig, Phys. Chem. Chem. Phys. **10**, 4119 (2008)

[5] C. Hattig and A. Kohn, J. Chem. Phys. **117**, 6939 (2002)

Chapter 7

Concluding remarks and future scope

This is the concluding chapter wherein the relevant applicability of the thesis is discussed followed by the future scope and discussion on some of the ongoing projects.

7.1 Summary

This thesis presented new developments toward calculation of transition dipole moments within the Fock-space multi-reference coupled cluster (FSMRCC) framework. A couple of lower scaling methods within the FSMRCC singles and doubles scheme was also developed and tested for certain molecular systems.

The first chapter gave a brief introduction to the single reference based many body methods, highlighting the relevant working equations for the single reference coupled cluster (SRCC) method. This was followed by the theory of equation of motion coupled cluster. The need to move beyond single reference based methods came next, followed by the effective Hamiltonian based multi-reference CC methods. The Fock-space MRCC theory was discussed in details together with the theory of constrained variation approach within the *(1,1)* valence sector.

The second chapter comprised the entire formulation and developmental work pertaining to the calculation of transition dipole moments within FSMRCC methodology. The actual implementation of the codes (as given in chapter 3 and 4) were tested through calculating and evaluating the TDM and oscillator strength of a few selected molecules, that were compared with other available theoretical models. Oscillator strengths were also reported for a number of molecules in three different approaches for ground to excited states of closed shell molecules. Among the three methods developed to evaluate TDM (and eventually relate it to oscillator strength) FSCC-T method is the cheapest in terms of computational time. Although this suffers from an infinite series, inclusion of sufficient number of terms (refer equation 2.22 and section 2.4.1) in the dipole strength calculation, will reduce the error that arises due to the non-terminating nature of the equation. The left and right transition moments in FSCC-Λ method have a natural termination (as opposed to FSCC-T method) due to linearized left vectors that can contract with only a handful of *T*-amplitudes giving rise to an overall connected form. Though the bi-orthogonal method is conceptually perhaps the best method within FSCC to evaluate transition moments, it is computationally very expensive. Even for a small system under study, the solution of the lambda equations is the rate determining step in calculating TDM. Another drawback of this method is that, only one root can be solved at a time. In order to calculate TDM for a particular state, the entire set of lambda equations have to solved starting from the *(1,1)* sector till the *(0,0)* sector. This is in contrast with the

expectation value method, where the entire set of transition moments can be obtained in one go. The semi-bi-orthogonal method, strikes a balance between the two approaches. The left transition moment is solved in a similar manner to that of FSCC-Λ, while the right transition moment is solved like the expectation value method. Thus, the left transition moment is now a naturally terminating series and we no longer have to solve for the entire lambda equations. Solving for an extra set of $\Lambda^{(0,0)}$ will be sufficient. Thus, FSCC-ΛT can be an attractive choice to evaluate TDM and oscillator strength within FSCC framework. This method can also evaluate TDM for all target states in one shot, i.e. it is not state dependent. In case of evaluating transition moments for the doublet radicals, the FSCC-T and FSCC-Λ methods provide transition moments that are in close proximity to each other and to any other available theoretical methods. Thus, both these methods are equally suitable for calculation of the same specifically for open shell systems.

The fifth chapter developed new approximate methods within the FSCC singles and doubles (SD) scheme to calculate direct difference of energies and electric response properties. The various perturbative truncation schemes within FSCCSD were presented in this chapter. The series of approximate methods were labeled as FSCC(n), where n denotes the leading order of corrected correlation energy within the FSCCSD scheme. An error analysis of the various difference energies like, ionization potential (IP), electron affinity (EA) and excitation energies (EE) showed that FSCC(4) method had nearly converged energy values as that of FSCCSD. The FSCC(3) method had a higher error bar as compared to FSCC(4). But both these methods scale as N^6 which is the same as FSCCSD. The FSCC(2) and FS-CC2 methods have reduced scaling of N^5. The error analysis shows an average error bar of 0.15eV to 0.2 eV for both the lower scaling methods for difference energies. Thus, these two methods were further tested for electric response properties like, dipole moment, polarizabilities and transition moments. The electric response properties were calculated by finite difference method (finite difference of energies) while the dipole strength was reported for the FSCC-T method. The averaged error analysis showed that the FS-CC2 method performed better than FSCC(2) method for polarizabilities of all the sectors and the dipole strengths. In case of dipole moments, the averaged error was similar for the *(0,1)* and *(1,0)* sectors, but for the higher valence *(1,1)* sector, FS-CC2 outperformed it. Thus, it can be concluded that among

FS-CC2 and FSCC(2) methods, the FS-CC2 method can be the method of choice when calculating electric response properties or transition moments for excited states.

7.2 Future directions

The work presented in this thesis was fundamental development within FSMRCCSD framework. The developed theories has been tested on a number of small molecular systems. As a first step, a larger test system can be chosen and a benchmark study can be initiated for the lower scaling methods to exploit their versatility. Such a study would serve as a reference for future developments in this area.

Another interesting case study would be to further exploit the FSCC(2) and FS-CC2 methods for the specific problem of electron attachment. In studying EA/EE, there is a large storage requirement for four particle type of integrals. It would be worthwhile to make further approximations within the lower scaling methods, that would not only reduce computational time but also storage area in hard drives. Such a method would find suitability for treating molecules with much larger number of atoms.

The transition moments were developed within the class of FSCC singles and doubles scheme. Inclusion of full/partial triples can be implemented for all the different methods developed in this thesis.

7.3 Ongoing projects

One of the ongoing project that is connected to the work presented in this thesis is, calculation of transition moment for the doublet radical pertaining to the case of electron attachment i.e. *(1,0)* sector. Another work is a benchmark study of transition moments from the ground to a few low lying excited states for a larger set of test molecules. A number of CC based methods have claimed to reproduce transition moments of closed shell molecules. We aim to reproduce results from all these methods and compare them with the methods developed by us for a systematic case study.

We have compared results for TDM in FSCC-T technique for the lower scaling methods. The same reduced scaling can also be extended to FSCC-ΛT and FSCC-Λ methods. We are also involved in truncating the de-excitation amplitudes in

a similar footing, as is done for the similarity transformed Hamiltonian of the ground state sector. This is an ongoing work where we are also looking into the perturbative truncation of the higher valence effective Hamiltonian, in order to reduce scaling for all other higher valence rank sectors with respect to the cluster operators.

Appendix A

Triplet excitation energies for all systems as referred to in chapter 5

Triplet Energies	States	FS-CC2	FSCC(2)	FSCC(3)	FSCC(4)	FSCCSD
NH_3	1e to $4a_1$	13.233	13.670	13.793	13.316	13.302
	1e to $5a_1$	14.867	14.886	14.983	14.937	14.922
	1e to 3e	15.326	15.345	15.456	15.409	15.393
	2e to $4a_1$	11.694	11.713	11.844	11.793	11.778
	2e to $5a_1$	13.650	13.670	13.793	13.742	13.726
	2e to 3e	13.302	13.321	13.426	13.378	13.363
	$3a_1$ to $4a_1$	5.785	5.831	5.918	5.834	5.823
	$3a_1$ to $5a_1$	7.336	7.378	7.445	7.370	7.357
	$3a_1$ to 3e	7.447	7.489	7.557	7.481	7.468
BH	$2\sigma_g$ to 1π	14.863	14.917	15.260	15.117	15.128
	$2\sigma_g$ to $4\sigma_g$	13.285	13.327	13.590	13.459	13.462
	$2\sigma_g$ to $5\sigma_g$	15.495	15.543	15.327	15.177	15.189
	$2\sigma_g$ to 3π	14.916	14.970	15.327	15.177	15.189
	$2\sigma_g$ to $6\sigma_g$	0.890	0.893	1.510	1.376	1.374
	$3\sigma_g$ to 1π	6.156	6.188	6.746	6.580	6.580
	$3\sigma_g$ to $4\sigma_g$	6.991	7.025	7.586	7.416	7.417
	$3\sigma_g$ to $5\sigma_g$	0.889	0.893	1.510	1.376	1.374
	$3\sigma_g$ to 3π	0.889	0.893	1.510	1.376	1.374
	$3\sigma_g$ to $6\sigma_g$	7.843	7.883	8.437	8.256	8.259
HF	$3\sigma_g$ to $4\sigma_g$	13.592	13.518	13.499	13.568	13.547
	$3\sigma_g$ to $5\sigma_g$	17.472	17.378	17.361	17.451	17.429
	$3\sigma_g$ to $6\sigma_g$	18.570	18.468	18.459	18.557	18.535
	$3\sigma_g$ to 3π	18.450	18.368	18.346	18.431	18.410
	1π to $4\sigma_g$	10.191	10.100	10.077	10.168	10.146
	1π to $5\sigma_g$	13.842	13.744	13.699	13.801	13.779
	1π to $6\sigma_g$	14.883	14.780	14.739	14.845	14.824
	1π to 3π	14.396	14.317	14.260	14.349	14.330
	1π to 4π	14.397	14.318	14.261	14.629	14.609
H_2S	$2b_2$ to $6a_1$	11.313	11.357	11.614	11.492	11.489
	$2b_2$ to $3b_2$	13.044	13.094	13.341	13.209	13.207
	$5a_1$ to $6a_1$	9.203	9.247	9.515	9.380	9.379
	$5a_1$ to $3b_2$	11.216	11.269	11.503	11.363	11.363

	$2b_1$ to $6a_1$	6.318	6.363	6.615	6.474	6.475
	$2b_1$ to $3b_2$	8.253	8.302	8.537	8.398	8.398
CO	$4\sigma_g$ to $6\sigma_g$	0.60284	0.60390	0.60750	0.60301	0.60226
	$4\sigma_g$ to 3π	0.53216	0.52850	0.53134	0.53430	0.53211
	$4\sigma_g$ to $7\sigma_g$	0.66093	0.65488	0.64585	0.66279	0.66305
	1π to 3π	0.50829	0.50767	0.50531	0.50554	0.50408
	1π to $6\sigma_g$	0.43476	0.43212	0.43299	0.43513	0.43286
	$5\sigma_g$ to $7\sigma_g$	0.38925	0.39755	0.40563	0.39447	0.39509
H_2O	$1b_2$ to $4a_1$	0.50686	0.50567	0.50769	0.50818	0.50749
	$1b_2$ to $2b_2$	0.58179	0.58036	0.58180	0.58277	0.58200
	$3a_1$ to $4a_1$	0.37182	0.37094	0.37191	0.37231	0.37162
	$3a_1$ to $2b_2$	0.44043	0.43923	0.43969	0.44054	0.43978
	$1b_1$ to $4a_1$	0.28990	0.28929	0.28955	0.28976	0.28911
	$1b_1$ to $2b_2$	0.36054	0.35964	0.35925	0.35989	0.35917
CH^+	$2\sigma_g$ to 1π	0.35477	0.35564	0.37714	0.37217	0.37236
	$3\sigma_g$ to 1π	0.02292	0.02279	0.04886	0.04426	0.04418
CH_4	$1T_2$ to $3a_1$	0.38547	0.38788	0.39546	0.39130	0.39116
	$1T_2$ to $4T_2$	0.43755	0.44020	0.44762	0.44320	0.44305
	$1T_2$ to $5T_2$	0.44574	0.44845	0.45588	0.45139	0.45124
	$1T_2$ to $6T_2$	0.44572	0.44843	0.45587	0.45138	0.45123
	$2T_2$ to $3a_1$	0.38547	0.38788	0.39546	0.39130	0.39116
	$2T_2$ to $4T_2$	0.44573	0.44844	0.45588	0.45139	0.45124
	$2T_2$ to $5T_2$	0.43751	0.44017	0.44759	0.44317	0.44302
	$2T_2$ to $6T_2$	0.43751	0.44017	0.44759	0.44316	0.44301

List of Publications

1. "Fock-space multi-reference coupled cluster response with the effect of triples on dipole moment of ClO and SF radicals" L. Ravichandran, D. Bhattacharya, N. Vaval and S. Pal, *J. Chem. Sci.* 124, 223 (2012)

2. "Electronic transition dipole moments and dipole oscillator strength within Fock-space multireference coupled cluster framework: An efficient and novel approach" D. Bhattacharya, N. Vaval and S. Pal, *J. Chem. Phys.* 138, 094108 (2013)

3. "Electronic transition dipole moment: A semi-biorthogonal approach within valence universal coupled cluster framework" D. Bhattacharya, N. Vaval, S. Pal, *Int. J. Quantum Chem.* 114, 1212 (2014)

4. "Perturbative order analysis of the similarity transformed Hamiltonian in Fock-space coupled cluster theory: Difference energy calculations" D. Bhattacharya, A. K. Dutta, J. Gupta and S. Pal, Mol. Phys. (2015) *(in press)*

5. "Transition moments of radical cations under the Fock-space coupled cluster singles and doubles approximation" D. Bhattacharya, N. Vaval and S. Pal, *J. Chem. Phys.* (to be submitted)

ERRATUM

ERRATUM

ERRATUM